UNIVERSIDADE FEDERAL DE SANTA MARIA
CENTRO DE CIÊNCIAS NATURAIS E EXATAS
PROGRAMA DE PÓS-GRADUAÇÃO EM BIODIVERSIDADE ANIMAL

Micheli Stefanello

DESCRIÇÃO, TAXONOMIA, FILOGENIA E EVOLUÇÃO CRANIANA DE NOVOS PROBAINOGNÁTIOS NÃO-MAMALIAFORMES (CYNODONTIA: EUCYNODONTIA) SUL-BRASILEIROS

Santa Maria, RS
2022

Micheli Stefanello

DESCRIÇÃO, TAXONOMIA, FILOGENIA E EVOLUÇÃO CRANIANA DE NOVOS PROBAINOGNÁTIOS NÃO-MAMALIAFORMES (CYNODONTIA: EUCYNODONTIA) SUL-BRASILEIROS

Tese apresentada ao Curso de Doutorado do Programa de Pós-Graduação em Biodiversidade Animal, Área de Concentração em Sistemática e Biologia Evolutiva, da Universidade Federal de Santa Maria (UFSM, RS), como requisito parcial para obtenção do grau de **Doutora em Ciências Biológicas – Área Biodiversidade Animal**.

Orientador: Prof. Dr. Leonardo Kerber

Santa Maria, RS
2022

This study was financied in part by the Coordenação de Aperfeiçoamento de Pessoal de Nível Superior - Brasil (CAPES) - Finance Code 001

Stefanello, Micheli
DESCRIÇÃO, TAXONOMIA, FILOGENIA E EVOLUÇÃO CRANIANA DE NOVOS PROBAINOGNÁTIOS NÃO-MAMALIAFORMES (CYNODONTIA: EUCYNODONTIA) SUL-BRASILEIROS / Micheli Stefanello.- 2022.
137 p.; 30 cm

Orientador: Leonardo Kerber
Tese (doutorado) - Universidade Federal de Santa Maria, Centro de Ciências Naturais e Exatas, Programa de Pós-Graduação em Biodiversidade Animal, RS, 2022

1. Período Triássico 2. Cinodontes 3. Prozostrodontia 4. Cladística 5. Origem dos Mammaliaformes I. Kerber, Leonardo II. Título.

Sistema de geração automática de ficha catalográfica da UFSM. Dados fornecidos pelo autor(a). Sob supervisão da Direção da Divisão de Processos Técnicos da Biblioteca Central. Bibliotecária responsável Paula Schoenfeldt Patta CRB 10/1728.

Declaro, MICHELI STEFANELLO, para os devidos fins e sob as penas da lei, que a pesquisa constante neste trabalho de conclusão de curso (Tese) foi por mim elaborada e que as informações necessárias objeto de consulta em literatura e outras fontes estão devidamente referenciadas. Declaro, ainda, que este trabalho ou parte dele não foi apresentado anteriormente para obtenção de qualquer outro grau acadêmico, estando ciente de que a inveracidade da presente declaração poderá resultar na anulação da titulação pela Universidade, entre outras consequências legais.

Micheli Stefanello

DESCRIÇÃO, TAXONOMIA, FILOGENIA E EVOLUÇÃO CRANIANA DE NOVOS PROBAINOGNÁTIOS NÃO-MAMALIAFORMES (CYNODONTIA: EUCYNODONTIA) SUL-BRASILEIROS

Tese apresentada ao Curso de Doutorado do Programa de Pós-Graduação em Biodiversidade Animal, Área de Concentração em Sistemática e Biologia Evolutiva, da Universidade Federal de Santa Maria (UFSM, RS), como requisito parcial para obtenção do grau de **Doutora em Ciências Biológicas – Área Biodiversidade Animal**.

Aprovada em 12 de setembro de 2022:

_____

Leonardo Kerber, Prof. Dr. (UFSM)
(Presidente/Orientador)

_____

Átila Augusto Stock da Rosa, Prof. Dr. (UFSM)

_____

Marina Bento Soares, Prof.ª Dra. (UFRJ)

_____

Ane Elise Branco Pavanatto, Dra.

_____

Tomaz Panceri Melo, Dr.

Santa Maria, RS
2022

Dedico esta Tese aos meus pais, Delvi Tedeu Stefanello e Elisabeth Garlet Stefanello, que não mediram esforços para proporcionar-me educação e estudos de qualidade.

AGRADECIMENTOS

Agradeço, primeiramente, à Universidade Federal de Santa Maria (UFSM), onde tive a oportunidade e o privilégio de permanecer por quase onze anos, e durante estes conquistar os títulos de Licenciada em Ciências Biológicas, Mestra e por fim, o tão sonhado título de Doutora.

Agradeço imensamente ao meu orientador, Prof. Dr. Leonardo Kerber, pela orientação, ensinamentos e incentivos constantes, e também por possibilitar meu crescimento e seguimento na área a qual tenho muito apreço, carinho e interesse.

Ao Prof. Dr. Sérgio Dias da Silva, por ter aceitado me orientar durante todo o mestrado e parte deste doutorado, principalmente por ter aberto as portas do mundo da paleontologia para mim e ter me proporcionado estudar fósseis tão incríveis.

Aos colegas do Centro de Apoio à Pesquisa Paleontológica (CAPPA) da Quarta Colônia da UFSM, pela convivência, troca de conhecimentos e por terem me auxiliado de diferentes formas ao longo desses anos, entre o mestrado e o doutorado.

Ao Dr. Agustín Guillermo Martinelli por todo o aprendizado, sugestões e discussões sobre o fascinante mundo dos cinodontes.

Ao Prof. Dr. Átila Augusto Stock Da Rosa, à Prof.ª Dra. Marina Bento Soares, à Prof.ª Dra. Ane Elise Branco Pavanatto e ao Prof. Dr. Tomaz Panceri Melo, pela participação como membros da banca examinadora dessa tese.

Ao Secretário, Sidnei Cruz, e ao Coordenador, Prof. Dr. Andre Schuch, do Programa de Pós-Graduação em Biodiversidade Animal (PPGBA) da UFSM, por estarem sempre dispostos a auxiliar-me nos problemas burocráticos e pela oportunidade de desenvolver este estudo.

À Coordenação de Aperfeiçoamento de Pessoal de Nível Superior (CAPES), pela bolsa de estudo concedida.

Por fim, agradeço à toda a minha família e amigos pelo apoio constante. Em especial, agradeço aos meus pais, Delvi e Elisabeth, por toda a educação, incentivo e amor. Às minhas irmãs, Francieli, Gisieli e Alessandra, pelo apoio incondicional. Ao meu marido, Luciano, por toda compreensão, companheirismo, carinho e amor. À minha amiga, Sheila, pela amizade, momentos de descontração e apoio emocional nos momentos mais difíceis. Enfim, agradeço a todos que de alguma forma contribuíram ao longo dessa jornada.

Não é a terra que é frágil. Nós é que somos frágeis. A natureza tem resistido a catástrofes muito piores do que as que produzimos. Nada do que fazemos destruirá a natureza. Mas podemos facilmente nos destruir.

James Lovelock

RESUMO

DESCRIÇÃO, TAXONOMIA, FILOGENIA E EVOLUÇÃO CRANIANA DE NOVOS PROBAINOGNÁTIOS NÃO-MAMALIAFORMES (CYNODONTIA: EUCYNODONTIA) SUL-BRASILEIROS

AUTORA: Micheli Stefanello
ORIENTADOR: Leonardo Kerber

Cynodontia compreende um grande clado de sinápsidos que inclui numerosas espécies, tanto não-Mammaliaformes quanto Mammaliaformes. Formas não-mamaliaformes estavam entre os componentes mais conspícuos da paleofauna continental de tetrápodes terrestres durante o Triássico, com ocorrência em toda a Pangeia. Menos inclusivo, o clado Probainognathia reúne uma grande variedade de tamanhos e morfologias dentárias, exibindo um registro fóssil abundante nas sucessões faunísticas do Triássico Médio e Superior, sobretudo no Brasil e na Argentina. O presente trabalho tem por objetivo estudar a anatomia craniana, mandibular e dentária de novos espécimes (CAPPA/UFSM 0208, CAPPA/UFSM 0262 e CAPPA/UFSM 0210) de cinodontes probainognátios não-mamaliaformes do Triássico Superior, coletados na região da Quarta Colônia, região central do Rio Grande do Sul. Os espécimes foram tomografados e sua anatomia descrita formalmente. Os materiais apresentam estruturas morfológicas diagnósticas tanto do clado Probainognathia, quanto do clado menos inclusivo Prozostrodontia. CAPPA/UFSM 0262 e CAPPA/UFSM 0208 correspondem a um novo gênero e espécie de cinodonte prozostrodonte não-mamaliaforme, *Agudotherium gassenae* Stefanello et al., 2020a, para o Triássico Superior do Sul do Brasil. O novo táxon consiste, em um dentário esquerdo (holótipo, CAPPA/UFSM 0262) e direito (parátipo, CAPPA/UFSM 0208), com dentes incisivos, caninos e pós-caninos preservados. A nova espécie difere claramente de outros cinodontes não-mamaliaformes carnianos e norianos conhecidos, por possuir uma combinação única de características morfológicas. *Agudotherium gassenae* fornece novas evidências sobre a diversidade de cinodontes probainognátios não-mamaliaformes, bem como para o conhecimento da irradiação adaptativa de Prozostrodontia, ocorrido durante o final do período Triássico. Já CAPPA/UFSM 0210 compreende um novo e mais completo espécime de *Prozostrodon brasiliensis* (BARBERENA; BONAPARTE; TEIXEIRA, 1987), representado por um crânio com dentários desarticulados. Dada à completude do espécime, o novo material de *P. brasiliensis* fornece informações anatômicas adicionais para a região posterior do crânio, ajudando a preencher lacunas no caminho evolutivo das transformações sofridas dentro do clado Cynodontia, que levaram o desenvolvimento de características mamalianas conhecidas atualmente. Os novos dados anatômicos, por meio da investigação cladística, revelam um novo clado endêmico de cinodontes sul-americanos – Prozostrodontidae. Este clado ilustra a primeira radiação de prozostrodontes carnianos para o Gondwana ocidental. Por fim, o conjunto de espécimes estudado contribui para o conhecimento e compreensão sobre a evolução craniana e diversificação de Prozostrodontia não-Mammaliaformes durante o final do período Triássico.

Palavras-chave: Período Triássico. Cinodontes. Prozostrodontia. Origem dos Mammaliaformes.

ABSTRACT

DESCRIPTION, TAXONOMY, PHYLOGENY, AND CRANIAL EVOLUTION OF NEW NON-MAMALIAFORM PROBAINOGNATHIANS (CYNODONTIA: EUCYNODONTIA) SOUTHERN BRAZIL

AUTHOR: Micheli Stefanello
ADVISOR: Leonardo Kerber

Cynodontia comprises a large synapsid clade that includes numerous species, both non-Mammaliaformes and Mammaliaformes. Non-mammaliaform forms were among the most conspicuous components of the continental paleofauna of terrestrial tetrapods during the Triassic, occurring throughout Pangea. Less inclusive, the clade Probainognathia has a great variety of size and dental morphology, exhibiting an abundant fossil record in the faunal successions of the Middle and Late Triassic, especially in Brazil and Argentina. The present work aims to study the cranial, mandibular, and dental anatomy of new specimens (CAPPA/UFSM 0208, CAPPA/UFSM 0262, and CAPPA/UFSM 0210) of non-mammaliaform probainognathian cynodonts from the Upper Triassic, collected in the region of Quarta Colônia, central region of Rio Grande do Sul. The specimens were CT scanned, and their anatomy formally described. The materials present diagnostic morphological structures of both the Probainognathia clade and the less inclusive Prozostrodontia clade. CAPPA/UFSM 0262 and CAPPA/UFSM 0208 correspond to a new genus and species of non-mammaliaform prozostrodontian cynodont, *Agudotherium gassenae* Stefanello et al., 2020a. The new taxon consists of a left dentary (holotype, CAPPA/UFSM 0262) and a right dentary (paratype, CAPPA/UFSM 0208), with preserved incisors, canines, and postcanines. The new species clearly differs from other known non-mammaliaform Carnian and Norian cynodonts in having a unique combination of morphological features. *Agudotherium gassenae* provides new evidence on the diversity of non-mammaliaform probainognathian cynodonts and the knowledge of the adaptive irradiation of Prozostrodontia, which occurred during the late Triassic period. CAPPA/UFSM 0210 comprises a new and more complete specimen of *Prozostrodon brasiliensis* (BARBERENA; BONAPARTE; TEIXEIRA, 1987), represented by a complete skull with disarticulated dentaries. Given the completeness of the specimen, the new material from *P. brasiliensis* provides additional anatomical information for the posterior region of the skull, helping to fill in gaps in the evolutionary path of the transformations undergone within the non-Mammaliaformes Cynodontia clade, which led to the currently known Mammalian pattern. The new anatomical data, through cladistic investigation, reveal a new endemic clade of South American cynodonts – Prozostrodontidae. This clade illustrates the first radiation of Carnian prozostrodontians to western Gondwana. Finally, the set of specimens studied contributes to the knowledge and understanding of the cranial evolution and diversification of non-Mammaliaform Prozostrodontia during the late Triassic period.

Key words: Triassic period. Cynodonts. Prozostrodontia. Origin of the Mammaliaforms.

LISTA DE FIGURAS

TEXTO INTEGRADOR

ARTIGO 1 – A new prozostrodontian cynodont (Eucynodontia, Probainognathia) from the Upper Triassic of Southern Brazil

LISTA DE TABELAS

ARTIGO 2 – A complete skull of a stem mammal from the Late Triassic of Brazil illuminates the early evolution of prozostrodontians

LISTA DE SIGLAS

CAPPA	Centro de Apoio à Pesquisa Paleontológica da Quarta Colônia
MMACR	Museu Municipal Aristides Carlos Rodrigues
MVP	Museu Vicente Pallotti
PVSJ	Instituto y Museo de Ciencias Naturales
UFRGS	Universidade Federal do Rio Grande do Sul
UFSM	Universidade Federal de Santa Maria

SUMÁRIO

APRESENTAÇÃO

A presente tese de doutorado está estruturada de acordo com as normas do Manual de Dissertações e Teses (MDT) da Universidade Federal de Santa Maria (UFSM) e atende as exigências do Programa de Pós-Graduação em Biodiversidade Animal (PPGBA). A tese integra os requisitos necessários para a obtenção do título de Doutora em Biodiversidade Animal, sendo composta por um breve texto integrador, artigos científicos e considerações finais. A metodologia empregada na tese está descrita em cada um dos trabalhos científicos.

O texto integrador inclui uma contextualização do clado Cynodontia, de um de seus grupos menos inclusivos, Probainognathia, com enfoque especial ao clado Prozostrodontia. Também, são apresentadas algumas das principais mudanças anatômicas ocorridas na linhagem Cynodontia, as quais foram, posteriormente, estabelecidas no clado Mammalia. Sequentemente à contextualização introdutória, segue a apresentação dos objetivos da tese.

O Artigo 1 refere-se à descrição de um novo gênero e espécie de cinodonte prozostrodonte para o Triássico Superior do Sul do Brasil. A nova espécie, *Agudotherium gassenae* Stefanello et al., 2020a, consiste em um dentário esquerdo (holótipo, CAPPA/UFSM 0262) e direito (parátipo, CAPPA/UFSM 0208) com dentes incisivos, caninos e pós-caninos preservados. O artigo encontra-se publicado no periódico científico *Journal of Vertebrate Paleontology* (DOI: 10.1080/02724634.2020.1782415) (STEFANELLO et al., 2020a). Enquanto que no dataset do Artigo 1, publicado na revista científica *MorphoMuseuM* (DOI: 10.18563/journal.m3.120), são apresentados os dados dos modelos tridimensionais e da microtomografia computadorizada (Micro-CT) dos dentários e dentes de *A. gassenae* (STEFANELLO et al., 2020b).

O Artigo 2 apresenta a descrição anatômica de um novo e mais completo espécime de *Prozostrodon brasiliensis* (CAPPA/UFSM 0210), descoberto em estratos do Triássico Superior do Sul do Brasil. O novo material, excepcionalmente bem preservado, representado pelo crânio e dentários, fornece informações adicionais sobre a radiação inicial de Cynodontia e revela um novo clado de cinodontes sul-americanos. O manuscrito é apresentado de acordo com as normas de formatação exigidas pelo periódico científico *Journal of Mammalian Evolution*, no qual o mesmo foi submetido. Na seção conclusões é apresentada uma breve recapitulação dos resultados em relação aos objetivos propostos para esta tese.

TEXTO INTEGRADOR

1 INTRODUÇÃO

1.1 CONTEXTUALIZAÇÃO DO CLADO CYNODONTIA

Os cinodontes (Cynodontia Owen, 1861) compreendem um grande clado de sinápsidos que inclui numerosas espécies, tanto não-Mammaliaformes quanto Mammaliaformes, estas últimas incluindo Mammalia Linnaeus, 1758 como clado coronal (HOPSON; KITCHING, 2001; LIU; OLSEN, 2010) (Figura 1). Formas não-mamaliaformes estavam entre os componentes mais conspícuos da paleofauna continental de tetrápodes terrestres durante o Triássico, ocorrendo em grande parte das regiões do supercontinente Pangeia (ABDALA; NEVELING; WELMAN, 2006; ABDALA et al., 2009; MUSSER et al., 2009; ABDALA; RIBEIRO, 2010; BONAPARTE; MIGALE, 2010). O registro mais antigo de Cynodontia data do Permiano Superior e é representado por *Charassognathus gracilis* Botha; Abdala; Smith, 2007 e *Abdalodon diastematicus* Kammerer, 2016, da Bacia de Karoo, África do Sul, sendo que estes representam a primeira radiação adaptativa de Cynodontia (BOTHA; ABDALA; SMITH, 2007; KAMMERER, 2016).

Durante o Triássico, principalmente Médio e Superior, os cinodontes tornaram-se abundantes e taxonomicamente diversos, distribuindo-se e ocupando diferentes nichos nos ecossistemas terrestres (ABDALA et al., 2009; ABDALA; RIBEIRO, 2010). A maioria dos táxons foi extinta até o final do Triássico, mas os sobreviventes da linhagem Mammaliaformes passaram a se diversificar a partir desse momento. Além dos mamaliaformes, duas outras famílias, Tritheledontidae e Tritylodontidae, romperam o limite Triássico-Jurássico (KEMP, 2005), sendo que apenas representantes dessa última sobreviveram até o início do Cretáceo (WATABE; TSUBAMOTO; TSOGTBAATAR, 2007; MUSSER et al., 2009).

Eucynodontia Kemp, 1982 é considerado um clado bastante estável (ROWE, 1988; LIU; OLSEN, 2010), o qual inclui todos os cinodontes mais derivados que *Thrinaxodon liorhinus* Seeley, 1894 (KEMP, 1982; HOPSON; BARGHUSEN, 1986; LIU; OLSEN, 2010), ou, em outra definição, o clado menos inclusivo incluindo Mammalia e *Exaeretodon frenguelli* Cabrera, 1943 (HOPSON; KITCHING, 2001). Eucynodontia é composto por dois grandes clados menos inclusivos principais, Cynognathia Hopson; Barghusen, 1986 e Probainognathia Hopson, 1990 (HOPSON; KITCHING, 2001; BONAPARTE; MARTINELLI; SCHULTZ, 2005; ABDALA,

2007; LIU; OLSEN, 2010; RUTA et al., 2013; MARTINELLI; SOARES; SCHWANKE, 2016; MARTINELLI et al., 2017a, b; WALLACE; MARTÍNEZ; ROWE, 2019; KERBER et al., 2022) (Figura 1). Os cinognátios incluem táxons basais de hábitos carnívoros (como por exemplo, o gênero *Cynognathus*) e táxons derivados, como Traversodontidae, que agrupam uma associação altamente diversa de formas com hábitos herbívoros e/ou onívoros, apresentando uma dentição transversamente alargada (CROMPTON, 1972; LIU; ABDALA, 2014). Por outro lado, os probainognátios reúnem numerosas formas carnívoras, insetívoras, onívoras e herbívoras, com uma grande variedade de tamanhos e morfologias dentárias, possuindo desde dentes pós-caninos setoriais comprimidos labiolingualmente até dentes pós-caninos quadrilaterais/multicuspidados (por exemplo, Tritylodontidae) (Figura 2). Como mencionado anteriormente, em Probainognathia, inclui-se o clado Mammaliaformes, e por sua vez, Mammalia (LUO, 1994; HOPSON; KITCHING, 2001; BONAPARTE; MARTINELLI; SCHULTZ, 2005; MARTINELLI; ROUGIER, 2007; LIU; OLSEN, 2010; OLIVEIRA; SOARES; SCHULTZ, 2010; BONAPARTE; SOARES; MARTINELLI, 2012).

Figura 1 – Cladograma mostrando as relações filogenéticas de Cynodontia e de seus clados menos inclusivos

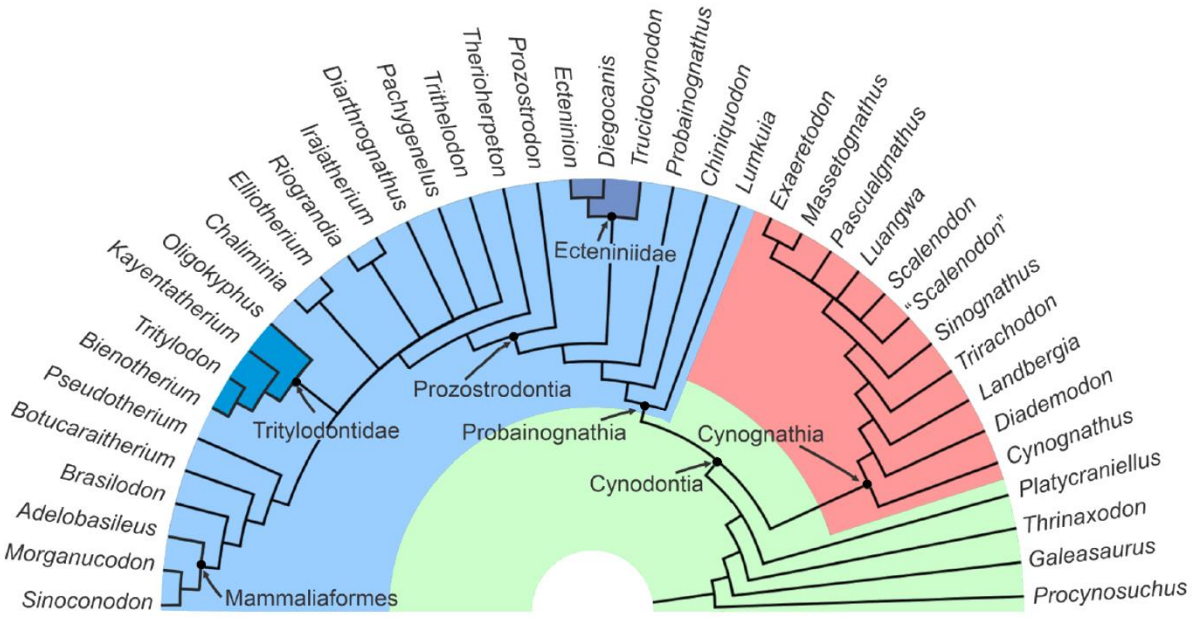

Fonte: (Modificada, KERBER et al., 2022).

Figura 2 – Diversidade de crânios de Probainognátios sul-americanos.
Trucidocynodon riograndensis (A), *Chiniquodon theotonicus* (B), *Probainognathus jenseni* (C), *Protheriodon estudianti* (D), *Riograndia guaibensis* (E), *Chaliminia musteloides* (F), *Brasilodon quadrangularis* (G-H)

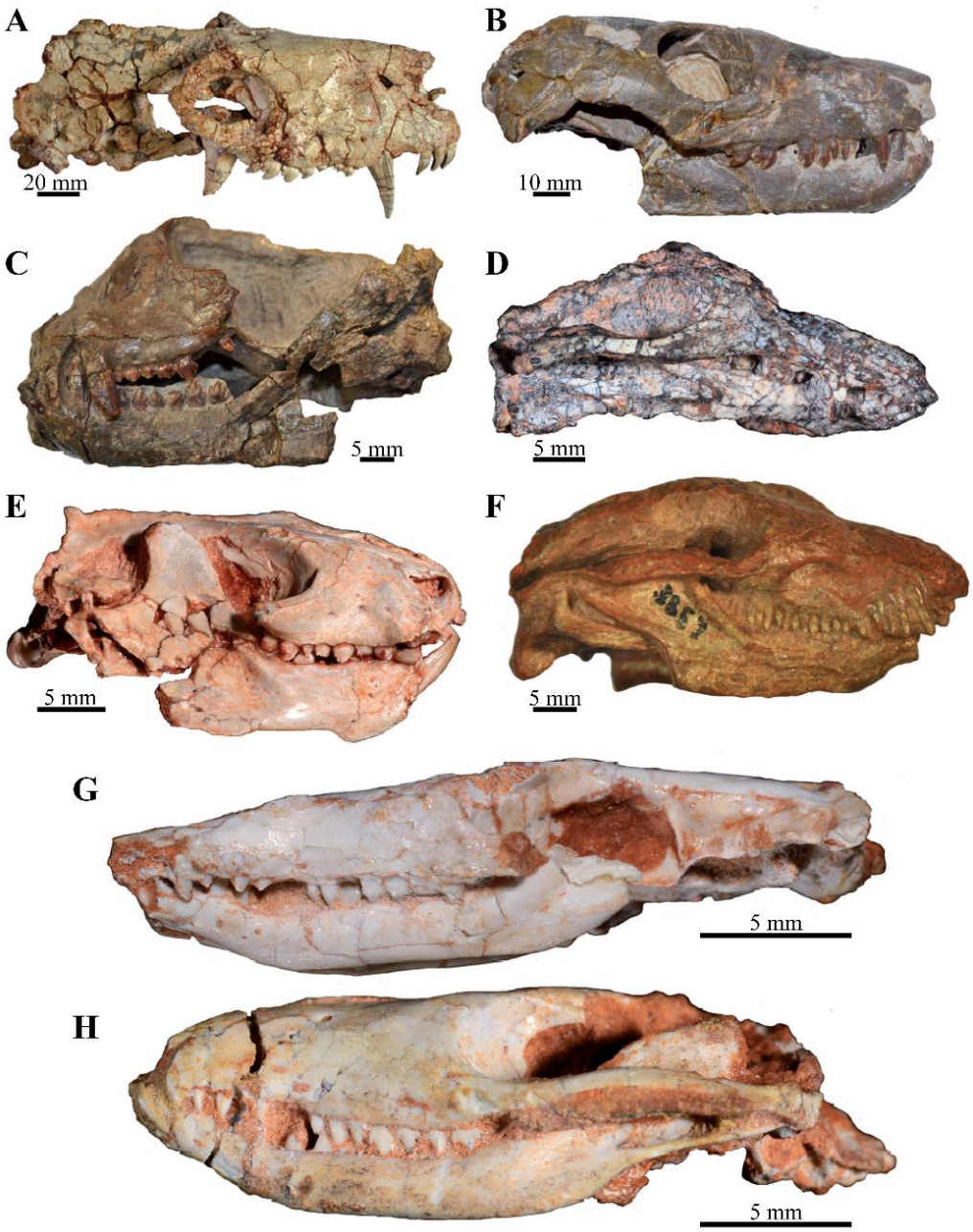

Fonte: (Modificada, MARTINELLI; SOARES, 2016).

O clado Probainognathia vem evidenciando seu monofiletismo em diversas análises cladísticas (vide BONAPARTE et al., 2003; BONAPARTE; MARTINELLI; SCHULTZ, 2005; ABDALA, 2007; MARTINELLI; ROUGIER, 2007; LIU; OLSEN, 2010; SOARES; MARTINELLI; OLIVEIRA, 2014; MARTINELLI; SOARES; SCHWANKE, 2016). Originalmente, foi definido como o grupo mais inclusivo incluindo *Probainognathus jenseni* Romer, 1970 e excluindo *Exaeretodon* (HOPSON; KITCHING, 2001). Os principais caracteres sinapomórficos apresentados pelo clado são: ausência de forame parietal; ausência de ectopterigoide; borda posterior do palato secundário situada no nível da margem anterior da órbita; crista lambdoide separada do arco zigomático por um entalhe em forma de "V"; ausência de expansão lateral das costelas; e cavidade glenoide sem ou com pouca participação do pró-coracoide (sensu HOPSON; KITCHING, 2001).

Probainognathia exibe um registro fóssil abundante na fauna Gonduânica Triássica. Na América do Sul, sobretudo no Brasil e na Argentina, são conhecidas cerca de vinte espécies nas assembleias faunísticas do Triássico Médio e Superior (BONAPARTE, 1966, 1969, 1971; MARTÍNEZ; FORSTER, 1996; MARTÍNEZ; MAY; FORSTER, 1996; ABDALA; BARBERENA; DORNELLES, 2002; BONAPARTE et al., 2003; OLIVEIRA; SOARES; SCHULTZ, 2010; SOARES; SCHULTZ; HORN, 2011; MARTÍNEZ; FERNANDEZ; ALCOBER, 2013; MARTINELLI; SOARES, 2016; MARTINELLI; SOARES; SCHWANKE, 2016; MARTINELLI et al., 2017a, b), de modo que, até o momento, as rochas triássicas brasileiras apresentam a maior diversidade para o grupo (ABDALA; GAETANO, 2018; ABDALA et al., 2020) (Figura 3).

Até o presente, as rochas triássicas aflorantes no Brasil com presença de fósseis são restritas ao Estado do Rio Grande do Sul, onde a incidência de cinodontes probainognátios é assinalada em estratos da Supersequência Santa Maria (ZERFASS et al., 2003; LANGER et al., 2007; HORN et al., 2014), ocorrendo em quase todas as subdivisões da unidade, como por exemplo: *Chiniquodon theotonicus* von Huene, 1936, *Protheriodon estudianti* Bonaparte; Soares; Schultz, 2006, *Candelariodon barberenai* Oliveira et al., 2011, *Bonacynodon schultzi* Martinelli; Soares; Schwanke, 2016 e *Aleodon cromptoni* Martinelli et al., 2017a com ocorrência na Sequência Pinheiros-Chiniquá (Zona de Associação (ZA) de *Dinodontosaurus*, Ladiniano/Carniano); *Santacruzgnathus abdalai* Martinelli; Soares; Schwanke, 2016 e alguns espécimes referidos a *Chiniquodon* sp. (ABDALA; RIBEIRO; SCHULTZ, 2001; MELO et al.,

2022) pertencendo à Sequência Santa Cruz (ZA de *Santacruzodon*, Carniano); *Therioherpeton cargnini* Bonaparte; Barberena, 1975, *Prozostrodon brasiliensis* (BARBERENA; BONAPARTE; TEIXEIRA, 1987), *Charruodon tetracuspidatus* Abdala; Ribeiro, 2000, *Trucidocynodon riograndensis* Oliveira; Soares; Schultz, 2010 e *Alemoatherium huebneri* Martinelli et al., 2017b fazendo parte da Sequência Candelária (ZA de *Hyperodapedon*, Carniano/Noriano); *Riograndia guaibensis* Bonaparte; Ferigolo; Ribeiro, 2001, *Brasilodon quadrangularis* Bonaparte et al., 2003, *Brasilitherium riograndensis* Bonaparte et al., 2003, *Irajatherium hernandezi* Bonaparte; Martinelli; Schultz, 2005, *Minicynodon maieri* Bonaparte et al., 2010 e *Botucaraitherium belarminoi* Soares; Martinelli; Oliveira, 2014 com ocorrência na seção superior da Sequência Candelária (ZA de *Riograndia*, Noriano) (ZERFASS et al., 2003; HORN et al., 2014; LANGER; RAMEZANI; DA ROSA, 2018) (Figura 3). *B. riograndensis* e *M. maieri* foram considerados estágios ontogenéticos de *B. quadrangularis* (LIU; OLSEN, 2010; MARTINELLI et al., 2017c).

Recentemente, um novo gênero e espécie de cinodonte probainognátio foi descrito para o Triássico Superior do Sul do Brasil. A nova espécie, *Agudotherium gassenae* Stefanello et al. 2020a, foi coletada no Sítio Niemeyer, interior do município de Agudo, Rio Grande do Sul, Brasil (PAVANATTO et al., 2018), pertencente à Sequência Candelária, Supersequência Santa Maria (ZERFASS et al., 2003; LANGER et al., 2007; HORN et al., 2014). Dada à proximidade geográfica e à semelhança litológica, Marsola et al. (2018) correlacionam os sítios ASERMA e Concórdia à localidade-tipo de *Sacisaurus agudoensis* Ferigolo; Langer, 2007 tendo esta uma fauna fossilífera que apoia a sua inclusão na ZA de *Riograndia* (idade noriana) (LANGER; RAMEZANI; DA ROSA, 2018; MARSOLA et al., 2018; MIRON et al., 2020. MÜLLER, 2021). Adicionalmente, o traversodontídeo *Siriusgnathus niemeyerorum* Pavanatto et al., 2018 é conhecido para essas duas primeiras localidades fossilíferas (MIRON et al., 2020), além da localidade tipo, Sítio Niemeyer (PAVANATTO et al., 2018). Sendo, assim, infere-se que este seja atribuído à ZA de *Riograndia* (início do noriano) (MIRON et al., 2020, MÜLLER, 2021) (Figura 3). Até o momento, esse sítio fossilífero não apresenta idade absoluta disponível e os fósseis guias típicos característicos para a ZA (por exemplo, o cinodonte *R. guaibensis*, o rincocéfalo *Clevosaurus brasiliensis* Bonaparte; Sues, 2006 e/ou o dicinodonte *Jachaleria candelariensis* Araújo; Gonzaga, 1980) ainda são desconhecidos (STEFANELLO et al., 2020a). Dessa forma, não se pode afirmar com precisão se, de fato, *A. gassenae* pertence à seção superior da Sequência Candelária ou a uma ZA ainda não reconhecida.

Figura 3 – Distribuição bioestratigráfica de Probainognathia não-Mammaliaformes para o Triássico Sul-brasileiro
Abreviações: **Ind,** Induano; **Ole,** Olenekiano; **ZA,** Zona de Associação;
Símbolos: ***,** Espécies sinonímias; **(?),** Espécie sem idade conhecida.

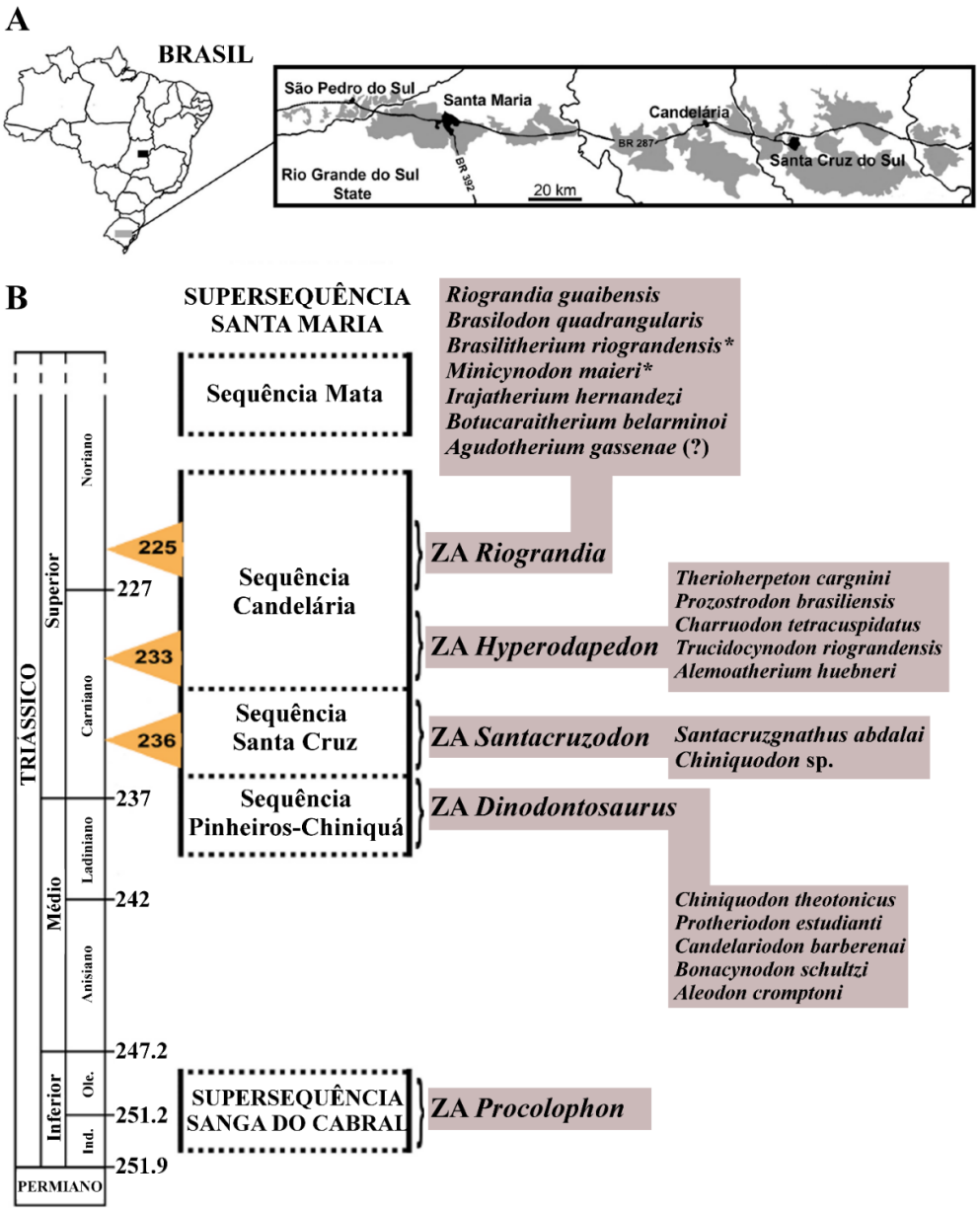

Fonte: (Modificada, ABDALA et al., 2020).

O crescente aumento da diversidade no registro fóssil de Probainognathia não-Mammaliaformes é notável e reflete as principais modificações anatômicas (tais como, aumento da caixa craniana, especialização da dentição e do padrão de oclusão dentária, palato secundário alongado, aquisição de uma articulação crânio-mandibular formada pelo dentário e esquamosal, dentre outras) ocorridas no esqueleto desses animais antes da aquisição de um padrão morfológico mamaliano.

1.1.1 Principais transformações anatômicas ocorridas em Probainognathia

Cinodontes probainognátios triássicos da América do Sul são táxons chave na investigação da origem e evolução dos caracteres mamalianos. O crescente número de descobertas de prozostrodontes de pequeno porte para o Triássico Superior no Sul do Brasil e Argentina (BONAPARTE; BARBERENA, 1975, 2001; BONAPARTE; FERIGOLO; RIBEIRO, 2001; BONAPARTE et al., 2003; BONAPARTE; MARTINELLI; SCHULTZ, 2005; MARTINELLI et al., 2005; SOARES; MARTINELLI; OLIVEIRA, 2014; MARTINELLI; SOARES; SCHWANKE, 2016; MARTINELLI et al., 2017a, b; GUIGNARD; MARTINELLI; SOARES, 2018; WALLACE; MARTÍNEZ; ROWE, 2019; STEFANELLO et al., 2020a; KERBER et al., 2022) melhoraram, consideravelmente, o conhecimento sobre o grupo, formando a base para a compreensão da maioria das transformações crânio-mandibulares e dentais que ocorreram antes do estabelecimento de características comumente associados a mamíferos (LUO, 1994, 2007; SIDOR; HOPSON, 1998; HOPSON; KITCHING, 2001; SIDOR, 2003; KIELAN-JAWOROWSKA; CIFELLI; LUO, 2004; KEMP, 2005; RUTA et al., 2013; BOTHA-BRINK; SOARES; MARTINELLI, 2018).

O registro fóssil de Cynodontia mostra que a aquisição de características mamalianas foi gradual e tais caracteres apomórficos foram se acumulando e, posteriormente, culminaram no aparecimento de feições típicas de mamíferos (KEMP, 2012; RUTA et al., 2013). Transformações anatômicas cruciais, ocorridas, principalmente, em Probainognathia não-Mammaliaformes, possibilitaram importantes adaptações, as quais estão relacionadas a complexas mudanças nas regiões rostral, palatal e basicraniana, na articulação crânio-mandibular e na dentição, bem como alterações significativas no esqueleto pós-craniano (SIDOR; HOPSON, 1998; SIDOR, 2003; KIELAN-JAWOROWSKA; CIFELLI; LUO, 2004; KEMP, 2005). Algumas das principais mudanças anatômicas crânio-mandibulares e dentais que surgiram na linhagem Cynodontia são brevemente comentadas a seguir.

As mudanças na cavidade nasal foram significativas tanto em cinodontes não-Mammaliaformes quanto Mammaliaformes, pois permitiram incrementos na respiração, olfato e no metabolismo (HILLENIUS, 1992, 1994; ROWE; MACRINI; LUO, 2011; CROMPTON et al., 2017). Em formas mais derivadas de probainognátios, a superfície interna da cavidade nasal tem um maior desenvolvimento anteroposterior, relacionado, principalmente, à redução da vacuidade

orbital que sofre maior ossificação (LUO, 1994; HOPSON; KITCHING, 2001). Nesses cinodontes, o surgimento de cristas na superfície interna na maxila tem sido interpretado como possível evidência para a presença de estruturas turbinais (HILLENIUS, 1994). Delicadas ossificações, descritas para o interior da cavidade nasal do prozostrodonte *Brasilodon quadrangularis*, foram interpretadas como sendo possíveis turbinais ossificados (RUF et al., 2014; CROMPTON et al., 2017). Em adição, Ruben et al. (2012) sugerem que o desenvolvimento dos turbinais respiratórios podem estar relacionados a uma função termorreguladora. Recentemente, Araújo et al. (2022) discutiram o surgimento da endotermia em mamíferos e sugerem que em alguns prozostrodontes derivados (como por exemplo, *B. quadrangularis* e *Pseudotherium argentinus*), tritilodontídeos e mamaliaformes já seriam considerados endotérmicos, sendo que a possibilidade de endotermia é de 95% para o clado.

O remodelamento da região palatal, com a formação de um palato ósseo secundário alongado, é outra importante mudança estabelecida no grupo (Figura 4). O desenvolvimento dessa parede óssea, tanto medial quanto anteroposterior, permitiu a separação das vias aéreas e da cavidade bucal, proporcionando melhorias na respiração e olfato, também na função mastigatória (MAIER; HEEVER; DURAND, 1996). Em relação à última, o progressivo fechamento do palato secundário permitiu maior habilidade para o processamento nutricional do alimento antes da deglutição, exploração de novos itens alimentares, bem como propiciou o ato de mamar (HOPSON; BARGHUSEN, 1986; MAIER; HEEVER; DURAND, 1996). Em formas mais avançadas de probainognátios, como chiniquodontídeos, triteledontídeos, brasilodontídeos e mamaliaformes (BONAPARTE et al., 2003; BONAPARTE; MARTINELLI; SCHULTZ, 2005; SIDOR; HANCOX, 2006), o palato ósseo secundário é tão alongado quanto o conhecido nos mamíferos, atingindo a borda posterior ao nível dos últimos dentes pós-caninos (HOPSON; BARGHUSEN, 1986) (Figura 4).

Figura 4 – Desenvolvimento do palato ósseo secundário em Synapsida
Abreviações: **ch,** coana; **ect,** ectopterigoide; **max,** maxila; **pal,** palatino; **pmx,** pré-maxila; **pt,** pterigoide; **vo,** vômer.

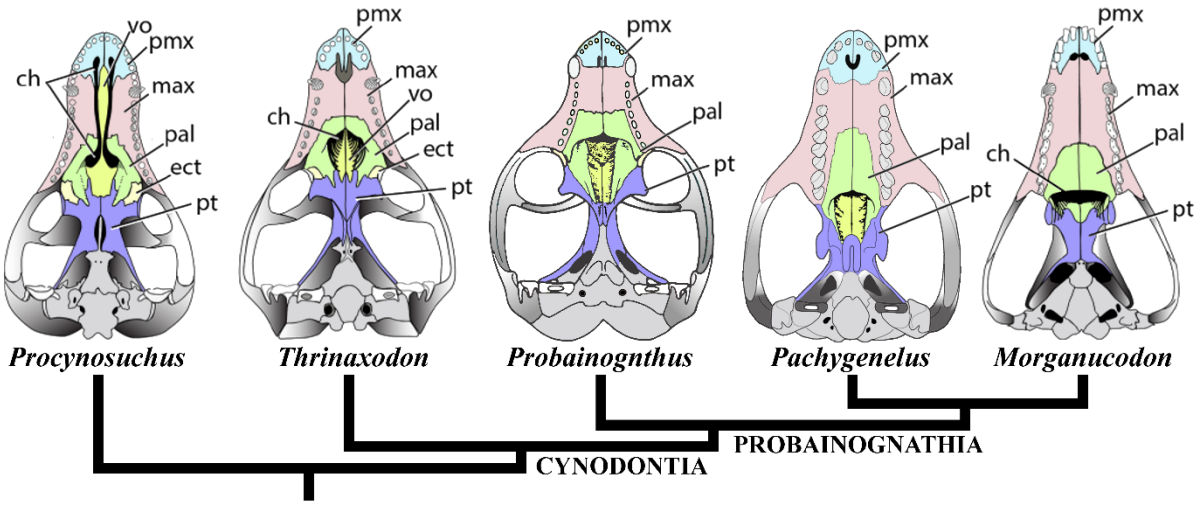

Fonte: (Modificada, ROWE; SHEPHERD, 2016)

O aumento progressivo do volume da caixa craniana, relacionado ao desenvolvimento do encéfalo, é, provavelmente, um dos pontos mais importantes na evolução dos cinodontes (HOPSON; BARGHUSEN, 1986; ROWE, 1988), uma vez que tais mudanças têm correlação direta ao desenvolvimento de um sistema neuronal mais eficaz e com maior capacidade de percepção de estímulos do meio (SOARES; DORNELLES, 2009). Esse aumento da caixa craniana pode estar relacionado também com o desenvolvimento do neocórtex, intimamente relacionado com o tamanho expressivo do cérebro em mamíferos, quando comparado a outros grupos. Essas modificações craniais levaram a maior ossificação no neurocrânio, além de alterações cruciais na parede lateral da caixa craniana e na região basicraniana (ROUGIER; WIBLE; HOPSON, 1992; LUO, 1994).

Importantes modificações relacionadas à reconfiguração dos ossos basicranianos possibilitaram mudanças na evolução do ouvido (interno, médio e externo), acarretando melhorias significativas na audição para esses cinodontes e, posteriormente para os primeiros mamíferos (ROUGIER; WIBLE; HOPSON, 1992; LUO, 1994; LUO; CROMPTON; LUCAS, 1995; ROUGIER; WIBLE, 2006; RODRIGUES; RUF; SCHULTZ, 2013). Um promontório se desenvolve para acomodar o canal coclear (LUO, 1994, 2001; LUO; CROMPTON; LUCAS, 1995). Este é originado pela fusão dos ossos proótico e opistótico, que passam a ser chamados de

petrosal. A presença de um único osso torna, possivelmente, o ouvido interno mais rígido e, portanto, mais isolado e menos suscetível a interferências (LUO, 2001).

Em cinodontes probainognátios mais basais (por exemplo, *Probainognathus jenseni*), a região basicraniana apresenta uma asa do basisfenóide desenvolvida lateralmente e uma clara sutura entre os ossos proótico e opistótico (LUO, 1994). Nos prozostrodontes *Prozostrodon brasiliensis* e *P. argentinus*, a asa do basisfenóide torna-se mais curta e o osso petrosal é fusionado, mas sem a formação de um promontório, enquanto em *Adelobasileus cromptoni* e *B. quadrangularis*, a asa do basisfenóide sofre um encurtamento ainda maior e se observa um promontório incipiente (LUO, 1994; LUO; CROMPTON; LUCAS, 1995; BONAPARTE; MARTINELLI; SCHULTZ, 2005; BONAPARTE; SOARES; MARTINELLI, 2012; RODRIGUES; RUF; SCHULTZ, 2013). A condição de *Morganucodon oehleri* e outros mamaliaformes caracteriza-se por uma asa do basisfenóide reduzidas ou ausentes, além da formação de um promontório para alojar a cóclea (ROUGIER; WIBLE; HOPSON, 1992; LUO, 1994) (Figura 5).

Outra mudança importante na região basicraniana tem relação com a posição dos forames jugular e perilinfático (=fenestra rotunda). A condição primitiva, encontrada em *Thrinaxodon liorhinus*, por exemplo, é caracterizada pela confluência total das duas aberturas (ROUGIER; WIBLE; HOPSON, 1992; WIBLE; HOPSON, 1993; RODRIGUES; RUF; SCHULTZ, 2013; LUO; SCHULTZ; EKDALE, 2016; LUO; MANLEY, 2020). Em alguns prozostrodontes (como em *P. argentinus*, *P. brasiliensis* e *B. quadrangularis*), os forames apresentam uma separação parcial entre eles, embora ainda posicionados em uma fossa comum (LUO, 1994; RODRIGUES; RUF; SCHULTZ, 2013; WALLACE; MARTÍNEZ; ROWE, 2019). Enquanto na condição derivada existe uma separação óssea entre os forames jugular e perilinfático, está observada, por exemplo, em *Pachygenelus monus*, *Riograndia guaibensis* e Mammaliaformes (LUO; WIBLE, 2005; ROUGIER; WIBLE, 2006; SOARES; SCHULTZ; HORN, 2011) (Figura 5).

Figura 5 – Desenvolvimento da região basicraniana em Cynodontia
Abreviações: **Bo**, basioccipital; **Bs**, basisfenóide; **bsw**, asa do basisfenóide; **ce**, cavum epiptericum; **fv**, fenestra vestibuli; **jf**, fenestra jugular; **Op**, opistótico; **Pe**, petrosal; **plf**, forame perilinfático; **ppf**, forame pterygoparoccipital; **Pr**, proótico; **pro**, promontório.

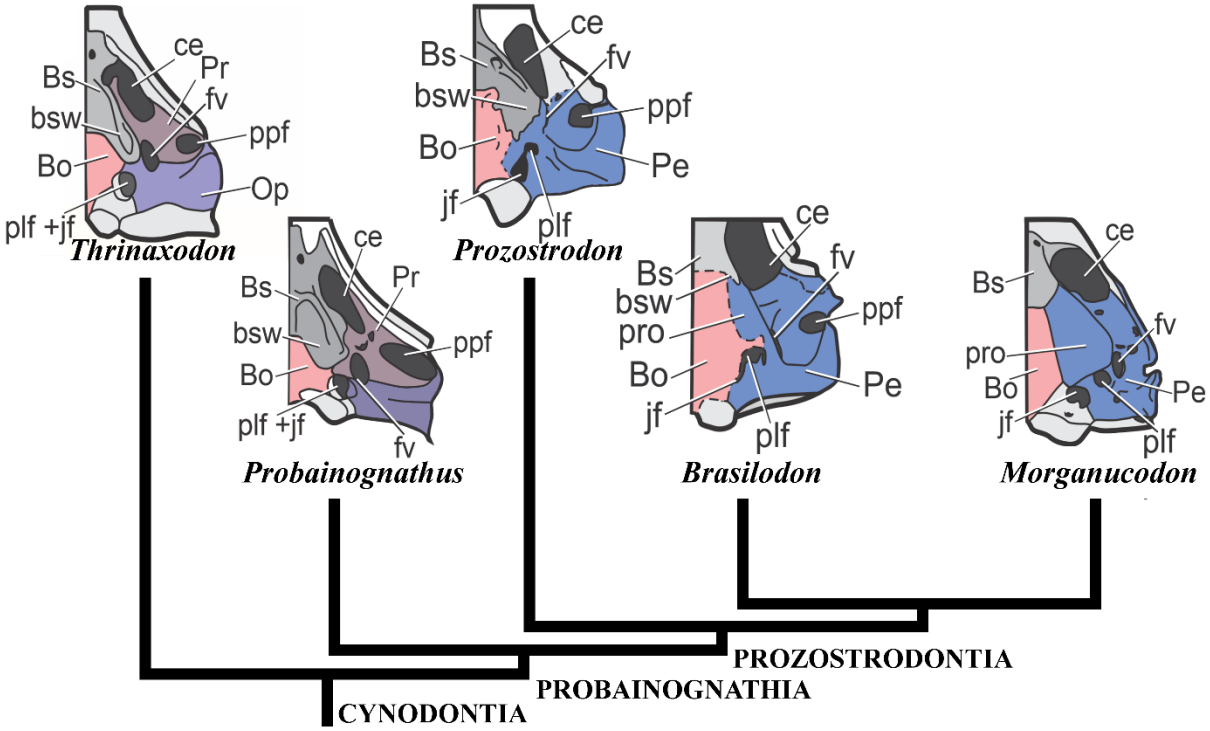

Fonte: (STEFANELLO et al. em revisão).

Na parede lateral da caixa craniana desses cinodontes ocorre outra mudança notória, similar à condição derivada encontrada em *B. quadrangularis* e em mamaliaformes, alguns prozostrodontes (como, *P. brasiliensis* e *P. argentinus*) e triteledontídeos apresentam saídas separadas para os ramos maxilar (V_2) e mandibular (V_3) do nervo trigêmeo, o quais estão localizados na lâmina lateral do proótico/petrosal e do aliesfenoide (BONAPARTE; MARTINELLI; SCHULTZ, 2005; RODRIGUES; RUF; SCHULTZ, 2013). Em contrapartida, em cinodontes basais é reconhecida uma única saída para o V_{2+3}, posicionada entre o proótico e o aliesfenoide (ROUGIER; WIBLE; HOPSON, 1992).

Em relação à dentição, Cynodontia é um dos primeiros clados de terápsidos a apresentar heterodontia, dentes com formas e funções distintas, apresentando incisivos, caninos e pós-caninos (SOARES, 2015). Contudo, diferentemente dos mamaliaformes, que possuem um alto grau de diferenciação dentária, os cinodontes possuem dentes pós-caninos bastante semelhantes entre si, e, por esse motivo, não podem ser reconhecidos como verdadeiros pré-molares e molares

(KIELAN-JAWOROWSKA; CIFELLI; LUO, 2004; KEMP, 2005; ROWE; MACRINI; LUO, 2011; MANLEY, 2012; LAUTENSCHLAGER et al., 2016).

Os mecanismos de substituição dentária reconhecidos nos cinodontes são diversos e, possivelmente, podem estar relacionados com a dieta alimentar de cada grupo específico (MARTINELLI; BONAPARTE, 2011; ABDALA; JASINOSKI; FERNANDEZ, 2013). De forma geral, o padrão primitivo de substituição dentária é do tipo polifiodonte, sendo este identificado em vários táxons, como, por exemplo, no cinodonte basal *T. liorhinus* e no triteledontídeo derivado *P. monus*. Na dentição polifiodonte, os dentes podem ser substituídos, constantemente, ao longo da vida do animal (CROMPTON; LUO, 1993; ABDALA; JASINOSKI; FERNANDEZ, 2013; O'MEARA; DIRKS; MARTINELLI, 2018). Além dos cinodontes, a polifiodontia é observada também em répteis e nos demais sinápsidos não-mamaliaformes. Em contrapartida, os cinodontes gonfodontes apresentam uma substituição dentária relativamente diferenciada, que consiste basicamente na perda de dentes anteriores e na adição de dentes mais complexos posteriormente (HOPSON, 1971; LIU; SUES, 2010).

Entretanto, em algumas formas mais avançadas de prozostrodontes e triteledontídeos, é reconhecido um menor número de substituições dentárias ao longo da vida do animal, atestado pelo acentuado e uniforme grau de desgaste no esmalte dos dentes pós-caninos (KIELAN-JAWOROWSKA; CIFELLI; LUO, 2004; KEMP, 2005; MARTINELLI; BONAPARTE, 2011; ABDALA; JASINOSKI; FERNANDEZ, 2013). Em *B. quadrangularis*, por exemplo, o mecanismo de substituição é alternado, sendo comparável a aquele encontrado no mamaliaforme *Sinoconodon rigneyi* (MARTINELLI; BONAPARTE, 2011; MARTINELLI et al., 2017c). Já a condição típica mamaliana, observada em *M. oehleri*, é representada por uma substituição dentária difiodonte (dentição decídua e permanente), um padrão de oclusão preciso, e por um crescimento determinado (CROMPTON, 1974; LUCKETT, 1993; KIELAN-JAWOROWSKA; CIFELLI; LUO, 2004; LUO et al., 2015; O'MEARA; DIRKS; MARTINELLI, 2018).

Um dos aspectos cruciais da evolução dentária dos cinodontes é a subdivisão da raiz dos dentes pós-caninos. Grande parte dos táxons de cinodontes mais basais apresentam apenas uma raiz para os pós-caninos, contrastando com o padrão de raízes bifurcadas presente nos mamaliaformes (SULEJ et al., 2018). Entretanto, em alguns cinodontes derivados, tais como, o prozostrodonte *B. quadrangularis* e em triteledontídeos, observa-se uma tendência à bifurcação das raízes pós-caninas. Esses dentes são incipientemente divididos e apresentam um sulco

longitudinal (lingual e/ou labial) que forma uma constrição, o que caracteriza a condição prévia para uma raiz dupla presente nos mamaliaformes (BONAPARTE; BARBERENA, 1975, 2001; BONAPARTE; FERIGOLO; RIBEIRO, 2001; BONAPARTE et al., 2003; BONAPARTE; MARTINELLI; SCHULTZ, 2005; BONAPARTE; SOARES; MARTINELLI, 2012; SOARES; MARTINELLI; OLIVEIRA, 2014). A bifurcação das raízes pós-caninas é uma importante novidade evolutiva, uma vez que dentes com raízes duplas são mais resistentes às tensões exercidas durante a mordida (SULEJ et al., 2020).

Por fim, uma última mudança desenvolvida em Cynodontia é comentada, esta refere-se à aquisição de uma articulação crânio-mandibular formada por um côndilo globoso do dentário que se encaixa na cavidade glenoide do esquamosal (CROMPTON; HYLANDER, 1986) (Figura 6). O desenvolvimento dessa articulação permitiu uma maior movimentação dentária, bem como proporcionou a liberação dos ossos pós-dentários, viabilizando a incorporação destes no ouvido médio, o que acarretou, por fim, melhorias significativas na audição (ALLIN, 1986; ALLIN; HOPSON, 1992; LUO, 2011; LUO; MANLEY, 2020).

Em cinodontes basais, a articulação entre crânio e mandíbula segue o padrão ancestral da grande maioria dos tetrápodes. Além do dentário, os ossos pós-dentários são robustos e ocupam um espaço considerável na mandíbula. Nessas formas mais basais, como, por exemplo em *T. liorhinus*, a articulação entre crânio e mandíbula se dá através de um dos ossos pós-dentários, o articular, e pelo osso quadrado do crânio (CROMPTON, 1972; ALLIN, 1975; ALLIN; HOPSON, 1992; HOPSON, KITCHING, 2001; KEMP, 2005) (Figura 6). Tal articulação quadrado-articular é comumente observada em saurópsidos e nos demais sinápsidos (LUO, 2011).

Alguns cinodontes triássicos, como *P. jenseni*, adquirem uma segunda articulação mandibular acessória, formada pelos ossos surangular, da mandíbula, e esquamosal, do crânio. Essa articulação passa a coexistir com a articulação quadrado-articular (CROMPTON, 1972; CROMPTON; LUO, 1993; KEMP, 2007). Nos probainognátios mais derivados, os ossos pós-dentários são extremamente reduzidos, alojando-se em um estreito sulco pós-dentário, enquanto no dentário desenvolve-se um processo articular alongado, quase atingindo o esquamosal (ALLIN; HOPSON, 1992; LUO, 2011) (Figura 6).

Em triteledontídeos e em *B. quadrangularis* (CROMPTON; LUO, 1993; BONAPARTE et al., 2003; BONAPARTE; MARTINELLI; SCHULTZ, 2005; SIDOR, HANCOX, 2006;

BONAPARTE; SOARES; MARTINELLI, 2012), a articulação quadrado-articular ainda é presente, mas, adicionalmente, o dentário passa a fazer contato com o osso esquamosal do crânio (LUO, 1994; SOARES; SCHULTZ; HORN, 2011). Por outro lado, na articulação dentário-esquamosal, reconhecida como o padrão mamaliano, a extremidade posterior do dentário forma um côndilo, que se encaixa na cavidade glenoide do osso esquamosal (CROMPTON; HYLANDER, 1986; CROMPTON; LUO, 1993; LUO, 1994).

Essas importantes mudanças relacionadas a articulação dentário-esquamosal possibilitaram transformações cruciais para alguns ossos componentes do crânio (quadrado) e da mandíbula (articular), conhecidos mais tarde como martelo e bigorna, respectivamente. Estes ossos, formam, juntamente com o estribo, os três ossículos do ouvido médio dos mamaliaformes. Por fim, esses ossículos possibilitaram mudanças imprescindíveis para o aparelho auditivo, as quais foram mantidas desde então pelos mamíferos (KERMACK et al., 1973; ALLIN, 1975; ALLIN; HOPSON, 1992; LUO, 2011; LUO; MANLEY, 2020) (Figura 6).

Figura 6 – Desenvolvimento da articulação crânio-mandibular em Cynodontia
Abreviações: **D**, dentário; **D-SQ**, articulação dentário-esquamosal; **Q-A**, articulação quadrado-articular, **SQ**, esquamosal.

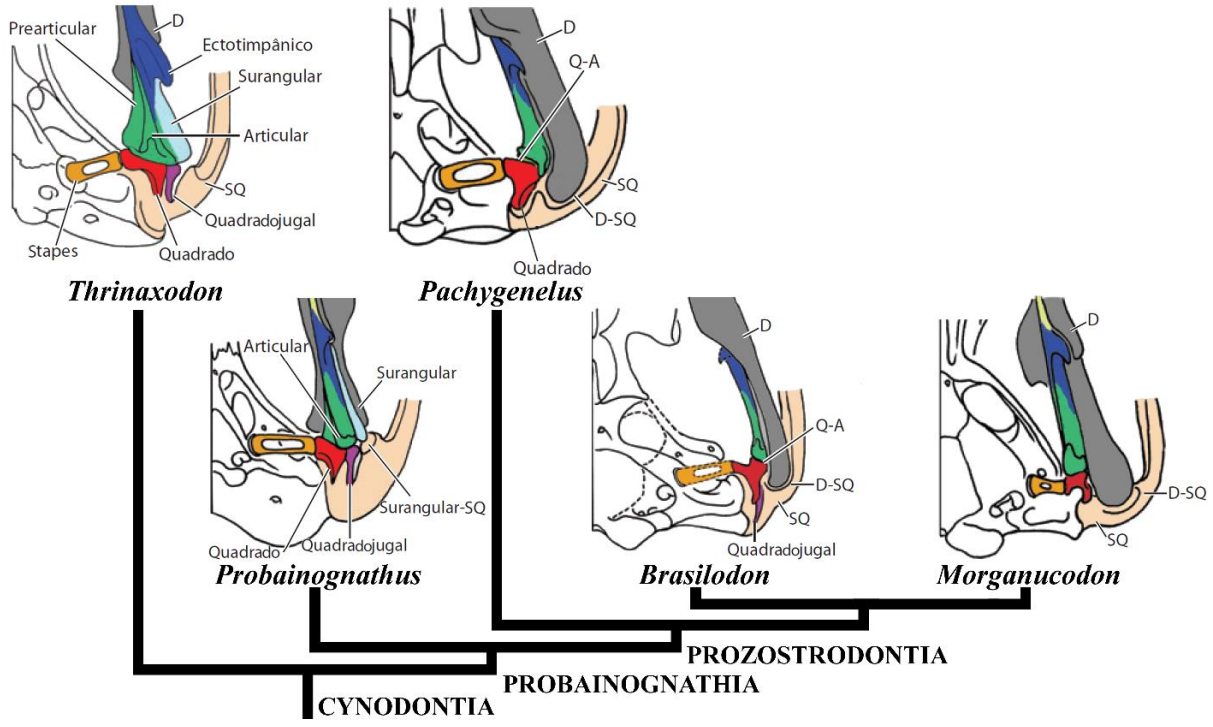

Fonte: (Modificada, LUO, 2011).

1.2 OBJETIVOS

1.2.1 Objetivo geral

- Estudar a anatomia craniana, mandibular e dentária de novos espécimes de cinodontes probainognátios não-mamaliaformes do Triássico Superior do Rio Grande do Sul e analisar, quando possível, suas afinidades e implicações filogenéticas.

1.2.2 Objetivos específicos

- Realizar identificação taxonômica e descrever a anatomia mandibular e dentária dos espécimes CAPPA/UFSM 0208 e CAPPA/UFSM 0262 (Artigo 1);
- Realizar identificação taxonômica e descrever a anatomia craniana, mandibular e dentária do espécime CAPPA/UFSM 0210, bem como analisar suas implicações filogenéticas e evolutivas (Artigo 2).

ARTIGOS CIENTÍFICOS

2 ARTIGOS CIENTÍFICOS

2.1 ARTIGO 1

O Artigo 1, intitulado: **“A new prozostrodontian cynodont (Eucynodontia, Probainognathia) from the Upper Triassic of Southern Brazil”**, foi publicado no periódico *Journal of Vertebrate Paleontology*, DOI: 10.1080/02724634.2020.1782415.

Journal of Vertebrate Paleontology e1782415 (12 pages)

DOI: 10.1080/02724634.2020.1782415

ARTICLE

A NEW PROZOSTRODONTIAN CYNODONT (EUCYNODONTIA, PROBAINOGNATHIA) FROM THE UPPER TRIASSIC OF SOUTHERN BRAZIL

MICHELI STEFANELLO, *[1,2] LEONARDO KERBER, *[1,2] AGUSTIN G. MARTINELLI, [3] and SÉRGIO DIAS-DA-SILVA [1]

[1]Programa de Pós-Graduação em Biodiversidade Animal, Universidade Federal de Santa Maria, 97105-120, Santa Maria, Rio Grande do Sul, Brazil, michelistefanello@hotmail.com; paleosp@gmail.com;

[2]Centro de Apoio à Pesquisa Paleontológica da Quarta Colônia, Universidade Federal de Santa Maria, Rua Maximiliano Vizzotto, 598, 97230-000, São João do Polêsine, Rio Grande do Sul, Brazil, leonardokerber@gmail.com;

[3]CONICET-Museo Argentino de Ciencias Naturales 'Bernardino Rivadavia,' Av. Ángel Gallardo, 470, C1405 DJR, Buenos Aires, Argentina, agustin_martinelli@yahoo.com.ar

ABSTRACT—Probainognathian cynodonts are well represented in the fossil record from the Middle and Upper Triassic of South America, especially in Brazil and Argentina. In this contribution, we describe a new genus and species of non-mammaliaform prozostrodontian cynodont from southern Brazil. The new taxon comes from the Niemeyer Site, a locality in which the traversodontid cynodont *Siriusgnathus niemeyerorum* is numerically dominant, whereas probainognathians and other tetrapods are comparatively scarce. The fauna from the Niemeyer Site was putatively assigned to the *Riograndia* Assemblage Zone (Norian age) recently, although none of the index fossils for that biozone (e.g., *Riograndia*, *Clevosaurus*, *Jachaleria*) have so far been discovered at this locality. The new cynodont taxon is based on a left lower jaw with the canine and six (pc2–pc7) well-preserved postcanines (CAPPA/UFSM 0262, holotype), and a second referred specimen (CAPPA/UFSM 0208, paratype), which includes a right lower jaw with incisors, canine, and seven (pc1–pc7) postcanines, with pc6–pc7 being the best preserved. These specimens have a robust dentary, a long and dorsoventrally tall Meckelian groove, unserrated canines, and unserrated, sectorial postcanine teeth with posteriorly inclined cusps and a poorly developed lingual cingulum. This combination of features is unknown in other Carnian and Norian non-mammaliaform cynodonts. The new taxon contributes to our knowledge of the evolutionary radiation of small prozostrodonts that occurred in western Gondwana during the Late Triassic and led to the emergence of several important cynodont groups, including Mammaliaformes.

http://zoobank.org/urn:lsid:zoobank.org:pub:FDC21881-532B-490A-96A1-A65EA5F62737

Citation for this article: Stefanello, M., L. Kerber, A. G. Martinelli, and S. Dias-Da-Silva. 2020. A new prozostrodontian cynodont (Eucynodontia, Probainognathia) from the Upper Triassic of southern Brazil. Journal of Vertebrate Paleontology. DOI: 10.1080/02724634.2020.1782415.

INTRODUCTION

Probainognathia (sensu Hopson and Kitching, 2001; Liu and Olsen, 2010) is a clade of cynodonts that originated during the early Middle Triassic (Martinelli et al., 2017a) and includes the crown group, Mammalia (Rowe, 1988). The non-mammaliaform probainognathians have a rich fossil record, and are abundant and diverse in the Triassic fauna from Gondwana. The South American record, so far known only from Brazil and Argentina, consists of about 20 species from Middle and Upper Triassic strata (Abdala and Ribeiro, 2010; Martinelli and Soares, 2016; Botha-Brink et al., 2018), most of them based upon relatively well-preserved specimens (Bonaparte, 1966, 1971; Martínez and Forster, 1996; Martínez et al., 1996, 2013; Bonaparte and Barberena, 2001; Bonaparte et al., 2001, 2003, 2005, 2006, 2010; Abdala and Giannini, 2002; Abdala and Ribeiro, 2010; Martinelli et al., 2005, 2016, 2017a, 2017b; Martinelli and Rougier, 2007; Oliveira et al., 2010, 2011a, 2011b; Soares et al., 2011a, 2011b, 2014; Wallace et al., 2019).

The taxonomic diversity and morphological disparity of Middle–Late Triassic South American probainognathian cynodonts are remarkable, and they form the primary basis for understanding the evolutionary transformations underlying the origin of the Mammaliaformes (e.g., Bonaparte et al., 2005; Martinelli et al., 2016). In Brazil, fossiliferous continental Triassic outcrops are restricted to the State of Rio Grande do Sul, which has yielded a diverse fauna of probainognathian cynodonts from the Santa Maria Supersequence (Zerfass et al., 2003; Langer et al., 2007, 2018; Abdala and Ribeiro, 2010; Horn et al., 2014; Martinelli and Soares, 2016). At the base of the supersequence, the Pinheiros-Chiniquá Sequence (*Dinodontosaurus* Assemblage Zone [AZ], late Ladinian/early Carnian) records the probainognathians *Chiniquodon theotonicus* von Huene, 1936, *Protheriodon estudianti* Bonaparte et al., 2006, *Candelariodon barberenai* Oliveira et al., 2011a, *Bonacynodon schultzi* Martinelli et al., 2016, and *Aleodon cromptoni* Martinelli et al., 2017b. Subsequently, the Santa Cruz Sequence (*Santacruzodon* AZ, early Carnian) includes relatively few probainognathian specimens, represented by the holotype of *Santacruzgnathus abdalai* Martinelli et al., 2016 and a few specimens referred to *Chiniquodon* sp. (Abdala et al., 2001). In the overlying Candelária Sequence, two AZs are recognized: (1) the *Hyperodapedon* AZ (late Carnian) includes the probainognathians *Therioherpeton cargnini*

*Corresponding authors.

Color versions of one or more of the figures in the article can be found online at www.tandfonline.com/ujvp.

Bonaparte and Barberena, 1975, *Prozostrodon brasiliensis* (Barberena et al., 1987), *Charruodon tetracuspidatus* Abdala and Ribeiro, 2000, *Trucidocynodon riograndensis* Oliveira et al., 2010, and *Alemoatherium huebneri* Martinelli et al., 2017a; (2) in the upper section of the sequence, the *Riograndia* AZ (Norian) includes the prozostrodonts *Riograndia guaibensis* Bonaparte et al., 2001, *Brasilodon quadrangularis* Bonaparte et al., 2003, *Brasilitherium riograndensis* Bonaparte et al., 2003, *Irajatherium hernandezi* Martinelli et al., 2005, *Minicynodon maieri* Bonaparte et al., 2010, and *Botucaraitherium belarminoi* Soares et al., 2014. However, this diversity is possibly overestimated, as it has been proposed that *Brasilodon*, *Brasilitherium*, and *Minicynodon* are synonymous, with the first taxon representing the valid name (Liu and Olsen, 2010; Martinelli, 2017; Martinelli et al., 2017c; Botha-Brink et al., 2018).

The Niemeyer Site is remarkable amongst southern Brazilian Upper Triassic localities because of the large number of fossils discovered so far. Although abundant, the fossil content is not diverse, with the numerically dominant taxon being the traversodontid cynodont *Siriusgnathus niemeyerorum* Pavanatto et al., 2018. The few fossils known from other taxa include fragmentary remains of indeterminate archosauromorphs and a few specimens of probainognathian cynodonts (Pavanatto et al., 2018). Recently, this fossiliferous site was tentatively assigned to the *Riograndia* AZ (Norian age; Langer et al., 2018), following the discovery of *Siriusgnathus* in other outcrops believed to represent this AZ (see Marsola et al., 2018; Miron et al., 2020). However, it is important to note that no absolute ages are currently available for this site, and no index fossils of the typical *Riograndia* AZ (e.g., the cynodont *Riograndia*, rhynchocephalian *Clevosaurus*, or dicynodont *Jachaleria*; Bonaparte et al., 2010; Soares et al., 2011b) have been recovered there. Additional investigation of the Niemeyer Site is needed to help resolve its precise age and to better understand the diversity of tetrapods represented there. In this contribution, we describe a new genus and species of probainognathian cynodont from this locality, improving our understanding of the diversification of this clade during the Late Triassic.

Institutional Abbreviations—**CAPPA/UFSM**, Centro de Apoio à Pesquisa Paleontológica da Quarta Colônia da Universidade Federal de Santa Maria, São João do Polêsine, Brazil; **MMACR-PV-T**, Museu Municipal Aristides Carlos Rodrigues (Paleovertebrates-Triassic Collection), Candelária, Brazil; **UFRGS PV-T**, Universidade Federal do Rio Grande do Sul, Paleontologia de Vertebrados, Porto Alegre, Brazil.

MATERIALS AND METHODS

The specimens are housed at CAPPA/UFSM, cataloged as CAPPA/UFSM 0262 and CAPPA/UFSM 0208. They were collected in sector 4 of the Niemeyer Site, in the municipality of Agudo, State of Rio Grande do Sul, Brazil (Pavanatto et al., 2018) (Fig. 1). The horizon of this locality is included in the Candelária Sequence (Santa Maria Supersequence; Zerfass et al., 2003; Horn et al., 2014) and tentatively referred to the *Riograndia* AZ (Miron et al., 2020), which has been dated as Norian in age (Langer et al., 2018). More details on geology, geochronology, and biostratigraphy regarding the Niemeyer Site are available in Pavanatto et al. (2018) and Miron et al. (2020).

CAPPA/UFSM 0262 comprises a left lower jaw with canine and six preserved postcanine teeth, and CAPPA/UFSM 0208 is a right lower jaw with incisors, canine, and seven postcanine teeth. Due to taphonomic processes and weathering, the postcanine dentition in CAPPA/UFSM 0208 is somewhat damaged. On the other hand, CAPPA/UFSM 0262 is better preserved, and their postcanines are almost complete.

CAPPA/UFSM 0262 and CAPPA/UFSM 0208 were scanned using a micro-CT Skyscan 1173 at the Laboratório de Sedimentologia e Petrologia (LASEPE), Pontifícia Universidade Católica do Rio Grande do Sul (PUCRS), Porto Alegre, Brazil. The analysis (parameters: voltage 85 kV; amperage 65 μa; pixel size 15,166 μm) generated a total of 3,443 slices for CAPPA/UFSM 0262, and 3,696 slices (parameters: voltage 80 kV; amperage 100 μa; pixel size 14,108 μm) for CAPPA/UFSM 0208. The tomograms were imported into Mimics Medical 21.0 for virtual reconstruction and virtual segmentation of structures. From this, it was possible to virtually remove the sedimentary matrix that covered part of the specimens and access data on its morphology. After these procedures, the resulting files (in .stl format) were imported to Design Spark Mechanical 2.0 and colored to improve visibility. The CT slices and 3D models are available at MorphoMuseuM (https://doi.org/10.18563/journal.m3/120).

SYSTEMATIC PALEONTOLOGY

THERAPSIDA Broom, 1905
CYNODONTIA Owen, 1861
EUCYNODONTIA Kemp, 1982
PROBAINOGNATHIA Hopson, 1990
PROZOSTRODONTIA Liu and Olsen, 2010
AGUDOTHERIUM GASSENAE, gen. et sp. nov.
(Figs. 2–4)

Holotype—CAPPA/UFSM 0262, a left lower jaw with canine and tooth positions for seven postcanines (alveolus of pc1 plus six functional postcanines [pc2–pc7] exposed) (Figs. 2A, B, 3, 4).

Paratype—CAPPA/UFSM 0208, a right lower jaw with two poorly preserved incisors, canine, and tooth positions for seven postcanines (functional pc1–pc7 exposed) (Figs. 2C, D, 4). Dental elements pc6 and pc7 are the best preserved.

Etymology—'Agudo,' in reference to the municipality of Agudo (state of Rio Grande do Sul, Brazil) where the specimens were found. The suffix 'therium' (from the Greek '*thērion*') means 'beast,' and is often used for mammals and closely related forms. The specific epithet honors Mrs. Valserina Maria Bulegon Gassen, former mayor of the city of São João do Polesine (State of Rio Grande do Sul, Brazil), for her valuable contribution in the creation of CAPPA/UFSM.

Locality and Horizon—Both specimens referred to *Agudotherium gassenae* were collected at the Niemeyer Site, municipality of Agudo, State of Rio Grande do Sul, Brazil. Candelária Sequence, Santa Maria Supersequence (Horn et al., 2014).

Diagnosis—*Agudotherium gassenae*, gen. et sp. nov., is a small probainognathian cynodont diagnosed by a unique suite of features not present in any other known prozostrodontian cynodonts: horizontal ramus of the dentary dorsoventrally deep (relative to most Late Triassic prozostrodonts) with rectilinear ventral margin; rectilinear, long, and dorsoventrally tall Meckelian groove, positioned at mid-height on the medial surface of the dentary; alveolar platform of incisors and canines positioned slightly dorsal to postcanine alveolar level; absence of serrations on mesial/distal edges of canine; smooth mesial and distal edges of individual cusps in postcanines; sectorial postcanines that increase in size and number of cusps posteriorly; posterior postcanines (pc6–pc7) with cusps a, c, and d posteriorly inclined (albeit to a lesser degree than in *Chiniquodon*), with the mesial edge of each cusp convex and the distal one almost straight; sectorial crown in posterior postcanines with main cusp 'a,' followed by two distal cusps ('c' and 'd') decreasing in size distally, and a mesial small cusp ('b'); relation of height in the cusps of pc6–pc7: a > c > b > d; postcanines with poorly developed lingual cingulum or cusps, which when present are located on the mesio- and distolingual edges of the crown.

Remarks—CAPPA/UFSM 0208 and CAPPA/UFSM 0262 were found at the same spot in the outcrop, in sector 4 (Niemeyer Site; Pavanatto et al., 2018), and represent right and left

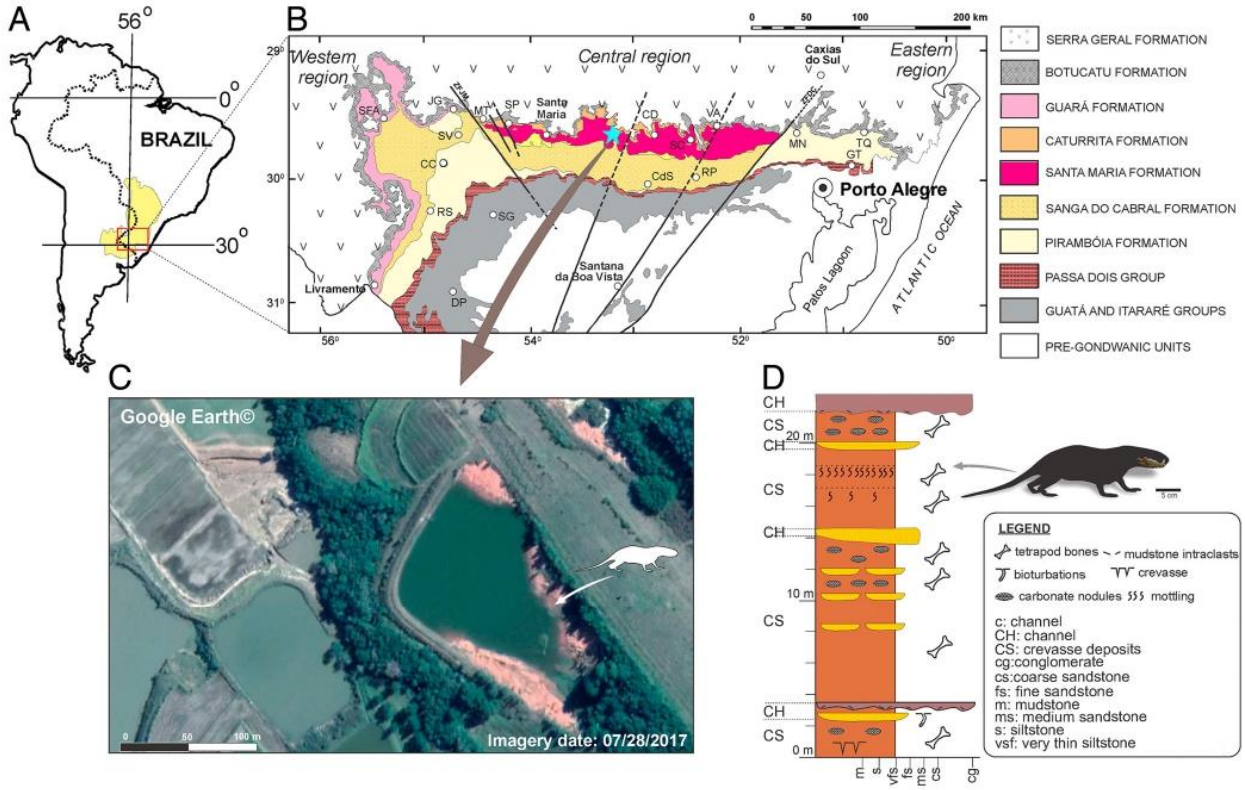

FIGURE 1. Location and geological context of the Niemeyer Site (Agudo, Rio Grande do Sul, Brazil). **A**, location map of the Paraná Basin in South America; **B**, sedimentary units in Southern Brazil (modified from Da-Rosa and Faccini, 2005); star indicates the Niemeyer Site; **C**, satellite image showing the location of the Niemeyer Site (©Google Earth); **D**, columnar geological profile of the Niemeyer Site. CAPPA/UFSM 0262 and CAPPA/UFSM 0208 were collected in sector 4 (**C**). Modified from Pavanatto et al. (2018).

hemimandibles of equivalent size. However, the first specimen was collected in 2017 and the second one in 2019. Thus, although they were found in the same location, have the same size and features, and represent counterparts of one another, we opt to treat them as distinct specimens in the absence of direct association demonstrating that they represent a single individual.

DESCRIPTION

Lower Jaw

CAPPA/UFSM 0262 (holotype) is an almost complete left lower jaw, measuring 50 mm in total preserved length (Figs. 2A, B, 4A, B). It is represented by the dentary, which preserves the symphysis, the horizontal ramus of the dentary with the Meckelian groove, part of the coronoid process, most of the postdentary trough, and part of its posterodorsal articular process. CAPPA/UFSM 0208 (paratype) is a right lower jaw, 51 mm in total preserved length, represented by most of the dentary plus small fragments of the postdentary bones (Figs. 2C, D, 4D, E).

The horizontal ramus of the dentary is dorsoventrally tall and has a straight ventral margin (Figs. 2, 4). In the holotype, the medial face of the dentary is covered by a hard layer of sedimentary matrix below the alveolar margin (Fig. 2A). The micro-CT scan indicates the presence of a rod of postdentary bones (possibly part of the articular plus prearticular complex) and it is possible to observe part of the Meckelian groove (Fig. 4B). In lateral view, at the highest portion of the dentary of the paratype specimen, a hard layer of sedimentary matrix covers both the coronoid process and postcanine teeth (Fig. 2D).

The symphysial region is anterodorsally projected, and its medial articular area has a relatively large, rough surface (Fig. 2A, C). The symphysial area is oval and inclined in an anterodorsal direction, with its posteroventral margin located around the level of pc1. The rugose symphysial surface likely indicates that it was not fused with its counterpart. The symphysis ascends anteriorly, angled upwards. This region is transversally broad, due to the large canine alveolus and root. The anterior portion of the symphysial region is slightly damaged in CAPPA/UFSM 0208 as well as in CAPPA/UFSM 0262, in which the place for the incisors is partially lost. The angle formed between the axes of the mandibular symphysis and the horizontal ramus of the dentary is ca. 132°.

Laterally, the horizontal ramus of the dentary is anteroposteriorly long and dorsoventrally tall (Fig. 2B, D). From the anterior to the posterior region, the dentary ramus increases in height. There is a large mental foramen laterally at the level of pc1–pc2 (Fig. 2B, D). In the paratype specimen, there are also small, randomly distributed vascular foramina below and anterior to the canine (Fig. 2D). The masseteric fossa extends across the horizontal ramus of the dentary towards the level of the last three postcanines (Fig. 2B, D).

The coronoid process of both specimens is broken near its base, lacking most of its body. It starts laterally to the posterior half of the last postcanine (pc7) and elevates abruptly posterodorsally (Fig. 2A–C). At this point, the base of the coronoid process is transversely broad and tapers dorsally. A rugose medial area at

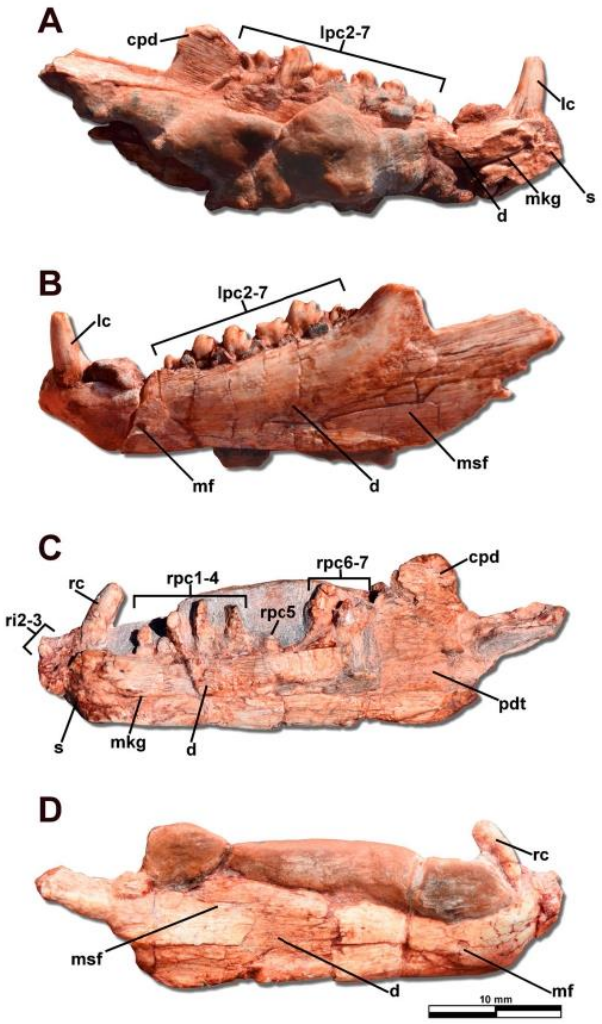

FIGURE 2. *Agudotherium gassenae*, gen. et sp. nov., CAPPA/UFSM 0262, holotype, left lower jaw in **A**, medial and **B**, lateral views. CAPPA/UFSM 0208, paratype, right lower jaw in **C**, medial and **D**, lateral views. **Abbreviations**: **cpd**, coronoid process of the dentary; **d**, dentary; **lc**, left canine; **lpc**, left postcanine; **mf**, mental foramen; **mkg**, Meckelian groove; **msf**, masseteric fossa; **pdt**, postdentary trough; **rc**, right canine; **ri**, right incisor; **rpc**, right postcanine; **s**, symphysis.

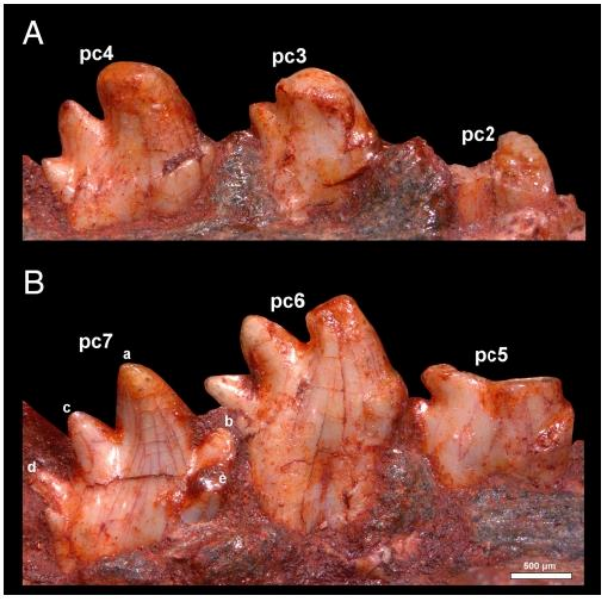

FIGURE 3. *Agudotherium gassenae* gen. et sp. nov., CAPPA/UFSM 0262, holotype, postcanine teeth in lingual view. **A**, anterior (pc2–pc4) and **B**, posterior postcanine dentition (pc5–pc7). In **B**, detail of the height relationship among all cusps of pc7 (a > c > b > d > e).

the base of this process likely indicates the attachment surface for the coronoid bone in CAPPA/UFSM 0208 (Fig. 2C). An angular process, like that reported for traversodontids (e.g., *Exaeretodon riograndensis* and *Siriusgnathus niemeyerorum*; Abdala et al., 2002; Pavanatto et al., 2018), is not evident. Posteriorly, the dentary exhibits subtle transverse widening, with a rounded posteroventral corner (Fig. 2B, D).

In medial view, the alveolar margin is straight, bearing a thin groove for the dental lamina. *Agudotherium gassenae* exhibits a conspicuous Meckelian groove running parallel to the ventral edge of the dentary (Fig. 2C). This groove is tall and deep, and is positioned at roughly the dorsoventral mid-height of the dentary. It extends anteriorly up to the symphysis and posteriorly emerges into the postdentary trough (Figs. 2C, 4B, E). The three-dimensional CT reconstructions highlight fragments of the postdentary bones in the posterior portion of the dentary of the holotype (Fig. 4B). The main fragment is large and long, placed over the postdentary trough, and likely corresponds to the articular plus prearticular complex. In addition, there is a laminar bone positioned over the posterior section of the Meckelian groove, separated from the main rod of postdentary bones, which can be interpreted as a fragment of the splenial (Fig. 4B).

Dentition of CAPPA/UFSM 0262

Incisors—The incisors were not preserved (Figs. 2A, B, 4A, B) because the anterior portion of the dentary is missing. However, the micro-CT revealed two incisor alveoli near to the canine, which can be interpreted as i2? and i3? (Fig. 4A, B). The position of the most distal alveolus indicates the lack of a diastema between incisors and canine.

Canine—The canine is missing only its apex (Figs. 2A, B, 4A, B). It is subcircular in cross-section at its base, slightly curved distally, with a mesially convex and distally (slightly) concave edge. Serrations on its mesial and distal edges are absent. The micro-CT data indicates that there is a short diastema between the canine and the alveolus of pc1, which has no preserved crown and root and its alveolus may have been in process of resorption (Fig. 4A, B).

Postcanines—CAPPA/UFSM 0262 preserves six postcanine (pc) teeth (Figs. 2A, B, 4A–C): pc2 to pc7. There is sedimentary matrix covering the space between the canine and pc2. However, the micro-CT revealed the presence of the alveolus for pc1 (Fig. 4A, B). The anterior postcanines (pc2–pc5) have partially preserved crowns, usually missing part of the main cusp, whereas the posterior postcanines (pc6–pc7) preserve almost complete crowns (Fig. 3A, B), the bases of which are slightly more bulbous those in the anterior postcanines. Postcanines 5–7 are partially imbricated, with the distal-most portion of the anterior tooth located labial to the mesial portion of the successive tooth (Fig. 3B).

The cusps of the postcanines are not serrated. The cusp pattern of pc2 to pc7 is variable, but generally, cusps are oriented in a

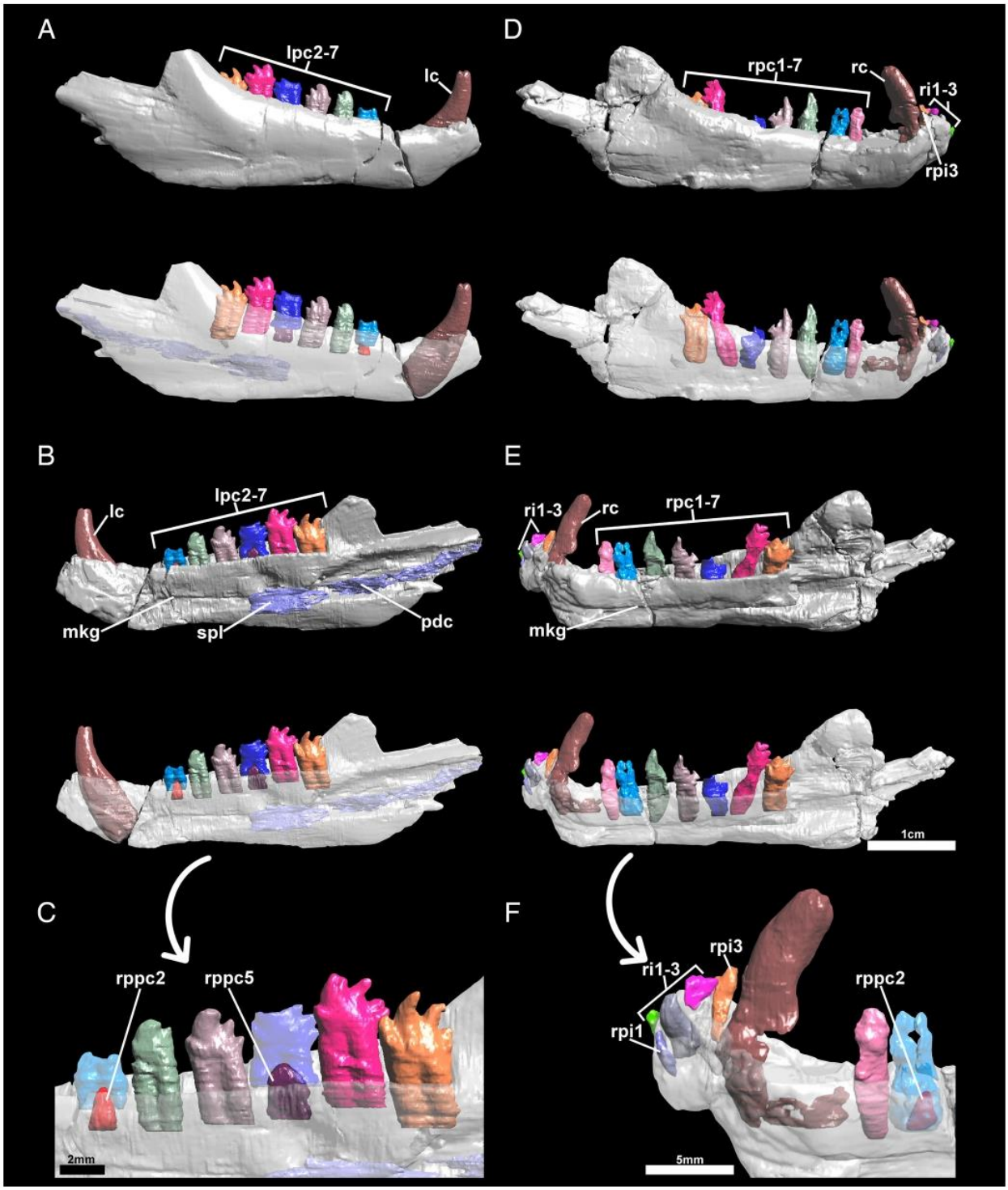

FIGURE 4. *Agudotherium gassenae*, gen. et sp. nov., three-dimensional reconstructions of the lower jaw and teeth. **A**–**C**, CAPPA/UFSM 0262, holotype, left lower jaw (reversed); **D**–**F**, CAPPA/UFSM 0208, paratype, right lower jaw. **A** and **D** in lateral view and **B**, **C**, **E**, and **F**, in medial view. Detail for the replacement incisors and postcanines in **C** and **F**. In **A**, **B**, **D**, and **E**, lower jaw with and without transparency; **C**, **F**, lower jaw and functional postcanine teeth (lpc2, lpc5, and rpc2) with transparency. **Abbreviations**: **lc**, left canine; **lpc**, left postcanine; **mkg**, Meckelian groove; **pdc**, postdentary bone complex; **rc**, right canine; **ri**, right incisor; **rpc**, right postcanine; **rpi**, replacement incisor; **rppc**, replacement postcanine; **slp**, splenial.

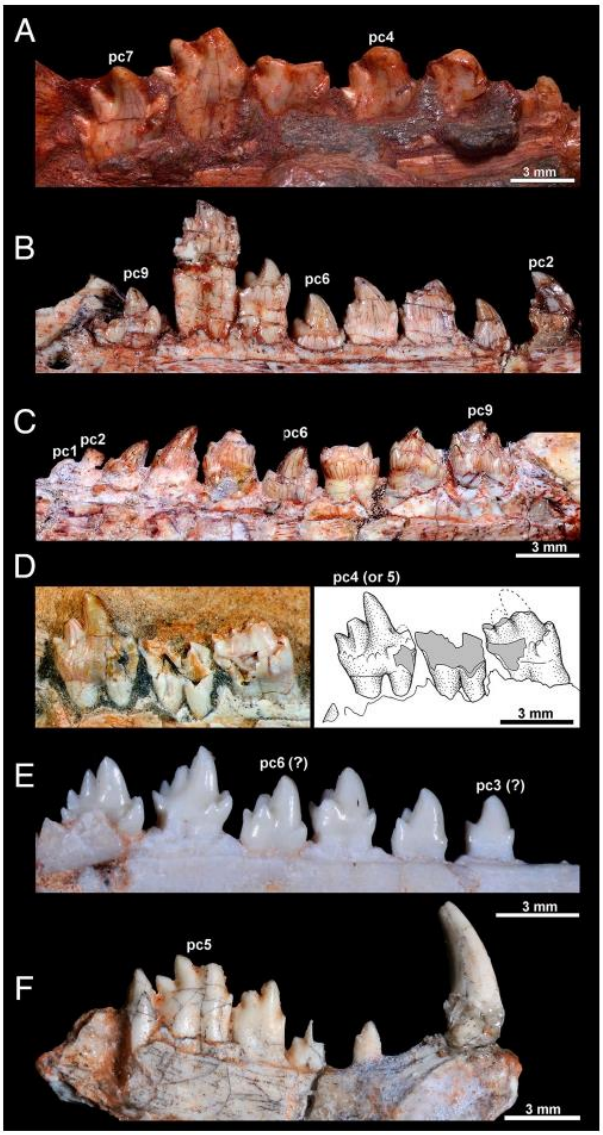

FIGURE 5. *Agudotherium gassenae* gen. et sp. nov., dentition compared with that of select probainognathians, all in lingual view. **A**, *Agudotherium gassenae*, CAPPA/UFSM 0262, holotype, left postcanine row. **B**, **C**, *Prozostrodon brasiliensis*, UFRGS-PV-248-T, holotype, **B**, left and **C**, right postcanine rows. **D**, *Botucaraitherium belarminoi*, MMACR-PV-003-T, holotype, detail by the last left postcanines; modified from Soares et al. (2014). **E**, *Brasilodon quadrangularis*, UFRGS-PV-0603-T, left postcanine row. **F**, *Irajatherium hernandezi*, UFRGS-PV-1029-T, right lower jaw (reversed). **Abbreviation**: **pc**, postcanine tooth.

mesiodistal line (Figs. 3, 5A). The main cusp occupies the mesial half of the crown, followed by distal cusp(s), which are slightly labially displaced. The cusps are slightly recurved distally, especially in the last three teeth (pc5–pc7), and constitute the sectorial portion of the crown. The lingual cingulum is poorly developed (Fig. 3). In pc2–pc4, the lingual cingulum is interrupted at its middle portion. It is developed in the mesiolingual corner of the crown by means of a subtle crest in pc2 and pc3, which in pc4 defines at least two accessory cusps. In the distolingual sector of the crown, the lingual cingulum is faint in pc2–pc3 and in pc4 there are tiny crenulations and a tiny cusp placed just lingual and ventral to cusp d (Fig. 3A). In pc5 to pc7 the crown has a long mesiodistal length, and the lack of continuity of the lingual cingulum is more evident. Nonetheless, pc5 and pc6 have a crest-like structure in the mesiolingual corner, similar to pc4, and pc7 has one discrete accessory cingular cusp in the mesiolingual and another in distolingual portion of the crown (Fig. 3B). The mesiolingual one is larger than the distolingual accessory cusp. It is possible to observe labial wear over the main cusp 'a' of pc3 and pc4, which seem to be functional teeth of an older generation than pc6 and pc7 (pc2 and pc5 have only partially preserved crowns) (Fig. 3).

Postcanines 2–5 are smaller and less complex than pc6–7, increasing in size posteriorly. Postcanines 6 and 7 are larger in length and height than pc2–pc5, indicating an increase in size and complexity in the posterior teeth (Fig. 3). Cusps a, c, and d of these last postcanines are more distally projected (Fig. 3B).

Postcanine 2 is damaged, and less than half of the crown is preserved (Fig. 3A). On the labial and lingual surfaces, the base of the tooth crown is incompletely subdivided, indicating the presence of an incipiently divided root. Postcanine 3 is slightly smaller than pc4, with subtle differences in their morphology. Postcanine 3 preserves two cups, a large main cusp (a) occupying most of the crown, followed by a smaller distal one (c) (Fig. 3A). The main cusp has a large wear facet facing dorsolabially. In this tooth, the lingual cingulum is developed on the mesiolingual side of the crown as a faint crest (Figs. 3A, 4B, C). Postcanine 4 is completely preserved, though the tip of the main cusp is worn (Fig. 3A). There are three cusps: a large main cusp (a) on the mesial half of the crown, followed by cusps c and d, with the relative heights of a > c > d. The distal cusp d is slightly labially displaced, in comparison with the main cusp a. The micro-CT revealed a possible mesial bulge that seems to indicate the presence of a reduced cusp b (Fig. 4C). The lingual cingulum forms a mesiolingual crest with at least two discrete accessory cusps, and at the distolingual side there are some crenulations and a discrete tiny accessory cusp near the base of cusp d.

Postcanine 5 is damaged and the apical half of its crown is missing (Fig. 3B). The main cusp (a) is almost entirely lost, retaining only its base. The cusp c is partially preserved and cusp d is complete (Figs. 3B, 4B, C). As in pc4, there is a mesial bulge that seems to indicate the presence of a reduced cusp b (Figs. 3B, 4B, C). A mesiodistal cingulum is evident, forming a crest-like structure (Fig. 3B). There are also very small distolingual accessory cusps observed in the micro-CT data (Fig. 4B, C).

The well-preserved pc6 and pc7 are sectorial, have large crowns, and display similar morphology (Fig. 3B). The main cusp (a) is followed by distal cusps (c and d) and a mesial cusp (b). The four larger cusps are oriented in mesiodistal line along the labial margin of the crown. Cusps a, c, and d are posteriorly inclined (Figs. 3B, 4C). In both teeth, the main cusp is asymmetrical and distally convex, with the mesial edge longer and more convex than the distal one. In pc6, the main cusp a has a distal edge shorter than the mesial one and its tip is missing (Fig. 3B). The distal cusps c and d are slightly labially displaced, in comparison with cusps a and b. In occlusal view, cusp b appears slightly more lingual than cusps a, c, and d. The height relationship among all cusps of pc6 is a ≥ c > b > d. The lingual cingulum is incomplete and poorly preserved, being more developed in the distolingual region of the crown (Fig. 3B).

Postcanine 7 is the best-preserved tooth, with four large cusps, and two smaller accessory cusps, mesio- and distolingually positioned (Fig. 3B). The main cusp a occupies the mesial half of the crown, followed by two cusps (c and d) that decrease in size posteriorly, positioned distally to it. The cusp d is positioned more distolabially. The mesial edge of cusp a descends to a small cusp b, positioned in the mesiolingual portion of the crown (Fig. 3B). The main cusp a is asymmetrical, with the

mesial edge longer and more convex than the distal one. This cusp is inclined distally and lingually. Cusps c and d display symmetrical mesial and distal edges. Cusps b and d are less developed than a and c, though cusp b is taller than cusp d. Cusp b is slightly lingually dislocated and seems to be asymmetrical, as in cusp a. Lingual to cusp b, there is evidence of one small mesiolingual accessory cusp, which is interpreted as cusp e (Fig. 3B) of the lingual cingulum. This accessory cusp is almost as large as cusp b. There is also a tiny cingular cusp below the base of cusp d. The height relationship among all cusps of pc7 is a > c > b > d > e.

The three-dimensional reconstructions show the presence of two replacement postcanines in CAPPA/UFSM 0262, which are placed below the functional pc2 and pc5 (Fig. 4B, C). The replacement pc2 is smaller than the replacement pc5 (Fig. 4C).

Dentition of CAPPA/UFSM 0208

Incisors—Three functional incisors (i1–i3) are present, but only part of i2 and i3 are externally visible (Figs. 2C, 4D–F). The i1 is positioned mesially to the crown of the functional i2, and is covered by sedimentary matrix. The partially preserved i2 is larger than the i3, which only preserves the crown base (Fig. 2C). They are anterodorsally inclined and located near the canine, no incisor–canine diastema is present. The digital renderings show two replacement incisors near to the functional teeth i1 and i3 (Fig. 4F).

Canine—The canine is missing its tip (Figs. 2C, D, 4D–F). Its features resemble those of the holotype.

Postcanines—The postcanine (pc) series of CAPPA/UFSM 0208 includes seven functional teeth (Figs. 2C, 4D, E). Unfortunately, pc1–pc5 are poorly preserved, hampering recognition of their cusps. Postcanine 5 preserves only part of the crown base. Postcanines 6 and 7 are better preserved than the other postcanines. As in CAPPA/UFSM 0262, those teeth are larger and broader than the previous postcanines (Fig. 4E) and there are no wear facets on their crowns.

Postcanines 6 and 7 exhibit the same morphology of the last postcanines (pc6–pc7) of the holotype (Fig. 4E). Postcanine 6 is displaced from the alveolus, partially exposing the roots (Fig. 4E). It is inclined distally. The main cusp a is broken in the tip, but this broken portion is distally displaced. Both cusps c and d are preserved. These cusps are positioned distally to main cusp a, and mesiolabial to the crown of pc7, indicating that pc6 is partially imbricated with pc7 (Fig. 4E). The cusp b is broken off.

Postcanine 7 is the best-preserved tooth (Fig. 4E), but the tip of all four cusps is damaged in some degree. The main cusp a is placed in the mesial half of the crown, followed by cusp c, positioned distally to it. Cusp a is slightly larger than cusp c. Cusp b is positioned in the mesial portion of the crown, whereas cusp d is positioned more distally, and it is comparatively smaller than the other cusps (Fig. 4E). In occlusal view, cusp b appears slightly more lingual than cusps c and d. Cusp a of pc7 is asymmetrical and distally convex, with the mesial edge longer and more convex than the distal one.

In pc7 the cingulum is well developed and not continuous and there are only diminutive mesiolingual cuspules. The root of the postcanine teeth exhibit incomplete subdivisions, presenting an incipient bifurcation with a well-developed longitudinal groove on the lingual surface. This incipient root division is more visible in pc6 and pc7, which display a large exposure of the dental root (Fig. 2C).

Similar to CAPPA/UFSM 0262, the three-dimensional CT reconstructions show the presence of one replacement postcanine, which would probably replace pc2 (Fig. 4F).

DISCUSSION

The new taxon, *Agudotherium gassenae*, gen. et sp. nov., is erected on the basis of two specimens, CAPPA/UFSM 0262 (holotype) and CAPPA/UFSM 0208 (paratype), which might correspond to the same individual. In general, the dentary with a reduced postdentary trough and large posterior articular process, unfused mandibular symphysis, sectorial postcanines with lingual accessory cusps, and roots with incipient division are traits shared with advanced non-mammaliaform probainognathian prozostrodonts (e.g., *Prozostrodon brasiliensis*, *Botucaraitherium belarminoi*, *Alemoatherium huebneri*, and *Brasilodon quadrangularis*; Bonaparte and Barberena, 2001; Bonaparte et al., 2005; Soares et al., 2014; Martinelli et al., 2017a). Furthermore, *Agudotherium* shares small size and reduced tooth replacement with the other prozostrodontian known cynodonts from the Upper Triassic of Brazil and Argentina. The assemblage of small cynodont taxa is extremely diverse, mainly in Triassic rocks from southern Brazil (e.g., Bonaparte et al., 2001, 2003, 2005, 2010; Martinelli et al., 2005, 2016, 2017a; Soares et al., 2011b, 2014), and the new taxon described herein can be added to this radiation.

The horizontal ramus of the dentary of *Agudotherium* is deep throughout its length in relation to postcanine crown height, which differs from the more slender dentary of *Brasilodon*, *Alemoatherium*, and *Santacruzgnathus abdalai* (Bonaparte et al., 2005; Martinelli et al., 2016, 2017a), although the height of the dentary can change during ontogeny, as observed in *Brasilodon* and *Sinoconodon* (Crompton and Luo, 1993; Martinelli, 2017). However, some other Late Triassic probainognathians also have deep dentaries (e.g., *Prozostrodon*, *Probainognathus jenseni*, *Candelariodon barberenai*, *Irajatherium hernandezi*, and *Riograndia guaibensis*; Bonaparte et al., 2001; Bonaparte and Barberena, 2001; Oliveira et al., 2011a; Martinelli et al., 2005, 2017d). The horizontal ramus of *Agudotherium* has its dorsal (alveolar) and its ventral margins diverge posteriorly, producing a triangular dentary in lateral view. This condition is shared with *Chiniquodon theotonicus* (Abdala and Giannini, 2002), *Botucaraitherium* (Soares et al., 2014), and *Pachygenelus monus* (Gow, 1980), but the rectilinear ventral margin of *Agudotherium* is not observed in the latter taxon. In comparison to the only two known specimens of *Prozostrodon* (see Pacheco et al., 2017), the jaws of *Agudotherium* are almost the same length as the smaller *Prozostrodon* specimen (CAPPA/UFSM 0123), but have a deeper dentary ramus (than even the larger specimen UFRGS-PV 248-T). In addition, *Prozostrodon* has more parallel ventral and dorsal borders of the horizontal ramus of the dentary (i.e., overall, it is less triangular) than in *Agudotherium*.

The unfused mandibular symphysis is a typical condition found in many derived probainognathians (e.g., *Prozostrodon*, *Botucaraitherium*, *Alemoatherium*, *Brasilodon*, *Riograndia*, *Irajatherium*, and *Chaliminia musteloides*; Bonaparte and Barberena, 2001; Bonaparte et al., 2001, 2003, 2005, 2012; Martinelli et al., 2005, 2017a; Martinelli and Rougier, 2007; Oliveira et al., 2011b; Soares et al., 2014). This feature is a synapomorphy of Prozostrodontia (Liu and Olsen, 2010), whereas in most non-prozostrodontian cynodonts the dentaries are fused with no evidence of a medial suture (e.g., earlier-diverging probainognathians including *Candelariodon*, chiniquodontids, and ecteniniids; Abdala and Giannini, 2002; Oliveira et al., 2011a; Martínez et al., 2013; Martinelli et al., 2017d). An unfused mandibular symphysis is also reported in basal (non-eucynodonts) cynodonts, such as *Procynosuchus delaharpeae*, *Thrinaxodon liorhinus*, and *Galesaurus planiceps* (Martinelli et al., 2017c).

The Meckelian groove in *Agudotherium* is dorsoventrally tall, anteroposteriorly long and rectilinear, and located at about mid-height on the dentary. This feature is similar to that of

most non-mammaliaform cynodonts (Luo, 1994), with only few possible exceptions such as *Brasilodon* and early mammaliaforms (e.g., *Morganucodon oehleri*), having a reduced and ventrally directed Meckelian groove that converges with the ventral edge of the jaw. Notably, the Meckelian groove of *Agudotherium* is wider and placed in a higher position than in *Prozostrodon* (Bonaparte and Barberena, 2001; Pacheco et al., 2017), *Candelariodon* (Oliveira et al., 2011a; Martinelli et al., 2017d), and *Irajatherium* (Martinelli et al., 2005). The trough for the postdentary bones is relatively reduced, as in most non-mammaliaform prozostrodontians, such as *Botucaraitherium* and *Prozostrodon* (UFRGS-PV 248-T). Both coronoid processes are mostly broken, but their anterior base starts just lateral to the last postcanine (pc7), as in most probainognathians; however, some taxa have an erupting (non-functional) last postcanine that is covered by the coronoid process, as in the smaller specimen of *Prozostrodon* (CAPPA/UFSM 0123) and the holotype of *Botucaraitherium* (MMACR-PV-003-T).

Based on the digital reconstructions, it is possible to observe three functional incisors (i1–i3) in *Agudotherium*, as in adult *Brasilodon* (UFRGS-PV 0628-T; Bonaparte et al., 2003, 2005; Martinelli et al., 2017c), *Riograndia* (Bonaparte et al., 2001; Soares et al., 2011b), *Irajatherium* (Martinelli et al., 2005; Oliveira et al., 2011b), *Chaliminia* (Martinelli and Rougier, 2007), and several other probainognathians (e.g., *Lumkuia fuzzi*, *Probainognathus*). In contrast, in the holotype of *Prozostrodon* (UFRGS-PV 248-T) (Bonaparte and Barberena, 2001), and the referred specimen (CAPPA/UFSM 0123) (see Pacheco et al., 2017) there are four lower incisors.

The new species does not exhibit a diastema between the last incisor and the canine, as in most prozostrodontians (Bonaparte and Barberena, 2001; Martinelli et al., 2005, 2017d; Oliveira et al., 2011b; Soares et al., 2011b, 2014), but differs from the tritheledontid *Chaliminia*, which exhibits an incisor/canine diastema equivalent to the anteroposterior length of one incisor (Martinelli and Rougier, 2007).

The canine is large and posteriorly curved, as in *Prozostrodon*, *Botucaraitherium*, and *Candelariodon* (Bonaparte and Barberena, 2001; Oliveira et al., 2011a; Soares et al., 2014, Martinelli et al., 2017d). Its mesial edge is shorter and more convex than the distal one. Contrarily, in *Alemoatherium* the mesial edge is slightly convex, but the distal one is almost straight (Martinelli et al., 2017a). The canine of *Agudotherium* does not possess serrations on its distal edge, as in *Botucaraitherium* and *Alemoatherium* (Soares et al., 2014; Martinelli et al., 2017a). Interestingly, the holotype of *Prozostrodon* has tiny serrations on the distal edge of the canine. Although badly preserved, and only observed after detailed further preparation of the holotype (UFRGS-PV0248-T), they are definitely present and further aid in distinguishing *Prozostrodon* from *Agudotherium*. The relative size of the canine is also noticeable in *Agudotherium*, similar to most probainognathians but differing from that of tritylodontids, *Chaliminia* and *Riograndia*, which have reduced canines.

A diastema between the canine and the postcanine series is present, as in other non-mammaliaform prozostrodontians (e.g., *Prozostrodon*, *Brasilodon*, *Chaliminia*, *Irajatherium*, *Botucaraitherium*, and *Candelariodon*; Bonaparte and Barberena, 2001; Bonaparte et al., 2003, 2012; Martinelli et al., 2005, 2017d; Martinelli and Rougier, 2007; Oliveira et al., 2011a, 2011b; Soares et al., 2014). This condition differs from that of *Riograndia* and *Alemoatherium*, in which the diastema is greatly reduced or absent (Bonaparte et al., 2001; Soares et al., 2011b; Martinelli et al., 2017a). However, this is a trait that changes considerably during ontogeny. The complete loss of the anterior postcanines and concomitantly the enlargement of the diastema between the canine and the postcanine series is a pattern frequently found in derived cynodonts (e.g., Hopson, 1971; Kemp, 1982; Martinelli and Bonaparte, 2011; Abdala et al., 2013; Soares et al., 2014; Pacheco et al., 2017) and mammaliaforms (e.g., Crompton and Luo, 1993; Luo et al., 2004).

The height of the incisor alveolar platform and the canine base is different from the condition found in most other prozostrodonts. The alveolar line of the incisor and the canine is positioned at a level only slightly above the alveolar level of the postcanine series, similar to *Botucaraitherium* (Soares et al., 2014), whereas that of *Prozostrodon*, *Brasilodon*, and *Irajatherium* is quite elevated in comparison (Bonaparte and Barberena, 2001; Bonaparte et al., 2003, 2005; Martinelli et al., 2005; Oliveira et al., 2011b; Pacheco et al., 2017).

The morphology of the postcanine teeth is triconodont-like, resembling the pattern of some basal cynodonts (e.g., *Thrinaxodon*) and particularly of several probainognathians (e.g., *Prozostrodon*, *Probainognathus*, *Therioherpeton*, *Meurthodon*, *Pachygenelus*), including early mammaliaforms (e.g., *Sinoconodon*). *Agudotherium gassenae* has posterior postcanines with four main cusps (a–d), which are oriented in a mesiodistal line, with cusp b slightly displaced lingually. The cingulum is developed on the mesio- and distolingual corners, and varies from a crest-like structure in anterior postcanines to accessory cusps in the more posterior ones. This pattern is reminiscent of that of *Brasilodon*, as seen in UFRGS-PV-0603-T (see Fig. 5E), but cusps a, c, and d are upright and not curved in *Brasilodon* as they are in *Agudotherium*. The crown pattern is also quite similar to *Prozostrodon* and *Botucaraitherium* (Fig. 5B–D), in which some of the postcanines have cusps slightly recurved posteriorly. Those two taxa, however, have much more complex lingual cingula than *Agudotherium*, including several discrete accessory cusps. Among Brazilian Triassic probainognathians, *Agudotherium* also resembles the condition in *Irajatherium* to some degree (Fig. 5F); however, all the postcanines of this latter taxon are much more sectorial, with a considerably sized cusp c (comparable to cusp a in the posterior postcanines) and with no conspicuous lingual cingulum. *Irajatherium* is also smaller in absolute size, has the incisor alveolar platform placed well above the postcanine alveolar margin, has a first incisor substantially larger than the remaining ones, a more slender horizontal ramus of the dentary, and a Meckelian groove positioned near the ventral border of the dentary (Martinelli et al., 2005; Oliveira et al., 2011b).

The anterior/middle postcanine teeth are smaller and less complex than in the posterior ones, similar to *Candelariodon*, *Prozostrodon*, *Brasilodon*, and *Botucaraitherium* (Bonaparte et al., 2003, 2005; Oliveira et al., 2011a; Soares et al., 2014) (Fig. 5A–E), in which the anterior postcanine dentition is well-differentiated from the posterior. In *Irajatherium*, *Pachygenelus*, *Riograndia*, *Probainognathus*, chiniquodontids, and ecteniniids, the morphological transition is more gradual (Gow, 1980; Bonaparte et al., 2001; Martinelli et al., 2005, 2007, 2016).

In the most complex postcanines, the main cusp (a) is asymmetrical and distally convex, with the mesial edge longer and more convex than the distal one. In contrast, cusp a in *Santacruzgnathus* is symmetrical and not curved posteriorly (Martinelli et al., 2016). The sectorial portion of cusp a in *Botucaraitherium* and *Alemoatherium* appears to be taller than in *Agudotherium* and *Prozostrodon* (Fig. 5A–D). Furthermore, cusps a and c of the new species are taller, whereas cusps b and d have almost the same height, a feature also observed in *Botucaraitherium*, *Santacruzgnathus*, and *Alemoatherium* (Bonaparte and Barberena, 1975; Soares et al., 2014; Martinelli et al., 2016, 2017a). Nonetheless, cusp b of *Agudotherium*, *Santacruzgnathus*, and *Alemoatherium* is higher than cusp d, whereas the reverse is true in *Botucaraitherium*, with cusp d higher than b. In occlusal view, cusp b is slightly more lingual than cusps c and d in *Agudotherium*, as in *Alemoatherium* (Martinelli et al., 2017a).

The digital renderings revealed replacement incisors and postcanines in CAPPA/UFSM 0262 and CAPPA/UFSM 0208. In the

former (the holotype), there are two replacement postcanines, erupting below the positions of the second and fifth functional postcanines, showing a pattern of alternating dental replacement. In CAPPA/UFSM 0208 it is also possible to observe the presence of replacement incisors, for the first and third functional incisors, and a replacement postcanine below the second functional postcanine. The tooth replacing the fifth functional postcanine is in a more advanced stage of development and eruption than the one replacing the second functional postcanine. In contrast, the tooth replacing pc3 is more developed than that replacing pc7 in the referred specimen of *Botucaraitherium* (MMACR-PV-044-T; Martinelli et al., 2017e), suggesting a somewhat different pattern of replacement. Regarding the incisors, the non-functional third tooth in CAPPA/UFSM 0208 is better developed than the first.

The micro-CT data show no evidence of an additional, non-erupted tooth posterior to the last functional postcanine tooth in either jaw of *Agudotherium*. The presence of such a non-erupted tooth, still within its crypt, would be evidence that the individual was still growing (Bonaparte and Barberena, 2001). Several specimens of cynodonts in different ontogenetic stages preserve a posterior, non-erupted tooth inside its crypt, e.g., *Prozostrodon* (UFRGS-PV 248-T and CAPPA/UFSM 0123; Barberena et al., 1987; Bonaparte and Barberena, 2001; Pacheco et al., 2017) and *Botucaraitherium* (MMACR-PV-044-T; Soares et al., 2014; Martinelli et al., 2017e), indicating that these specimens were still growing at the time of death. The absence of this feature in the known material of *Agudotherium* suggests that posterior dentition replacement has ceased and the specimens represent mature individuals. Alternatively, it could mean that the timing of postcanine formation and eruption is different in this taxon than in related forms, and the posteriormost tooth was too early in development to be visible in these specimens (which, as discussed above, may represent one individual). Only additional specimens will elucidate the details of tooth replacement in this species.

The presence of a lingual cingulum is considered a derived feature among probainognathians and is present in early mammaliaforms (e.g., *Morganucodon oehleri*; Mills, 1971; Parrington, 1973). However, the presence of this structure is also known in certain basal cynodonts (e.g., *Thrinaxodon*; Abdala et al., 2013) and is quite variable in prozostrodonts, although usually present (e.g., in *Brasilodon*, *Santacruzgnathus*, *Alemoatherium*, and *Candelariodon*; Bonaparte et al., 2003, 2005, 2012; Oliveira et al., 2011a; Martinelli et al., 2016, 2017a, 2017d). In *Agudotherium*, a complete lingual cingulum is absent but, instead, mesio- and disto-lingual structures (crest or accessory cusps) similar to those of *Brasilodon* (Fig. 5E) are present, differing considerably from the complete, multicuspidate cingulum of *Prozostrodon* and *Botucaraitherium* (Barberena et al., 1987; Bonaparte and Barberena, 2001; Pacheco et al., 2017; Martinelli et al., 2017e) (Fig. 5B–D). In certain other South American prozostrodonts, such as *Therioherpeton* (Bonaparte and Barberena, 1975; Oliveira, 2006) and the ictidosaurs *Irajatherium*, *Chaliminia*, and *Riograndia* (Bonaparte et al., 2001; Martinelli et al., 2005; Martinelli and Rougier, 2007; Soares et al., 2011b; Oliveira et al., 2011b), the postcanine teeth have no lingual cingulum. However, teeth of the tritheledontid *Pachygenelus* do possess well-defined cingula, with minuscule cuspules that are more evident in the distal edge (Gow, 1980).

The postcanines of *Agudotherium* are imbricated, notably in pc5 to pc7. This pattern occurs in some basal probainognathians (e.g., *Chiniquodon*, *Ecteninion lunensis*, *Diegocanis elegans*, and *Trucidocynodon riograndensis*; Martínez and Forster, 1996; Martínez et al., 1996, 2013; Oliveira et al., 2010; Stefanello et al., 2018) and in some prozostrodonts (e.g., *Therioherpeton*, *Irajatherium*, and *Riograndia*; Bonaparte and Barberena, 2001; Oliveira, 2006; Oliveira et al., 2011b; Soares et al., 2011b).

The roots of the postcanine teeth in *Agudotherium* exhibit an incipient division, as is typical for Prozostrodontia (Bonaparte and Barberena, 1975, 2001; Bonaparte et al., 2001, 2003, 2005, 2006; Martinelli et al., 2005, 2016, 2017a; Martinelli and Rougier, 2007; Soares et al., 2011b, 2014). The presence of an incipient division of the postcanine roots is recognized in a number of different lineages of derived non-mammaliaform cynodonts (e.g., therioherpetids, brasilodontids, and tritheledontids), and the independent origin of this trait is accepted within the group (Shapiro and Jenkins, 2001; Bonaparte et al., 2005; Martinelli et al., 2005; Martinelli and Rougier, 2007). The presence of conspicuous division of roots in postcanines was already developed in Carnian forms (e.g., in *Prozostrodon* and dromatheriids; Sulej et al., 2018).

The incomplete nature of the known material of *Agudotherium gassenae* and the mosaic of dental features observed in the increasingly diverse array of non-mammaliaform prozostrodontians hamper a clear phylogenetic placement for this taxon. Features in the jaw and dentition of *Agudotherium* are shared with a variety of disparate taxa among advanced non-mammaliaform probainognathians, but the combination of these features is not known in any particular subclade. Among the known Norian prozostrodontian cynodonts, the overall mandibular and dentary morphology of *Agudotherium* is similar in some degree to that of *Brasilodon*, *Botucaraitherium*, and *Irajatherium* (Bonaparte et al., 2003; Martinelli et al., 2005; Soares et al., 2014) (Fig. 5A, D–F), but with differences from each taxon especially in the morphology, the distribution, and the relative size of the cusps and the cingulum of the postcanines (see Fig. 5A, D, E). *Brasilodon* differs from the new taxon by having a slender dentary, with its anterior portion anterodorsally projected and a discrete Meckelian groove. In addition, the main cusps are usually more upright in position (Fig. 5E). *Botucaraitherium* differs from the new cynodont because it has a multicuspidated lingual cingular shelf. Moreover, the sectorial portion of the main cusp a is higher and cusps d and b are distributed differently in the crown (Fig. 5D). The interlocking mechanism in *Brasilodon* and *Botucaraitherium* is more complex than in *Agudotherium*. The first two taxa have the distal cusp of the anterior postcanine fit into an embayment between the cusps of the succeeding postcanine, whereas in *Agudotherium* the postcanines only somewhat overlap lingually. *Irajatherium* differs from the new taxon by the shape of the dentary, position of the Meckelian groove, position of the incisor related to the postcanine series, and the complexity of the lingual cingulum in *Agudotherium* (Fig. 5A, F). *Irajatherium* was related to tritheledontids (Martinelli et al., 2005; Oliveira et al., 2011b) mainly due to the morphology of its upper and lower postcanines, size of the first lower incisor, and postcranial features (e.g., morphology of the femur similar to *Pachygenelus*) and the resemblances of the new taxon with this one might be indicating a relationship with this clade.

The Carnian prozostrodont *Prozostrodon* (Bonaparte and Barberena, 2001) differs from *Agudotherium* by having the anterior portion of the dentary projected anterodorsally and a complete lingual cingulum bearing numerous discrete accessory cusps (Fig. 5A–C). In addition, *Prozostrodon* has four incisor teeth whereas there are only three in *Agudotherium*. The distal edge of the canine of the new taxon does not have serrated margins; contrarily *Prozostrodon* presents tiny serrations in this tooth. Ultimately, *Agudotherium* also differs from the first probainognathian cynodont (CAPPA/UFSM 0100) reported at the Niemeyer Site, mainly due to the difference in mandibular size, with CAPPA/UFSM 0100 being much larger than new species. It is also different in the presence of the mesial edge of the canine curved posteriorly and the horizontal ramus of the dentary and the coronoid process lower dorsoventrally than CAPPA/UFSM 0100 (see Pavanatto et al., 2018). However, this specimen is still covered by a hard layer of sedimentary matrix, so it needs

FIGURE 6. Life reconstruction of *Agudotherium gassenae* gen. et sp. nov., by Márcio L. Castro.

further detailed preparation in order to yield additional anatomical information.

Our comparisons suggest that *Agudotherium gassenae* represents a derived taxon among non-mammaliaform prozostrodontian cynodonts. However, the available specimens of *Agudotherium* are fragmentary, and the radiation of small, advanced non-mammaliaform probainognathians has shown a great diversity of forms that at some point have a suite of apomorphies widely distributed within the clade. More specimens, not only of this new taxon but also of other related forms, together with a broad phylogenetic analysis are required to improve the real diversity and relationships of these mammal precursors.

CONCLUSIONS

We described a new probainognathian cynodont based on two specimens, CAPPA/UFSM 0262 and CAPPA/UFSM 0208, from the Upper Triassic of southern Brazil (Fig. 6). *Agudotherium gassenae*, gen. et sp. nov., is based on a unique combination of features not present in other cynodonts, such as a robust dentary, with the dorsoventrally deep dentary body and a rectilinear ventral margin; a Meckelian groove that is long and dorsoventrally tall, disposed rectilinearly in the dorsoventral half of the dentary; the absence of serrations on the mesial and distal edges of the canine; and unserrated sectorial postcanine teeth with posteriorly inclined cusps and with lingual cingulum restricted to the mesio- and distolingual corners of the crowns.

Because of the reduced number of codable characters in this material, it was not possible to clarify the phylogenetic relations of *Agudotherium* amongst cynodonts. Nonetheless, the new taxon seems to be related to sectorial-toothed non-mammaliaform prozostrodontians (e.g., *Brasilodon*, *Botucaraitherium*, *Irajatherium*; Bonaparte et al., 2003, 2005; Martinelli et al., 2005; Soares et al., 2014). Only further specimens with more analyses of variation in dental characters will help to elucidate its phylogenetic placement.

If the Niemeyer Site is correctly attributed to the *Riograndia* AZ, the presence of *Agudotherium* increases the diversity of prozostrodontian cynodonts, one of the most diverse worldwide. During the Late Triassic (Carnian and Norian), non-mammaliaform prozostrodontians had an intense adaptative radiation in western Gondwana, which illustrates the previous steps leading to Mammaliaformes (Martinelli and Soares, 2016; Wallace et al., 2019).

ACKNOWLEDGMENTS

We thank the Niemeyer family for kindly allowing the paleontological prospection and field work at their property; R. T. Müller, who found the specimen CAPPA/UFSM 0262; CAPPA/UFSM team for the support in the field work; Fundação de Amparo à Pesquisa do Estado do Rio Grande do Sul (FAPERGS 17/2551-0000816-2) and Conselho Nacional de Desenvolvimento Científico e Tecnológico (CNPq 422568/2018-0; research grant 309414/2019-9) to L.K.; Coordenação de Aperfeiçoamento de Pessoal de Nível Superior (CAPES) scholarship for M.S., Consejo Nacional de Investigaciones Científicas y Técnicas (CONICET-Argentina) to A.G.M., and Conselho Nacional de Desenvolvimento Científico e Tecnológico (research grant, process numbers 306352/2016-8) to S.D.S. We especially thank two anonymous reviewers and editor J. Fröbisch for comments that greatly improved the manuscript.

ORCID

Micheli Stefanello http://orcid.org/0000-0002-6669-9657
Leonardo Kerber http://orcid.org/0000-0001-8139-1493
Agustin G. Martinelli http://orcid.org/0000-0003-4489-0888
Sérgio Dias-da-Silva http://orcid.org/0000-0002-1262-0528

LITERATURE CITED

Abdala, F., and N. P. Giannini. 2002. Chiniquodontid cynodonts: systematic and morphometric considerations. Palaeontology 45:1151–1170.

Abdala, F., and A. M. Ribeiro. 2000. A new therioherpetid cynodont from the Santa Maria Formation (middle Late Triassic), southern Brazil. Geodiversitas 22:589–596.

Abdala, F., and A. M. Ribeiro. 2010. Distribution and diversity patterns of Triassic cynodonts (Therapsida, Cynodontia) in Gondwana. Palaeogeography, Palaeoclimatology, Palaeoecology 286:202–217.

Abdala, F., M. C. Barberena, and J. E. Dornelles. 2002. A new species of the traversodontid cynodont *Exaeretodon* from the Santa Maria Formation (Middle/Late Triassic) of southern Brazil. Journal of Vertebrate Paleontology 22:313–325.

Abdala, F., S. C. Jasinoski, and V. Fernandez. 2013. Ontogeny of the early Triassic cynodont *Thrinaxodon liorhinus* (Therapsida): dental morphology and replacement. Journal of Vertebrate Paleontology 33:1408–1431.

Abdala, F., A. M. Ribeiro, and C. L. Schultz. 2001. A rich cynodont fauna of Santa Cruz do Sul, Santa Maria Formation (Middle–Late Triassic), southern Brazil. Neues Jahrbuch für Geologie und Paläontologie-Monatshefte 11:669–687.

Barberena, M. C., J. F. Bonaparte, and A. M. S. Teixeira. 1987. *Thrinaxodon brasiliensis* sp. nov., a primeira ocorrência de cinodontes galessauros para o Triássico do Rio Grande do Sul; pp. 67–74 in Anais do X Congresso Brasileiro de Geologia, Rio de Janeiro, Brazil.

Bonaparte, J. F. 1966. Sobre nuevos Terápsidos Triásicos hallados en el centro de la Provincia de Mendoza, (Therapsida, Dicynodontia y Cynodontia). Acta Geológica Lilloana 8:95–100.

Bonaparte, J. F. 1971. Los tetrápodos del sector superior de la Formación Los Colorados, La Rioja, Argentina (Triásico Superior). Opera Lilloana 22:1–183.

Bonaparte, J. F., and M. C. Barberena. 1975. A possible mammalian ancestor from the Middle Triassic of Brazil (Therapsida-Cynodontia). Journal of Paleontology 49:931–936.

Bonaparte, J. F., and M. C. Barberena. 2001. On two advanced carnivorous cynodonts from the Late Triassic of Southern Brazil. Bulletin of the Museum of Comparative Zoology 156:59–80.

Bonaparte, J. F., J. Ferigolo, and A. M. Ribeiro. 2001. A primitive Late Triassic 'ictidosaur' from Rio Grande do Sul, Brazil. Palaeontology 44:623–635.

Bonaparte, J. F., A. G. Martinelli, and C. L. Schultz. 2005. New information on *Brasilodon* and *Brasilitherium* (Cynodontia, Probainognathia) from the Late Triassic of southern Brazil. Revista Brasileira de Paleontologia 8:25–46.

Bonaparte, J. F., M. B. Soares, and A. G. Martinelli. 2012. Discoveries in the Late Triassic of Brazil improve knowledge on the origin of mammals. Historia Natural, Fundación Felix de Azara, Tercera Serie 2:5–30.

Bonaparte, J. F., M. B. Soares, and C. L. Schultz. 2006. A new non-mammalian cynodont from the Middle Triassic of southern Brazil and its implications for the ancestry of mammals. Bulletin of the New Mexico Museum of Natural History and Science 37:599–607.

Bonaparte, J. F., A. G. Martinelli, C. L. Schultz, and R. Rubert. 2003. The sister group of mammals: small cynodonts from the Late Triassic of southern Brazil. Revista Brasileira de Paleontologia 5:5–27.

Bonaparte, J. F., C. L. Schultz, M. B. Soares, and A. G. Martinelli. 2010. La fauna local de Faxinal do Soturno, Triásico Tardío de Rio Grande do Sul, Brasil. Revista Brasileira de Paleontologia 13:233–246.

Botha-Brink, J., M. B. Soares, and A. G. Martinelli. 2018. Osteohistology of Late Triassic prozostrodontian cynodonts from Brazil. PeerJ 6:e5029.

Broom, R. 1905. Preliminary notice of some new fossil reptiles collected by Mr. Alfred Brown at Aliwal North, South Africa. Records of the Albany Museum 1:269–275.

Crompton, A. W., and Z.-X. Luo. 1993. Relationships of the Liassic mammals *Sinoconodon*, *Morganucodon oehleri*, and *Dinnetherium*; pp. 30–44 in F. S. Szalay, M. J. Novacek, and M. C. McKenna (eds.), Mammal Phylogeny: Mesozoic Differentiation, Multituberculates, Monotremes, Early Therians and Marsupials, Springer, New York.

Da-Rosa, Á. A. S., and U. F. Faccini. 2005. Delimitação de blocos estruturais de diferentes escalas em sequências mesozoicas do Estado do Rio Grande do Sul: implicações bioestratigráficas. Gaea-Journal of Geoscience 1:16–23.

Gow, C. E. 1980. The dentitions of the Tritheledontidae (Therapsida: Cynodontia). Proceedings of the Royal Society of London, Series B 208:461–481.

Hopson, J. A. 1971. Postcanine replacement in the gomphodont cynodont *Diademodon*. Zoological Journal of the Linnean Society 50:1–21.

Hopson, J. A. 1990. Cladistic analysis of therapsid relationships. Journal of Vertebrate Paleontology 10(3, Supplement):28A.

Hopson, J. A., and J. W. Kitching. 2001. A probainognathian cynodont from South Africa and the phylogeny of nonmammalian cynodonts. Bulletin of the Museum of Comparative Zoology 156:5–35.

Horn, B. L. D., T. M. Melo, C. L. Schultz, R. P. Philipp, H. P. Kloss, and K. Goldberg. 2014. A new third-order sequence stratigraphic framework applied to the Triassic of the Paraná Basin, Rio Grande do Sul, Brazil, based on structural, stratigraphic and paleontological data. Journal of South American Earth Sciences 55:123–132.

Huene, F. von. 1936. Die fossilen Reptilien des südamerikanischen Gondwanalands. C. H. Beck'sche Verlag, München, 332 pp.

Kemp, T. S. 1982. Mammal-like Reptiles and the Origin of Mammals. Academic Press, London, 363 pp.

Langer, M. C., J. Ramezani, and Á. A. Da Rosa. 2018. U-Pb age constraints on dinosaur rise from south Brazil. Gondwana Research 57:133–140.

Langer, M. C., A. M. Ribeiro, C. L. Schultz, and J. Ferigolo. 2007. The continental tetrapod bearing Triassic of south Brazil. Bulletin of the New Mexico Museum of Natural History and Science 41:201–218.

Liu, J., and P. E. Olsen. 2010. The phylogenetic relationships of Eucynodontia (Amniota, Synapsida). Journal of Mammalian Evolution 17:151–176.

Luo, Z.-X. 1994. Sister-group relationships of mammals and transformations of diagnostic mammalian characters; pp. 98–128 in N. C. Fraser and H.-D. Sues (eds.), In the Shadow of the Dinosaurs: Early Mesozoic Tetrapods, Cambridge University Press, New York.

Luo, Z.-X., Z. Kielan-Jaworowska, and R. L. Cifelli. 2004. Evolution of dental replacement in mammals. Bulletin of Carnegie Museum of Natural History 36:159–175.

Marsola, J. C. A., J. S. Bittencourt, Á. A. Da Rosa, A. G. Martinelli, A. M. Ribeiro, J. Ferigolo, and M. C. Langer. 2018. New sauropodomorph and cynodont remains from the Late Triassic *Sacisaurus* site in southern Brazil and its stratigraphic position in the Norian Caturrita Formation. Acta Palaeontologica Polonica 63:653–669.

Martinelli, A. G. 2017. Contribuições ao conhecimento dos cinodontes probainognátios (Therapsida, Cynodontia, Probainognathia) do Triássico da América do Sul e seu impacto na origem dos Mammaliaformes. Ph.D. dissertation, Universidade Federal do Rio Grande do Sul, Porto Alegre, Brazil, 645 pp.

Martinelli, A. G., and J. F. Bonaparte. 2011. Postcanine replacement in *Brasilodon* and *Brasilitherium* (Cynodontia, Probainognathia) and its bearing in cynodont evolution; pp. 179–186 in J. Calvo, J. Porfiri, B. González-Riga, and D. Dos Santos (eds.), Dinosaurios y Paleontología desde América Latina, Anales del III Congreso Latinoamericano de Paleontología, Editorial de la Universidad Nacional de Cuyo, Mendoza.

Martinelli, A. G., and G. W. Rougier. 2007. On *Chaliminia musteloides* Bonaparte (Cynodontia, Tritheledontidae) and the phylogeny of the Ictidosauria. Journal of Vertebrate Paleontology 27:442–460.

Martinelli, A. G., and M. B. Soares. 2016. Evolution of South American cynodonts. Contribuciones del Museo Argentino de Ciencias Naturales 'Bernardino Rivadavia' 6:183–197.

Martinelli, A. G., M. B. Soares, and C. Schwanke. 2016. Two new cynodonts (Therapsida) from the Middle-Early Late Triassic of Brazil and comments on South American probainognathians. PLoS ONE 11:e0162945.

Martinelli, A. G., J. F. Bonaparte, C. L. Schultz, and R. Rubert. 2005. A new tritheledontid (Therapsida, Eucynodontia) from the Late Triassic of Rio Grande do Sul (Brazil) and its phylogenetic relationships among carnivorous nonmammalian eucynodonts. Ameghiniana 42:191–208.

Martinelli, A. G., E. Eltink, Á. A. Da-Rosa, and M. C. Langer. 2017a. A new cynodont from the Santa Maria Formation, south Brazil, improves Late Triassic probainognathian diversity. Palaeontology 3:401–423.

Martinelli, A. G., M. B. Soares, T. V. De Oliveira, P. G. Rodrigues, and C. L. Schultz. 2017d. The Triassic eucynodont *Candelariodon barberenai* revisited and the early diversity of stem prozostrodontians. Acta Palaeontologica Polonica 62:527–542.

Martinelli, A. G., I. J. Corfe, P. G. Gill, A. Kallonen, E. J. Rayfield, P. B. Rodrigues, C. L. Schultz, and M. B. Soares. 2017c. *Brasilodon quadrangularis*, *Brasilitherium riograndensis* and *Minicynodon maieri* (Cynodontia): taxonomy, ontogeny and tooth replacement; p. 189 in Paleontologia em Destaque, Boletim de Resumos XXV Congresso Brasileiro de Paleontologia, Ribeirão Preto, São Paulo, Brazil.

Martinelli, A. G., C. F. Kammerer, T. P. Melo, V. D. P. Neto, A. M. Ribeiro, Á. A. Da-Rosa, C. L. Schultz, and M. B. Soares. 2017b. The African cynodont *Aleodon* (Cynodontia, Probainognathia) in the Triassic of southern Brazil and its biostratigraphic significance. PLoS ONE 12: e0177948.

Martinelli, A. G, M. Guignard, P. G. Rodrigues, M. B. Soares, M. Castro, A. H. Augustin, C. T. Martinho, C. N. Rodrigues, M. C. Langer, and C. L. Schultz. 2017e. Novas informações sobre a dentição de *Botucaraitherium belarminoi* (Cynodontia, Prozostrodontia) do Triássico Superior do Rio Grande do Sul; p. 50 in Reunião Regional Paleo RS 2017, Boletim de Resumos, Rio Grande, Rio Grande do Sul, Brazil.

Martínez, R. N., and C. A. Forster. 1996. The skull of *Probelesodon sanjuanensis*, sp. nov., from the Late Triassic Ischigualasto Formation of Argentina. Journal of Vertebrate Paleontology 16:285–291.

Martínez, R. N., E. Fernandez, and O. A. Alcober. 2013. A new nonmammaliaform eucynodont from the Carnian-Norian Ischigualasto Formation, northwestern Argentina. Revista Brasilera de Paleontologia 16:61–76.

Martínez, R. N., C. L. May, and C. A. Forster. 1996. A new carnivorous cynodonts from the Ischigualasto Formation (Late Triassic, Argentina), with comment on eucynodont phylogeny. Journal of Vertebrate Paleontology 16:271–284.

Mills, J. R. E. 1971. The dentition of *Morganucodon*. Zoological Journal of the Linnean Society 50:26–63.

Miron, L. R., A. E. B. Pavanatto, F. A. Pretto, R. T. Müller, S. Dias-da-Silva, and L. Kerber. 2020. *Siriusgnathus niemeyerorum* (Eucynodontia: Gomphodontia): the youngest South American traversodontid? Journal of South American Earth Sciences 97:102394.

Oliveira, E. V. 2006. Reevaluation of *Therioherpeton cargnini* Bonaparte and Barberena 1975 (Probainognathia, Therioherpetidae) from the Upper Triassic of Brazil. Geodiversitas 28:447–465.

Oliveira, T. V., A. G. Martinelli, and M. B. Soares. 2011b. New material of *Irajatherium hernandezi* Martinelli, Bonaparte, Schultz and Rubert 2005 (Eucynodontia, Tritheledontidae) from the Upper Triassic (Caturrita Formation, Paraná Basin) of Brazil. Paläontologische Zeitschrift 85:67–82.

Oliveira, T. V., M. B. Soares, and C. L. Schultz. 2010. *Trucidocynodon riograndensis* gen. nov. et sp. nov. (Eucynodontia), a new cynodont from the Brazilian Upper Triassic (Santa Maria Formation). Zootaxa 2382:1–71.

Oliveira, T. V., M. B. Soares, C. L. Schultz, and C. N. Rogrigues. 2011a. A new carnivorous cynodont (Synapsida, Therapsida) from the Brazilian Middle Triassic (Santa Maria Formation): *Candelariodon barberenai* gen. et sp. nov. Zootaxa 3027:19–28.

Owen, R. 1861. Palaeontology, or a Systematic Summary of Extinct Animals and their Geological Relationships. Adam and Black, Edinburgh, 463 pp.

Parrington, F. R. 1973. The dentition of earliest mammals. Zoological Journal of the Linnean Society 52:85–95.

Pacheco, C. P., A. G. Martinelli, A. E. B. Pavanatto, M. B. Soares, and S. Dias-da-Silva. 2017. *Prozostrodon brasiliensis*, a probainognathian cynodont from the Late Triassic of Brazil: second record and improvements on its dental anatomy. Historical Biology 30: 475–485.

Pavanatto, A. E. B., F. A. Pretto, L. Kerber, R. T. Müller, Á. A. Da-Rosa, and S. Dias-Da-Silva. 2018. A new cynodont-bearing fossiliferous site from the Upper Triassic of southern Brazil, with taphonomic remarks and description of a new traversodontid taxon. Journal of South American Earth Sciences 88:179–196.

Rowe, T. 1988. Definition, diagnosis and origin of Mammalia. Journal of Vertebrate Paleontology 8:241–264.

Shapiro, M. D., and F. A. Jenkins, Jr. 2001. A cynodont from the Upper Triassic of East Greenland: tooth replacement and double-rootedness. Bulletin of the Museum of Comparative Zoology 156:49–58.

Soares, M. B., F. Abdala, and C. Bertoni-Machado. 2011a. A sectorial toothed cynodont (Therapsida) from the Triassic Santa Cruz do Sul fauna, Santa Maria Formation, Southern Brazil. Geodiversitas 33:265–278.

Soares, M. B., A. G. Martinelli, and T. V. Oliveira. 2014. A new prozostrodontian cynodont (Therapsida) from the Late Triassic *Riograndia* Assemblage Zone (Santa Maria Supersequence) of Southern Brazil. Anais da Academia Brasileira de Ciências 86:1673–1691.

Soares, M. B., C. L. Schultz, and B. L. D. Horn. 2011b. New information on *Riograndia guaibensis* Bonaparte, Ferigolo and Ribeiro, 2001 (Eucynodontia, Tritheledontidae) from the Late Triassic of southern Brazil: anatomical and biostratigraphic implications. Anais da Academia Brasileira de Ciências 83:329–354.

Stefanello, M., R. T. Müller, L. Kerber, R. N. Martínez, and S. Dias-Da-Silva. 2018. Skull anatomy and phylogenetic assessment of a large specimen of Ecteniniidae (Eucynodontia: Probainognathia) from the Upper Triassic of southern Brazil. Zootaxa 4457:351–378.

Sulej, T., G. Niedźwiedzki, M. Tałanda, D. Dróżdż, and E. Hara. 2018. A new early Late Triassic non-mammaliaform eucynodont from Poland. Historical Biology 32:80–92.

Wallace, R. V., R. N. Martínez, and T. Rowe. 2019. First record of a basal mammaliamorph from the early Late Triassic Ischigualasto Formation of Argentina. PLoS ONE 14:e0218791.

Zerfass, H., E. L. Lavina, C. L. Schultz, A. J. V. Garcia, U. F. Faccini, and F. Chemale, Jr. 2003. Sequence stratigraphy of continental Triassic strata of southernmost Brazil: a contribution to southwestern Gondwana palaeogeography and palaeoclimate. Sedimentary Geology 161:85–105.

Submitted February 4, 2020; revisions received April 7, 2020;
accepted June 7, 2020.
Handling Editor: Jörg Fröbisch.

2.1.1 Dataset do Artigo 1

O Dataset do Artigo 1, intitulado: **“3D models related to the publication: A new prozostrodontian cynodont (Eucynodontia, Probainognathia) from the Upper Triassic of southern Brazil”**, foi publicado no periódico *MorphoMuseuM*, DOI: 10.18563/journal.m3.120.

Dataset

3D models related to the publication: A new prozostrodontian cynodont (Eucynodontia, Probainognathia) from the Upper Triassic of southern Brazil

Micheli Stefanello[1,2], Leonardo Kerber[1,2]*, Agustin Martinelli[3], Sérgio Dias-da-Silva[1]

[1] *Programa de Pós-Graduação em Biodiversidade Animal, Universidade Federal de Santa Maria, Santa Maria, Brazil, CEP 97105-900*
[2] *Centro de Apoio à Pesquisa Paleontológica da Quarta Colônia, Universidade Federal de Santa Maria, São João do Polêsine, Brazil, CEP 97230-000*
[3] *CONICET-Museo Argentino de Ciencias Naturales "Bernardino Rivadavia", Buenos Aires, Argentina, C1405DJR*
***Corresponding author**: leonardokerber@gmail.com

Abstract
The present 3D Dataset contains the 3D models and CT-Scan slices of the lower jaws and teeth analyzed in "A new prozostrodontian cynodont (Eucynodontia, Probainognathia) from the Upper Triassic of southern Brazil". https://doi.org/10.1080/02724634.2020.1782415

Keywords: Late Triassic, lower jaw, micro-CT, Prozostrodontia

Submitted:2020-05-31, published online:2020-10-08. https://doi.org/10.18563/journal.m3.120

Inv nr.	Description
CAPPA/UFSM0262_M3#546	3D surface of left lower jaw and cheek teeth
CAPPA/UFSM0262_M3#547	µCT data
CAPPA/UFSM0208_M3#548	3D surface of right lower jaw
CAPPA/UFSM0208_M3#549	µCT data

Table 1. List of models of *Agudotherium gassenae*. Collection: Centro de Apoio à Pesquisa Paleontológica da Quarta Colônia (CAPPA), Universidade Federal de Santa Maria, Brazil

INTRODUCTION

Agudotherium gassenae Stefanello et al. (2020) is a new non-mammaliaform prozostrodontian cynodont found in Brazil. The new taxon is described based on two lower jaws found in Upper Triassic strata from southern Brazil that share a combination of features unknown in other Carnian and Norian non-mammaliaform cynodonts. The new probainognathian cynodont furnishes new evidence on the knowledge of the adaptative radiation of small-sized prozostrodonts in western Gondwana that occurred during the Late Triassic and led to the emergence of several groups, including Mammaliaformes. This contribution contains the 3D models and µCT-Scan slices of the lower jaws and teeth of *Agudotherium gassenae* (Fig. 1 and table 1).

METHODS

The lower jaws of CAPPA/UFSM 0262 (holotype) and CAPPA /UFSM 0208 (Centro de Apoio à Pesquisa Paleontológica da Quarta Colônia, Universidade Federal de Santa Maria) were scanned using a micro-CT Skyscan 1173 at the Laboratório de Sedimentologia e Petrologia (LASEPE), Pontifícia Universidade Católica do Rio Grande do Sul (PUCRS), Porto Alegre, southern Brazil. The analysis (parameters: voltage 85 kV; amperage 65 µa; pixel size 15,166 µm) generated a total of 3443 slices for CAPPA/UFSM 0262, and 3696 slices (parameters: voltage 80 kV; amperage 100 µa; pixel size 14,108 µm) for CAPPA/UFSM 0208. The tomograms were imported into Mimics Medical 21.0 for virtual reconstruction and virtual segmentation of structures. The 3D surface models are provided in .ply format, and can therefore be opened with a wide range of freeware. The slices accompanying this publication were binned and converted to DICOM, resulting in 1578 slices, with pixel size 0.0282177 mm (CAPPA/UFSM 0262) and 1768 slices, with pixel size 0.0303324 mm (CAPPA/UFSM 0208).

ACKNOWLEDGEMENTS

This study is supported by Fundação de Amparo à Pesquisa do Estado do Rio Grande do Sul (FAPERGS 17/2551-0000816-2) and Conselho Nacional de Desenvolvimento Científico e Tecnológico (CNPq 422568/2018-0; research grant 309414/2019-9) to L.K.; Coordenação de Aperfeiçoamento de Pessoal de Nível Superior (CAPES) scholarship for M.S., Consejo Nacional de Investigaciones Científicas y Técnicas (CONICET-Argentina) to A.G.M., and Conselho Nacional de Desenvolvimento Científico e Tecnológico (research grant, process numbers 306352/2016-8) to S.D.S.

BIBLIOGRAPHY

Stefanello, M., Kerber, L., Martinelli, A. G., Dias-Da-Silva, S., 2020. A new prozostrodontian cynodont (Eucynodontia, Probainognathia) from the Upper Triassic of southern Brazil. Journal of Vertebrate Paleontology. https://doi.org/10.1080/02724634.2020.1782415

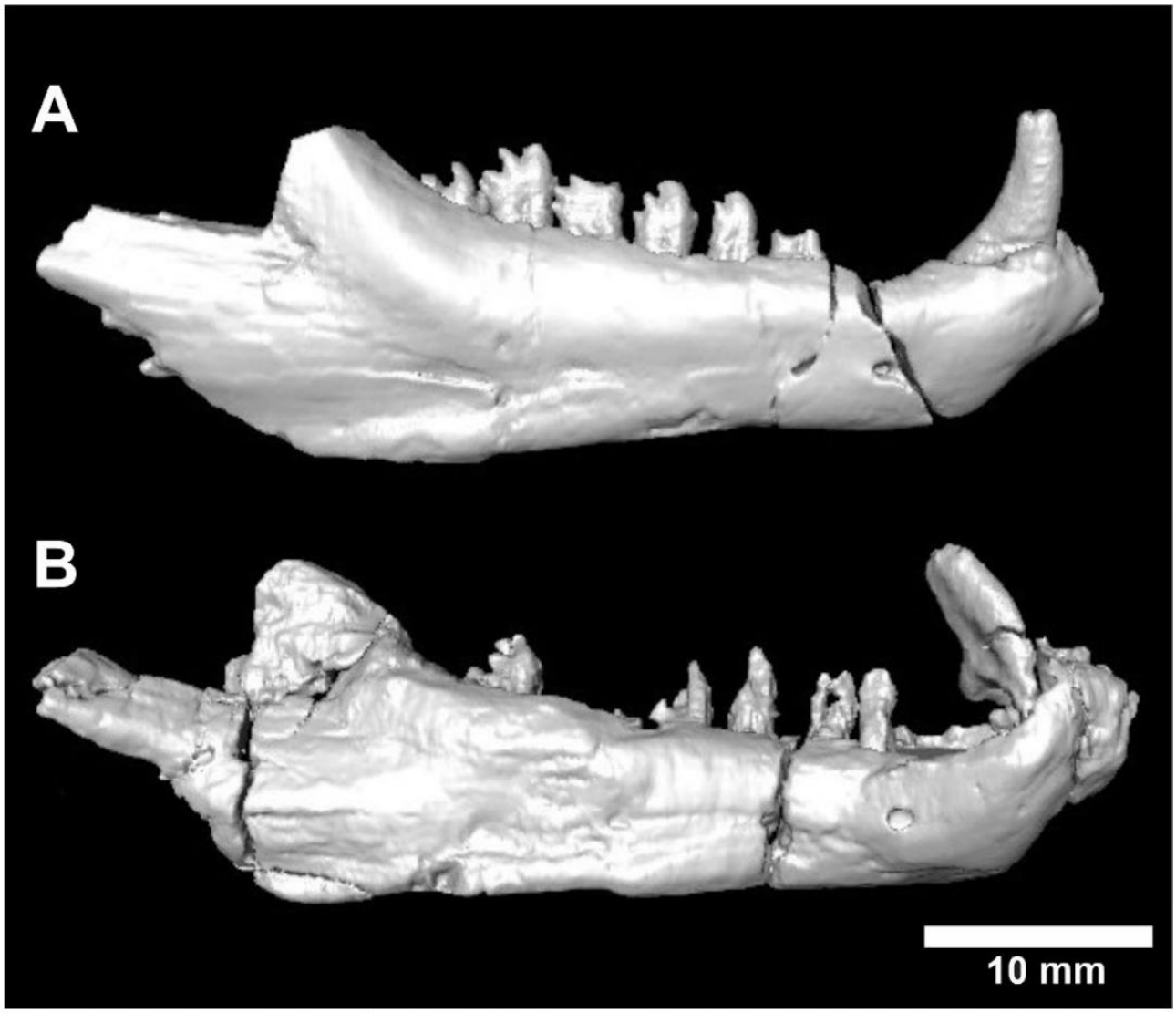

Figure 1. 3D models of the lower jaws and teeth of *Agudotherium gassenae* from the Upper Triassic of southern Brazil. **A:** Left lower jaw (reversed, CAPPA/UFSM 0262) in lateral view. **B:** right lower jaw (CAPPA/UFSM 0208) in lateral view.

ISSN: 2274-0422

2.2 ARTIGO 2

O Artigo 2, intitulado: **“A complete skull of a stem mammal from the Late Triassic of Brazil illuminates the early evolution of prozostrodontians”**, foi submetido para publicação no periódico científico *Journal of Mammalian Evolution* e está formatado de acordo com as normas do mesmo.

Track your submissions

A complete skull of a stem mammal from the Late Triassic of Brazil illuminates the early evolution of prozostrodontians

Corresponding Author: Leonardo Kerber

Journal of Mammalian Evolution

0eef3fd0-222e-49ec-8d37-6a29d5fa788d | v.1.0

Quality check in progress *about 19 hours ago*

A complete skull of a stem mammal from the Late Triassic of Brazil illuminates the early evolution of prozostrodonts

Micheli Stefanello[1,2]. Agustín G. Martinelli[3]. Rodrigo T. Müller[1,2]. Sérgio Dias-da-Silva[1]. Leonardo Kerber[1,2]

[1]Programa de Pós-Graduação em Biodiversidade Animal, Universidade Federal de Santa Maria, Av. Roraima, 1000, 97105-900, Santa Maria, RS, Brazil

[2]Centro de Apoio à Pesquisa Paleontológica da Quarta Colônia, Universidade Federal de Santa Maria (CAPPA/UFSM), Rua Maximiliano Vizzotto, 598, 97230-000, São João do Polêsine, RS, Brazil

[3]Sección Paleontologia de Vertebrados, Museo Argentino de Ciencias Naturales "Bernardino Rivadavia", Av. Ángel Gallardo, 470, C1405 DJR, Buenos Aires, Argentina

Corresponding authors: Micheli Stefanello (michelistefanello@hotmail.com), Leonardo Kerber (leonardokerber@gmail.com)

ORCID: MS, 0000-0002-6669-9657; AGM, 0000-0003-4489-0888; RTM, 0000-0001-8894-9875; SDS, 0000-0002-1262-0528; LK, 0000-0001-8139-1493

Abstract

Triassic cynodonts from South America are key taxa in the investigation of the emergence of mammalian characters. One of the most iconic species from the Carnian is *Prozostrodon brasiliensis*, found in Late Triassic strata from southern Brazil. This non-mammaliaform cynodont represents the earliest-diverging member of Prozostrodontia, a clade that encompasses Mammalia and their closest relatives. Previous descriptions of the skull of *Pr. brasiliensis* were based on specimens that did not preserve the posterior region, obscuring essential details of the basicranium. Here, we describe a new, complete, and exceptionally well-preserved skull of *Pr*. *brasiliensis* found in the same block as the holotype skeleton of the early predatory dinosaur *Gnathovorax cabreirai* and rhynchosaur specimens. Anatomical data from this specimen provide novel insights into the initial radiation of prozostrodontian cynodonts and reveal a new endemic clade of South American cynodonts – Prozostrodontidae – on the stem lineage of mammals.

Keywords Cynodontia, Probainognathia, Origin of mammaliaforms, Basicranium, Cladistics, Evolution.

Graphic abstract

Introduction

The Carnian (237-227 million years ago) is a stage in the Upper Triassic Series (Cohen et al. 2013). This interval of time is known for a climatic event of global proportions, the so-called Carnian Pluvial Event (CPE), which occurred approximately 234-232 million years ago (Furin et al. 2006; Ruffell et al. 2015). It is characterized by a shift from prevailing semiarid conditions to a humid and warm climate, with intense rainfall and relatively few arid climate intervals, followed by an intensification of aridity (Bernardi et al. 2018; Dal Corso et al. 2020). The Pangean biota was profoundly impacted by this event, and the fossil record highlights several faunal turnovers. The origins and/or radiations of several taxonomic groups have been associated with this time interval, such as those of conifers, insects, crocodiles, lizards, turtles, dinosaurs, and non-mammaliaform cynodonts (Bernardi et al. 2018; Dal Corso et al. 2020; Benton and Wu 2022).

During the Carnian, an important clade of non-mammaliaform cynodonts originated: the Prozostrodontia, which includes all the descendants of the most recent common ancestor of the Brazilian *Prozostrodon brasiliensis* and mammals (Liu and Olsen 2010; Abdala 2019). The earliest-diverging prozostrodont, *Pr*. *brasiliensis* itself, was discovered in the late Carnian strata of the *Hyperodapedon* Assemblage Zone (AZ) of the Candelária Sequence, Santa Maria, Brazil, in the 1980s. It was erected based on a partial cranium, mandible, and associated postcranial remains (Barberena et al. 1987; Bonaparte and Barberena 2001). Other records of this species include a right lower jaw from São João do Polêsine (Pacheco et al. 2017), and additional skull remains from the type locality (Kerber et al. 2020). During the preparation of the skeleton of the early

dinosaur *Gnathovorax cabreirai*, discovered in 2014 in Late Triassic strata from southern Brazil (Pacheco et al. 2019), a complete jaw of *Pr. brasiliensis* was found (Pacheco et al. 2017), and subsequently, an exceptional skull, which is described here. Using cladistic analysis and new data from this specimen, we recover a new clade representing the earliest radiation of Carnian prozostrodonts in western Gondwana.

Material and methods

Provenance

CAPPA/UFSM 0210 was collected at Marchezan site (29º37′52″S; 53º27′02″W), municipality of São João do Polêsine, Rio Grande do Sul, Brazil (*Hyperodapedon* AZ, Candelária Sequence, Santa Maria Supersequence) (Fig. 1). The fossiliferous level of the Cerro da Alemoa locality, another fossiliferous site of the *Hyperodapedon* AZ, was dated at a maximum depositional age of 233.23 ± 0.73 Ma (Carnian) (Langer et al. 2018).

Collection

CAPPA/UFSM 0210 was unearthed from a multitaxon association containing the herrerasaurid *Gnathovorax cabreirai* Pacheco et al. 2019, two *Hyperodapedon* rhynchosaurs, and a right lower jaw of *Prozostrodon brasiliensis* (Pacheco et at. 2017) (Figs. 1–2). The new specimen of *Pr. brasiliensis* is housed in the paleontological collection of the Centro de Apoio à Pesquisa Paleontológica da Quarta Colônia da Universidade Federal de Santa Maria.

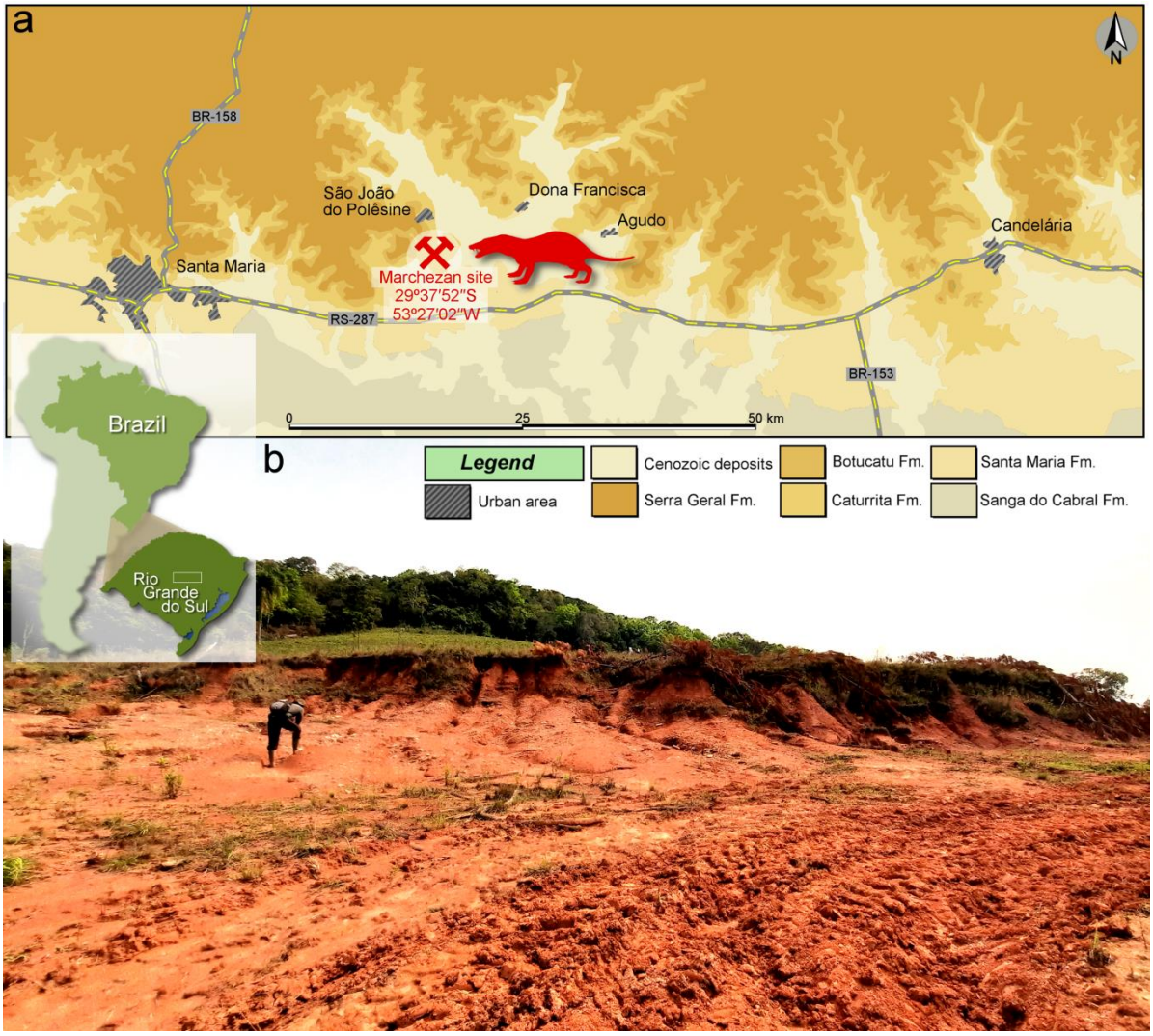

Fig. 1 Location of Marchezan Site, where the new specimen of *Prozostrodon brasiliensis* (CAPPA/UFSM 0210) was found. **a**. Map of the central region of Rio Grande do Sul, Brazil, and the surface distribution of the geologic units in the area; **b**. Photograph of the Marchezan Site, municipality of São João do Polêsine.

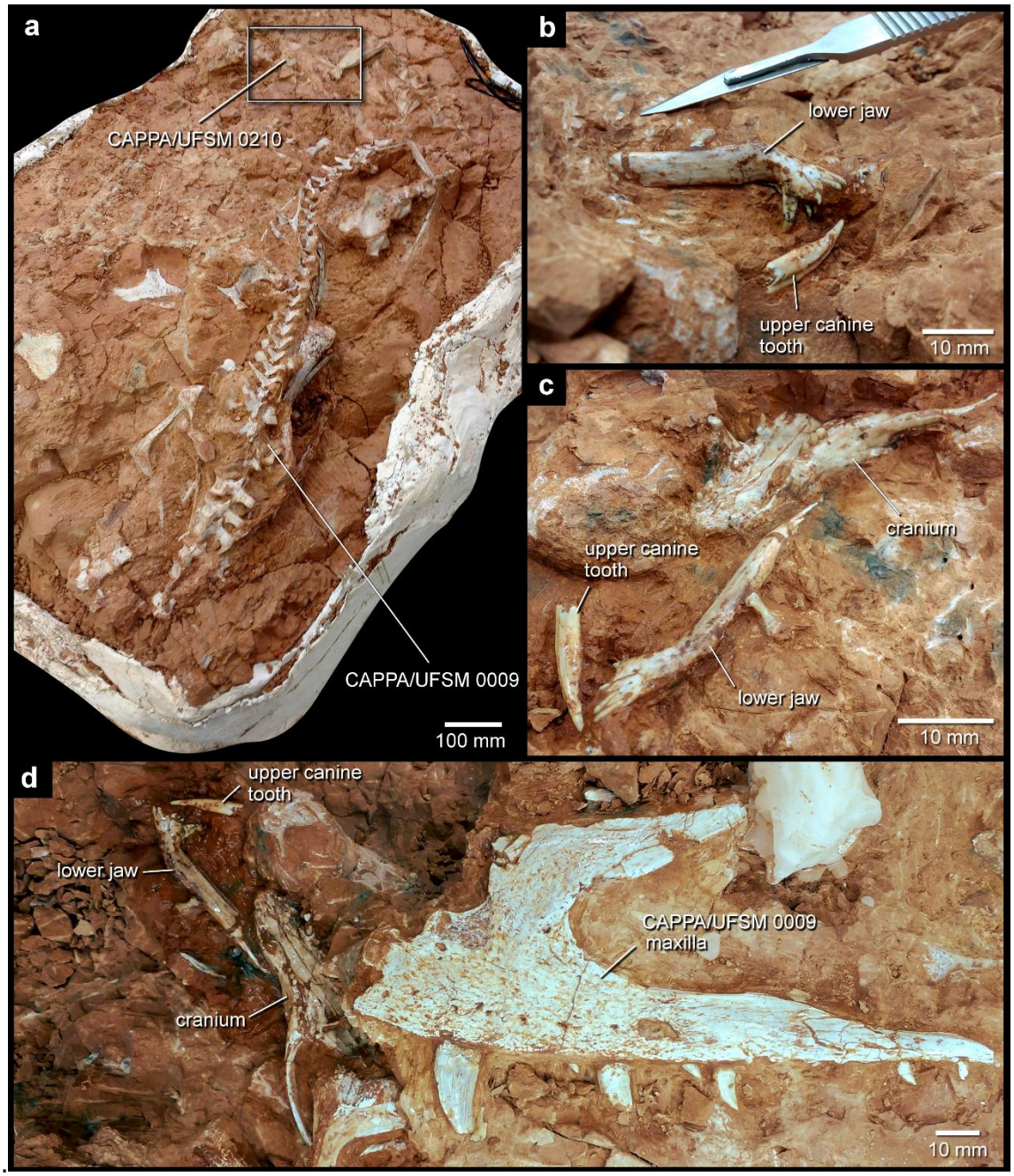

Fig. 2 Rock block with the skeleton of the dinosaur *Gnathovorax cabreirai* (CAPPA/UFSM 0009) (Pacheco et al. 2019). The rectangle in (**a**) shows the position of the new specimen of *Prozostrodon brasiliensis* (CAPPA/UFSM 0210) within the block; detail of the left lower jaw and upper canine tooth in situ *(***b**); cranium in ventral view, left lower jaw, and upper canine tooth in situ (**c**); The image (**d**) shows, from left to right, the

left lower jaw, the upper canine tooth, the cranium of CAPPA/UFSM 0210 in ventral view, and the left maxilla of CAPPA/UFSM 0009.

CT Scan and 3D modeling

The cranium of the specimen CAPPA/UFSM 0210 was scanned using a Nikon XT H 225 ST at the facilities of the University of Zurich, using 168 kV and 484 μA. This scan resulted in 2003 tomographic slices with a voxel size of 44.79 μm. The dentaries were scanned separately using a Skyscan™ 1173 at the Laboratório de Sedimentologia e Petrologia of Pontifícia Universidade Católica do Rio Grande do Sul (PUCRS), Porto Alegre (Brazil), using 85 kV and 65 μA. Each scanning resulted in 1200 tomographic slices with a voxel size of 15.16 μm. Avizo (FEI ThermoFisher Scientific) was employed to generate 3D models of the specimens

Phylogenetic analysis

The phylogenetic position of *Prozostrodon brasiliensis* was investigated employing the data matrix of Liu and Olsen (2010) with subsequent additions (Soares et al. 2014; Martinelli et al. 2016, 2017a, 2017b; Wallace et al. 2019; Kerber et al. 2022; Benoit et al. 2022). The new information from CAPPA/UFSM 0210 was combined with previous scores based on the holotype of *Pr. brasiliensis*. The complete list of modifications is presented in Online Resource. The final data matrix includes 154 characters and 39 operational taxonomic units (OTUs). The data matrix was analyzed in TNT v.1.5 (Goloboff and Catalano 2016). *Procynosuchus delaharpeae* was used to root the most parsimonious trees (MPTs), which were recovered with a heuristic search (random addition sequence + tree bisection reconnection) with 1000 replicates of Wagner trees

(with random seed = 0) and using tree bisection reconnection and branch swapping (holding ten trees save per replication). All characters received the same weight, and no characters were treated as ordered (additive).

Institutional abbreviations

CAPPA/UFSM, Centro de Apoio à Pesquisa Paleontológica da Quarta Colônia da Universidade Federal de Santa Maria, São João do Polêsine, Brazil; **MVP**, Museu Vicente Pallotti, Santa Maria, Brazil; **PVSJ**, Instituto y Museo de Ciencias Naturales, San Juan, Argentina; **UFRGS-PV-T**, Universidade Federal do Rio Grande do Sul, Paleontologia de Vertebrados (PV), Coleção Triássico (T), Porto Alegre, Brazil.

Availability of Data and Material

The dataset generated and analyzed during this study is included in this published article and its supplementary information files.

Systematic paleontology

Cynodontia Owen 1861

Probainognathia Hopson 1990

Prozostrodontia Liu and Olsen 2010

Prozostrodontidae clade nov.

Type genus *Prozostrodon brasiliensis* (Barberena et al. 1987).

Definition Most inclusive clade including *Prozostrodon brasiliensis* (Barberena et al. 1987) and *Pseudotherium argentinus* Wallace et al. 2019, but not *Therioherpeton cargnini* Bonaparte and Barberena 1975 nor *Morganucodon oehleri* Rigney 1963.

Diagnosis Prozostrodontids differ from other probainognathians by a unique combination of traits, which in association are not present in other clades: presence of a vertical septum of the vomer extending posteriorly to the level of the secondary palate; presence of prefrontal (absent in other prozostrodonts); fused prootic and opisthotic to form the petrosal (shared with most mammaliamorphs; sensu Rowe 1988); route of the venous drainage exiting from the back of the cavum epiptericum via a lateral flange vascular canal (shared with mammaliamorphs); maxillary and mandibular branches (V_{2+3}) of the trigeminal nerve exit via two foramina between the petrosal and alisphenoid (shared with tritylodontids); differentiated paroccipital process (shared with mammaliamorphs); and anteriormost one-cusped tooth not present in adults (shared with other prozostrodonts).

Prozostrodon brasiliensis (Barberena et al. 1987) (Figs. 3–6) (Table 1)

Holotype UFRGS-PV-0248-T consists of the anterior half of the skull with partial upper dentition, the right and left lower jaws with dentition, and several postcranial elements (see Bonaparte and Barberena 2001; Botha-Brink et al. 2018; Guignard et al. 2018).

Type locality and stratum Faixa Nova locality (Santa Maria, RS), *Hyperodapedon* AZ, Candelária Sequence, Santa Maria Supersequence, late Carnian (Langer et al. 2018).

Referred specimens CAPPA/UFSM 0123, right lower jaw with partial dentition (Pacheco et al. 2017); UFRGS-PV-0543-T, anterior portion of the skull with fragmented right lower jaw (Kerber et al. 2020).

New referred material CAPPA/UFSM 0210 comprises a complete and well-preserved skull with partial upper dentition, both lower jaws with partial dentition (Figs. 3–6), and some unprepared postcranial bones.

Emended diagnosis of *Prozostrodon brasiliensis* (Barberena et al. 1987) Probainognathian cynodont with the following association of features (autapomorphies marked with an asterisk): four upper incisors, increasing in size posteriorly; four lower incisors, slightly spatulate, decreasing in size posteriorly, with the apical third of the crown posteriorly inclined; lower canine with finely serrated distal margin; middle and posterior upper postcanine teeth with low crown, without distinctive cingula, with four mesiodistally aligned cusps (A–D), with cusps A>C≥B>>D*; posterior-most upper postcanine with distolabial accessory cusp; anterior lower postcanine teeth with conspicuous cusp a and small cusps b, c, and usually d; posterior lower postcanine teeth of ‘triconodont’ type, with cusps a>c>b>d, with continuous lingual cingulum bearing up to nine small discrete cusps*; length of the lower tooth row more than half the length of the dentary; lack of postorbital bone; lack of postorbital bar; lacrimal with large dorsal exposure; pronounced posterodorsal process of the premaxilla between the septomaxilla and maxilla; frontal, palatine, and orbitosphenoid contact in the orbital wall; secondary bony palate extended posteriorly beyond the last upper postcanine tooth; opisthotic and prootic fused, forming a petrosal bone; ribs without expanded processes; ‘Y’-shaped interclavicle; weakly twisted humerus with a perpendicularly projected deltopectoral crest, reaching the midshaft; expanded distal end representing about 58%

of the humeral length; presence of an ectepicondylar foramen; iliac blade with a reduced postacetabular portion and a well-developed anterodorsally projected preacetabular region; bulbous femoral head confluent with the greater trochanter and the shaft; short and medially projected lesser trochanter; and oval intertrochanteric fossa without marked trochanteric ridge (taken and modified from Bonaparte and Barberena 2001; Pacheco et al. 2017; Guignard et al. 2018; Kerber et al. 2020).

Description

Cranium

Rostral region CAPPA/UFSM 0210 has a long and narrow rostrum (Figs. 3a–b, 4a) (Table 1). The length of the rostral region is proportionally similar to the size of the temporal region of the cranium. The snout shows a marked constriction posterior to the upper canine root, which is confluent with the labial margin of the diastema (Figs. 3a–b, 4a). In the anterior portion of the rostrum, the premaxilla displays a large extranasal process, penetrating the maxilla and septomaxilla, but without contacting the nasal dorsolaterally (Fig. 4a). As in the prozostrodonts *Pseudotherium argentinus*, *Pachygenelus monus*, *Riograndia guaibensis*, and *Brasilodon quadrangularis*, the ascending process of the septomaxilla is long, far beyond the posterior border of the external nares (Figs. 3a, 4a).

The maxilla occupies most of the lateral surface of the rostral region (Figs. 3a, 4a). It forms a horizontal platform dorsal to the postcanine row in the posterior portion of the rostrum. On the lateral surface of the maxilla, there are three rostral alveolar foramina (Fig. 4a) (Benoit et al. 2019). The first one, a small opening more anteriorly

located, is positioned posterior to the canine alveolus bulge. Two other foramina are aligned dorsoventrally. They are placed dorsally to the diastema between the canine and the first postcanine (Fig. 4a). This arrangement is similar to that in the holotypes of *Prozostrodon brasiliensis* (UFRGS-PV-0248-T), *Therioherpeton cargnini*, and *Ps. argentinus*. However, the anteriormost foramen is not observable in UFRGS-PV-0248-T. In addition, a larger infraorbital foramen is positioned on the posterior portion of the lateral surface of the rostrum. It is located dorsally to the level of the posteriormost postcanines (Fig. 4a). The foramina arrangement and the branching pattern are similar to the pattern reconstructed for *B. quadrangularis* and tritylodontids (e.g., *Tritylodon longaevus*) (Benoit et al. 2019). According to the pattern recognized for these taxa, the maxillary canal is divided rostrally into the rostral alveolar and the infraorbital canals. The rostral alveolar canal is longer than the infraorbital canal, and it displays canals that open laterally to the surface of the maxillary bone. The infraorbital canal is comparatively short and opens laterally above the posterior postcanine teeth (Benoit et al. 2019). The zygomaticofacial foramen could not be identified.

The nasals comprised most of the dorsal surface of the rostral region of CAPPA/UFSM 0210 (Figs. 3a, 4a). A small foramen is present on this bone's dorsal surface, near the maxilla’s anterior contact.

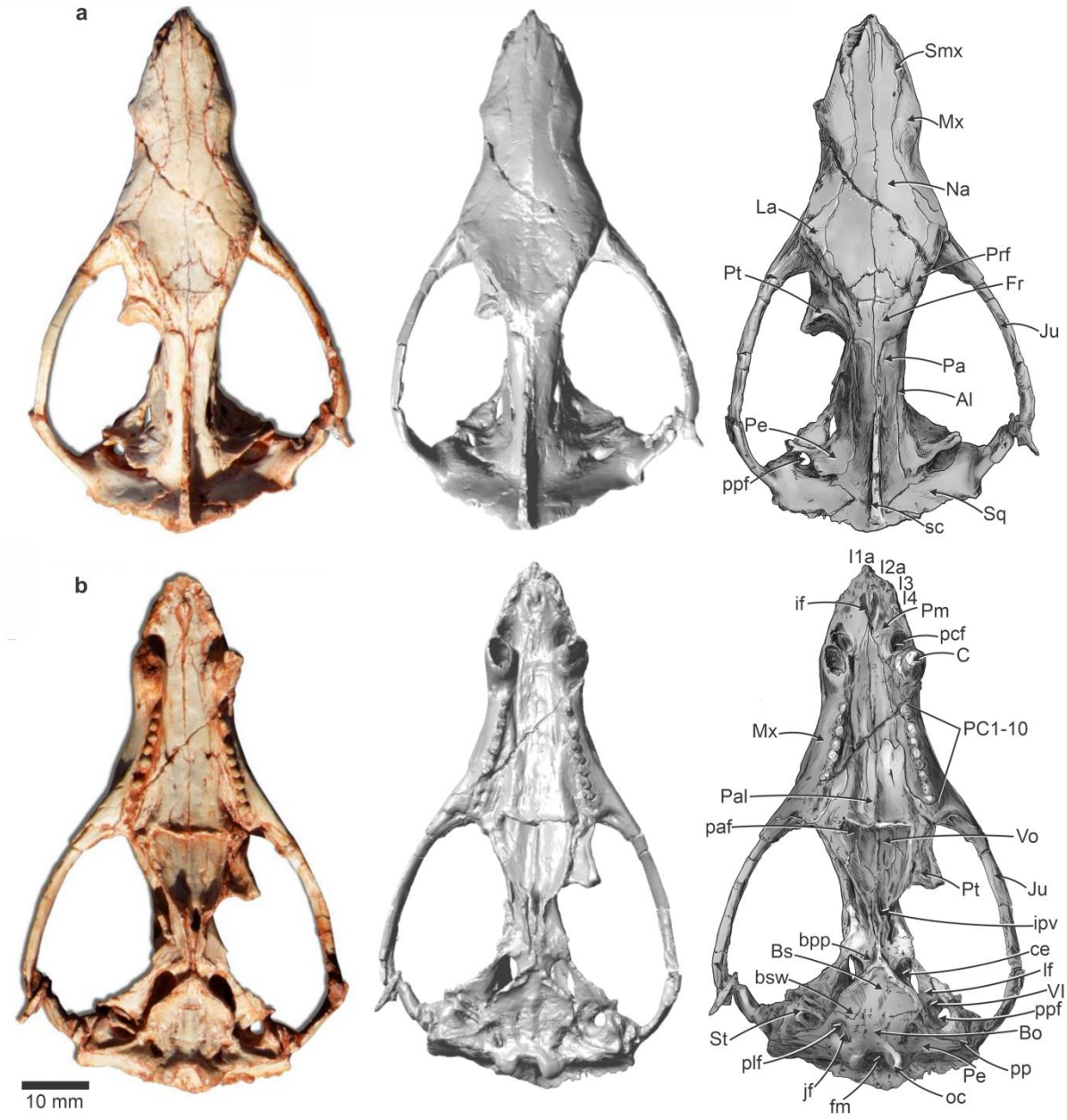

Fig. 3 Cranium of *Prozostrodon brasiliensis* (CAPPA/UFSM 0210) from the Late Triassic of southern Brazil. Photograph, tridimensional model, and schematic drawing, in dorsal (**a**) and ventral (**b**) views. Abbreviations: *Al* alisphenoid; *Bo* basioccipital; *bpp* basipterygoid process; *Bs* basisphenoid; *bsw* basisphenoid wing; *C* upper canine; *ce* cavum epiptericum; *fm* foramen magnum; *Fr* frontal; *I* upper incisor; *Ia* upper incisor alveolus; *if* incisive foramen; *ipv* interpterygoid vacuity; *jf* jugular foramen; *Ju* jugal; *La*

lacrimal; *lf* lateral flange; *Mx* maxilla; *Na* nasal; *oc* occipital condyle; *Pa* parietal; *paf* palatine flange; *pcf* paracanine fossa; *Pal* palatine; *Pc* upper postcanine; *Pe* petrosal; *plf* perilymphatic foramen; *Pm* premaxilla; *pp* paroccipital process; *ppf* pterygoparoccipital foramen; *Prf* prefrontal; *Pt* pterygoid; *sc* sagittal crest; *Smx* septomaxilla; *Sq* squamosal; *St* stapes; *VII* facial foramen; *Vo* vomer.

Orbital region In lateral view, the facial process of the lacrimal has a triangular shape (Fig. 4a). It is long and anteriorly developed, as in *T. cargnini*, but more developed than in *Ps. argentinus*. The lacrimal possesses a large anteroventral contact with the maxilla (Fig. 4a). The lacrimal foramen is located anteroventrally, near the border of the orbit.

The inner wall of the orbit of CAPPA/UFSM 0210 resembles the condition of *Ps. argentinus*. In these taxa, the orbital process of the lacrimal contributes broadly to forming the anteromedial wall of the orbit and meets the orbital process of the palatine, near the orbit floor (Fig. 4a). A fissure in the anterior rim of the orbit is pierced the maxillary foramen. It is positioned anteriorly to the wall of the orbit, between the lacrimal and palatine.

In lateral view, the prefrontal contributes to the anterodorsal margin of the orbit (Figs. 3a, 4a). The frontal borders the orbit and participates significantly in the medial wall of the orbit (Fig. 4a). As in the specimens UFRGS-PV-0248-T and UFRGS-PV-0543-T, the orbital process of the frontal contacts the orbital process of the palatine and the orbitosphenoid, similar to that of *M. oehleri* (Bonaparte and Barberena 2001). The orbital vacuity is delimited dorsally by the orbitosphenoid, anteriorly by the frontal, and posteriorly by the alisphenoid.

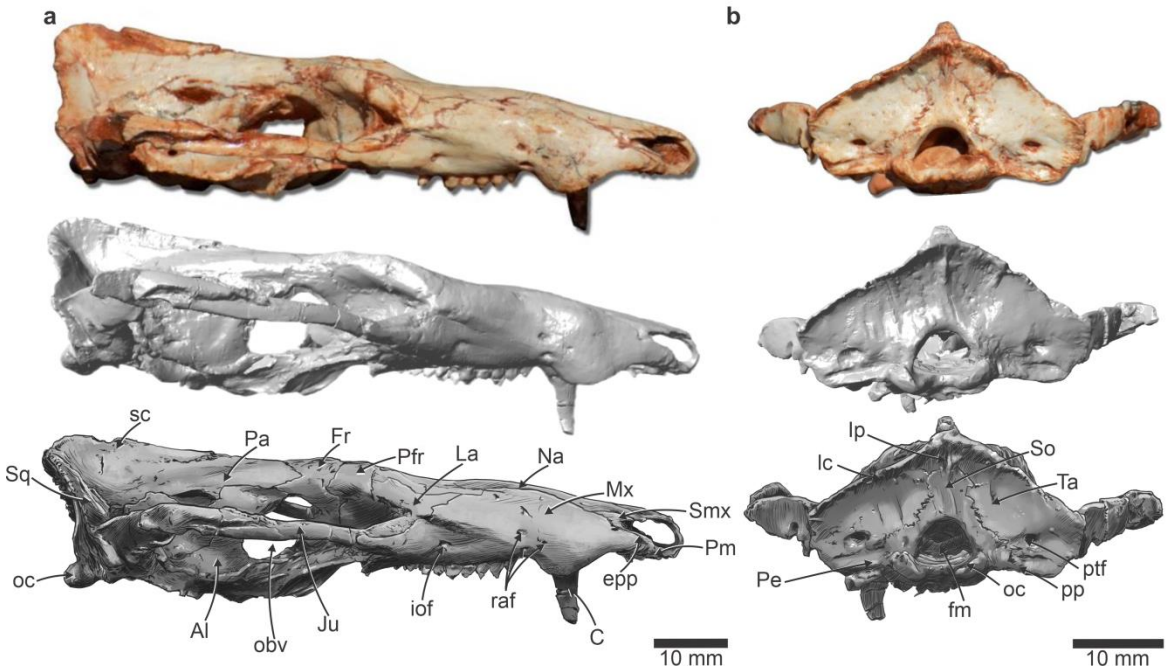

Fig. 4 Cranium of *Prozostrodon brasiliensis* (CAPPA/UFSM 0210) from the Late Triassic of southern Brazil. Photograph, tridimensional model, and schematic drawing, in right lateral (**a**) and posterior (**b**) views. Abbreviations: *Al* alisphenoid; *C* upper canine; *epp* extranasal process of the premaxilla; *fm* foramen magnum; *Fr* frontal; *iof* infraorbital foramen; *Ip* interparietal; *Ju* jugal; *La* lacrimal; *lc* lambdoidal crest; *Mx* maxilla; *Na* nasal; *obv* orbital vacuity; *oc* occipital condyle; *Pa* parietal; *Pe* petrosal; *Pm* premaxilla; *pp* paroccipital process; *ptf* posttemporal foramen; *Prf* prefrontal; *raf* rostral alveolar foramen; *sc* sagittal crest; *Smx* septomaxilla; *So* supraoccipital; *Sq* squamosal; *Ta* tabular.

Zygomatic arch Both zygomatic arches of CAPPA/UFSM 0210 are preserved (Figs. 3a–b, 4a). As in most prozostrodontians (e.g., *P. monus*, *B. quadrangularis*, and *T. cargnini*), the zygomatic arch is slender, dorsoventrally low, and formed mainly by the jugal. Differing from the pattern observed in more basal cynodonts, tritylodontids, and

Elliotherium kersteni, in which the zygomatic arch deepens posteriorly (Sidor and Hancox 2006), CAPPA/UFSM 0210 has uniform height throughout its length (Table 1).

The maxilla's posterior and ventral portion forms the zygomatic arch's root (Fig. 4a). As in the holotype (UFRGS-PV-0248-T) and *Ps. argentinus*, the anteroventral corner of the zygomatic arch lies at the same level as the postcanine line. In dorsal extension, the zygomatic arch occupies the portion below the middle of the orbit (Fig. 4a). This condition is similar to *P. monus*, *T. cargnini,* and *B. quadrangularis*. The lateralmost curvature of the arch is located at the level of the middle-posterior region of the cranium (Figs. 3a–b, 4a). Therefore, the temporal fossa is widest in the posterior region (Figs. 3a–b, 4a). In addition, the posteroventral process of the jugal is low, as in other prozostrodonts (e.g., *R. guaibensis*, *P. monus*, and *B. quadrangularis*). There is no evidence of an orbital process on the zygoma, and the postorbital process on the frontal is subtly defined.

Skull roof The frontal contributes significantly to the skull roof. The suture between the frontal and nasal is anteriorly convex, forming a triangular anterior projection at the anteromedial contact (Fig. 3a). This condition is similar to that of other specimens of *Pr. brasiliensis* (UFRGS-PV-0248-T; UFRGS-PV-0543-T).

The prefrontal also is observable in the dorsal view (Fig. 3a). The presence of the prefrontal bone is shared with most early diverging probainognathians (e.g., *Probainognathus jenseni*, *Chiniquodon theotonicus*, and ecteniniids) and also with the prozostrodontid *Ps. argentinus*. However, the prefrontal is absent in more derived forms, such as *T. cargnini*, tritylodontids, ‘ictidosaurs’, brasilodontids, and mammaliaforms.

As in other prozostrodonts, both the postorbital bone and the postorbital bar are absent in the new specimen of *Pr. brasiliensis*. Among prozostrodonts, the only taxon

retaining a postorbital bone is *Ps. argentinus*, although it is greatly reduced and does not form a postorbital bar (Wallace et al. 2019).

Palate The secondary osseous palate of CAPPA/UFSM 0210 is long and ventrally flat (Fig. 3b) (Table 1). Its posterior border extends back to the last postcanine level and the anterior orbital margin level. These traits are shared by derived prozostrodonts and early mammaliaforms (Kermack et al. 1981; Bonaparte and Barberena 1975; Bonaparte and Barberena 2001; Bonaparte et al. 2001, 2003, 2005; Wallace et al. 2019; Kerber et al. 2022), whereas in early divergent probainognathians the secondary palate is slightly (Romer et al. 1970; Abdala and Giannini 2000; Martinelli et al. 2016, 2017c) or considerably shorter (Martínez et al. 1996, 2013; Hopson and Kitching 2001; Oliveira et al. 2010; Benoit et al. 2022).

The premaxilla forms the anterior portion of the secondary palate (Fig. 3b). As in *Ps. argentinus* and *B. quadrangularis,* the medial margin of each premaxilla has a ventrally directed process that meets its counterpart at midline but does not fuse to it. The premaxilla does not form the posterior border of the incisive foramen, distinctly from *P. monus* and *C. theotonicus*, for example, in which the premaxilla encircles the incisive foramen. The maxilla comprises most of the anterior half of the secondary palate (Fig. 3b). The paracanine fossa is located in the anteriormost region of the palate, anteromedially to the upper canine (Fig. 3b). This pattern is also observed in most cynodonts (Bonaparte et al. 2003, 2005; Martinelli et al. 2005; Wallace et al. 2019; Kerber et al. 2022). As in *Ps. argentinus*, the maxilla is excluded from the border of the subtemporal fenestra (Wallace et al. 2019).

The palatine is anteroposteriorly elongated and forms the posterior half of the secondary palate (Table 1). The palatine flanges contact the vomer medially, which forms

the anterior portion of the primary palate (Fig. 3b). As in the holotype (UFRGS-PV-0248-T) and *Ps. argentinus*, there is an anteroposteriorly vertical septum on the vomerine surface extending posteriorly to the level of the secondary palate (Fig. 3b). The interpterygoid vacuities are open but poorly developed. They are anteroposteriorly elongated and transversely narrow (Fig. 3b). They are bordered laterally by the transverse processes of the pterygoids and posteriorly by the basisphenoid-parasphenoid complex. The interpterygoid vacuities are generally considered closed in adult specimens of non-prozostrodontian eucynodonts (e.g., traversodontids, and basal probainognathians) and apparently remained opened in most non-mammaliaform prozostrodonts as part of the reorganization of the mesocranium (Martinelli and Rougier 2007).

Temporal region The temporal region of the cranium of CAPPA/UFSM 0210 is anteroposteriorly subequal in length compared to the rostral region (Figs. 3a, 4a). The roof of the braincase is slightly vaulted and proportionally narrow, as in *Ps. argentinus* and *T. cargnini*, but less developed than in *B. quadrangularis* and *M. oehleri*.

The parietals form the roof of the endocranial cavity. At the midline, they are fused along the sagittal crest (Figs. 3a, 4a). Ventrally, they are in contact with the petrosal's anterior lamina and the alisphenoid's well-expanded ascending process. On the lateral side of the braincase, two foramina for the maxillary (V_2) and mandibular (V_3) branches of the trigeminal nerve are present between the petrosal and alisphenoid. This feature is shared with *Ps. argentinus* and tritylodontids (e.g., *T. longaevus* and *K. wellesi*) but differs from *P. jenseni* (Romer 1970) in which the trigeminal nerve exits via a single foramen. Conversely, in *B. quadrangularis* and early mammaliaforms (Kermack et al. 1981; Lucas and Hunt 1990; Crompton and Luo 1993; Bonaparte et al. 2003, 2005; Rodrigues et al.

2013), the foramina are exclusively on the anterior lamina of the petrosal. The sagittal crest continues posterolaterally to a well-developed lambdoidal crest, which forms the roof of the occiput (Fig. 4a–b). There is no evidence of a parietal foramen.

The parietal contacts the interparietal (=post-parietal), which contributes to the posterior end of the sagittal crest (Figs. 3a, 4a–b). Dorsally, the squamosal forms the anteroventral portion of the lambdoidal crest (Fig. 4a–b).

Basicranium The most striking feature of this region is the presence of a fused prootic and opisthotic, forming the petrosal (=periotic) but without developing a promontorium (Fig. 3b). Conversely, in the derived prozostrodont *B. quadrangularis,* the petrosal develops an incipient promontorium (Bonaparte et al. 2003, 2005, 2012; Rodrigues et al. 2013), and in mammaliaforms (Kermack et al. 1981; Lucas and Hunt 1990; Crompton and Luo 1993), the petrosal bears a well-defined promontorium.

In the medial portion of the basicranium, the parabasisphenoid complex is formed by the fusion of the basisphenoid and parasphenoid (Fig. 3b). The basipterygoid process of the basisphenoid extends anteriorly and contacts the pterygoid. The basisphenoid wings (=parasphenoid ala) are slightly reduced and bifurcated laterally (Fig. 3b). They extend near the anterior end of the pars cochlearis but do not participate in the border of fenestra vestibuli. In early mammaliaforms, the wings are reduced or absent (in, e.g., *M. oehleri* and *S. rigneyi*). In contrast, in *B. quadrangularis* and *A. cromptoni,* the basisphenoid wing is reduced and covers only a small portion of the pars cochlearis. The condition of CAPPA/UFSM 0210 resembles *Ps. argentinus* in that the basisphenoid wings are more expanded than in more derived forms but less developed than in *P. jenseni* (Luo 1994).

The anterior area of the cavum epiptericum is bordered by the medial expansion of the basipterygoid process of the basisphenoid and posteriorly by the lateral flange of the petrosal (Fig. 3b). The pterygoparoccipital foramen opens laterally as a thin notch (Fig. 3b). However, in dorsal view, the posterior process of this foramen surpasses the anterior one, making it appear closed. The open pterygoparoccipital foramen is a derived condition shared with other prozostrodonts (e.g., *P. monus*, *Ps. argentinus*, *R. guaibensis*, and *B. quadrangularis*) (Hopson and Rougier 1993; Bonaparte et al. 2005; Soares et al. 2011; Wallace et al. 2019), and mammaliaforms (Kermack et al. 1981; Luo 1994). In some eucynodonts, this foramen is completely closed laterally (e.g., gomphodonts, *C. theotonicus,* and *Lumkuia fuzzi*) (e.g., Hopson and Kitching 2001).

The anteriormost opening of the ventral exposure of the petrosal is here interpreted as the facial foramen (nerve VII; Rougier et al. 1992) (Fig. 3b). Posteromedially to this foramen, the fenestra vestibuli (=fenestra ovalis or oval window) is not rimmed and opens laterally (Fig. 3b). The specimen also preserves an incomplete right stapes (Fig. 3b). In the posteromedial portion of the basicranium, the jugular foramen and the perilymphatic foramen (=fenestra rotunda or round window) share a common ‘figure 8’-shaped fossa, without an ossified division/septum (Fig. 3b). The jugular foramen is anteroposteriorly elongated, while the perilymphatic foramen is smaller and is placed anterolaterally (Fig. 3b).

The lateral flange of the petrosal is quite similar to that of *Ps. argentinus* (Wallace et al. 2019), but less developed than in *B. quadrangularis* (Bonaparte et al. 2003), *A. cromptoni* (Lucas and Luo 1993), and *M. oehleri* (Kermack et al. 1981). The quadrate and the quadratojugal are not preserved.

Occipital region The interparietal and tabular, respectively, participate in the dorsal and lateral portions of the lambdoidal crest (Fig. 4b). The tabular surrounds the posttemporal foramen (Fig. 4b), unlike in *B. quadrangularis,* in which the foramen is located between the tabular and petrosal (Bonaparte et al. 2003). Ventral to this foramen, there is a posterior extension of the paroccipital process (Fig. 4b). This same pattern of arrangement of bones is observed in *L. fuzzi* and *Ps. argentinus* (Hopson and Kitching 2001; Wallace et al. 2019).

The exoccipital contributes to the lateral margin of the foramen magnum, whereas the supraoccipital and basioccipital delimitate the entire dorsal and ventral borders of this foramen, respectively (Fig. 4b).

Upper dentition Based on the alveoli and the right and left upper dentitions, CAPPA/UFSM 0210 presents four incisors (I), one canine (C), and ten postcanines (PC) (I4/C1/PC10) (Figs. 3b, 6a). Only the base of the crown of the fourth left incisor (I4) is preserved.

The upper left canine is long, slightly curved, and bears a sulcus on its labial surface, without serrations on its mesial and distal edges (Figs. 3b, 4a, 6a). The crown morphology of the canines resembles *Ps. argentinus*, whereas, in *B. quadrangularis,* it is transversely flat with a dorsoventrally smooth sulcus on the anterolateral surface (Bonaparte et al. 2005). There is a diastema between the canine and the first upper postcanine (Fig. 6a).

The morphology of the postcanine crowns is of the “triconodont” type, with cusps aligned mesiodistally (Figs. 3b, 6a), resembling the pattern observed in the other specimens of *Pr. brasiliensis*, prozostrodontian cynodonts (e.g., *T. cargnini*, *Ps. argentinus*, and *B. quadrangularis*; Bonaparte and Barberena, 2001; Bonaparte et al.

2005; Martinelli et al. 2017a, 2017b; Wallace et al. 2019), and also in early mammaliaforms (Kermack et al. 1981). The upper postcanine series of CAPPA/UFSM 0210 includes ten functional teeth. The preserved postcanine crowns increase in size and complexity posteriorly (Fig. 6a). The overall pattern of cusps disposition observed in postcanine crowns consists of three to four cusps disposed in line in the labial margin of the crown, without distinctive cingula (Fig. 6a). In contrast, the anterior/middle postcanine teeth comprise a large main cusp (A) and mesial and distal cusps, B and C, respectively, the posterior postcanines present four main cusps (A–D). In these last postcanines, the main cusp (A) is positioned in the mesial half of the crown, followed by three smaller mesial and distal cusps (B, C, and D, respectively) (Fig. 6a). The height pattern among all cusps is A>C≥B>>D. This same pattern is observed in posterior postcanines of *Pr. brasiliensis* (UFRGS-PV-0248-T).

Six postcanine teeth are preserved in the right postcanine series, plus four alveoli. The first five teeth have the crown preserved, except for the PC4, which preserves only half of the crown. The PC1 has two cusps (A-B), whereas the PC2-3 and PC5 have three aligned mesiodistally cusps (A-C). The crown of the PC6 is missing, having only the alveolus. There is a complete PC7, with an additional cusp (D) labially displaced compared to A-C. Distally to this last functional tooth, there are the alveoli to of the PC8-10 (Fig. 3b).

The left postcanine dentition preserves eight postcanine teeth plus two alveoli. Only the base of the crown of the PC1 is preserved. The first complete tooth is the PC2. The crown of the PC3 is missing. Distally to this alveolus, there are the functional teeth PC4-9. PC2 and PC4-6 have three aligned cusps (A-C), while the PC7-9 have four cusps mesiodistally aligned (A-D). Finally, the functional tooth PC10 is missing (Fig. 6a).

Lower jaw

The right and left lower jaws of CAPPA/UFSM 0210 have preserved complete dentary bones, lacking the postdentary bone complex (Figs. 5a–b, 6b–c).

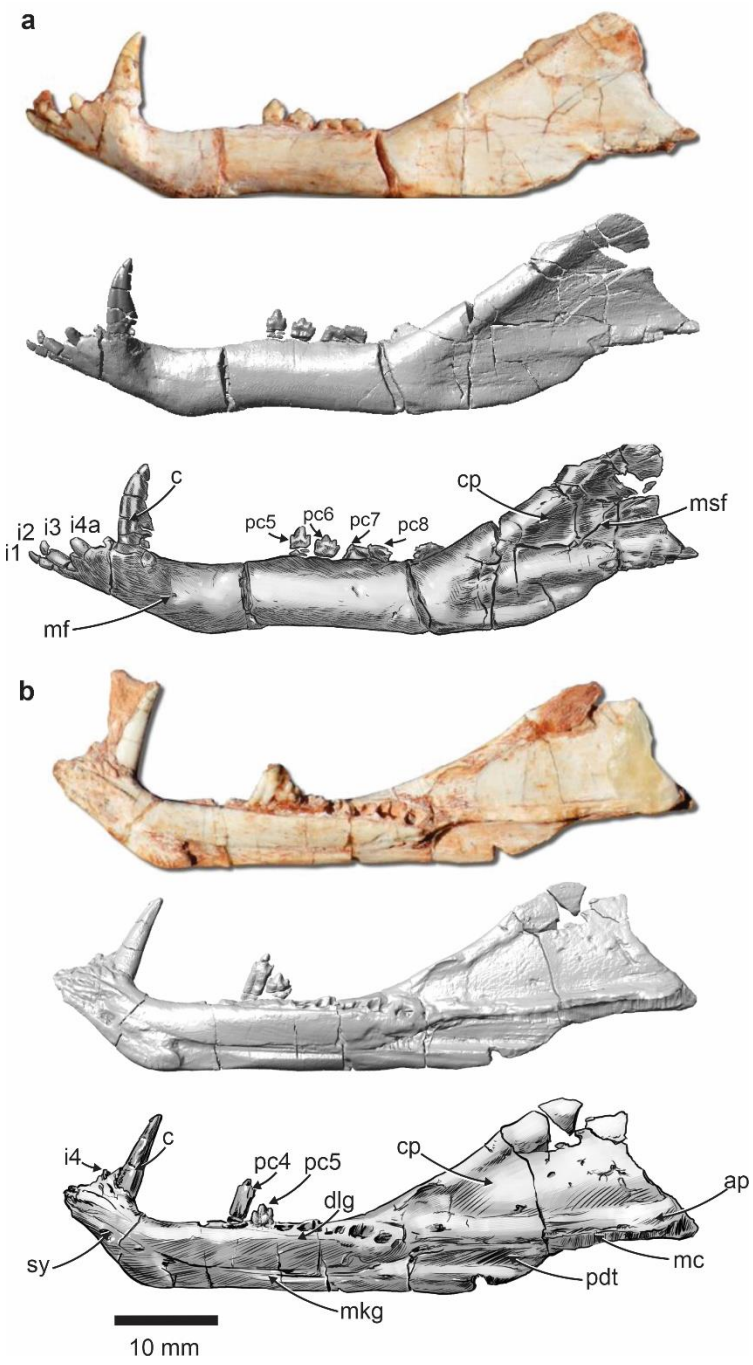

Fig. 5 Left and right lower jaws of *Prozostrodon brasiliensis* (CAPPA/UFSM 0210) from the Late Triassic of southern Brazil. Photograph, tridimensional model, and schematic drawing, in lateral (**a**) and medial (**b**) views. Abbreviations: *ap* articular process; *i* lower incisor; *ia* lower incisor alveolus; *c* lower canine; *cp* coronoid process; *dlg* dental lamina groove; *mc* medial crest; *mf* mental foramen; *msf* masseteric fossa; *mkg* Meckelian groove; *pc* lower postcanine; *pdt* postdentary trough; *sy* symphysis.

Dentary The dentary includes its horizontal ramus, the Meckelian groove, the coronoid process, the articular process, and the postdentary trough. In lateral view, the horizontal ramus is anteroposteriorly long (Fig. 5a–b), similar to that of other specimens of *Pr. brasiliensis* (UFRGS-PV-0248-T; UFRGS-PV-0543-T; CAPPA/UFSM 0123). In *B. quadrangularis*, *Santacruzgnathus abdalai*, *Alemoatherium huebneri*, and basal mammaliaforms (Bonaparte et al. 2005; Martinelli et al. 2016, 2017a), the ramus is slenderer. On the other hand, in some other Late Triassic probainognathians (e.g., *Irajatherium hernandezi*, *Candelariodon barberenai*, and *Agudotherium gassenae*; Martinelli et al. 2005, 2017b; Oliveira et al. 2011; Stefanello et al. 2020), the horizontal ramus of the dentary is more robust than in CAPPA/UFSM 0210. In addition, this ramus becomes slightly deeper posteriorly, evidencing the development of a well-defined masseteric fossa. The anterior portion of the dentary is anterodorsally projected (Fig. 5a). Therefore, the alveolar level of the incisors and canine is positioned slightly above the postcanine alveolar level (Fig. 5a–b). This feature is shared with other specimens of *Pr. brasiliensis* and also with *Botucaraitherium belarminoi*, *B. quadrangularis*, and *A. gassenae* (Bonaparte et al. 2005; Soares et al. 2014; Stefanello et al. 2020). On the lateral surface of the dentary, the mental foramen is located at the level of the canine

(Fig. 5a). Medially, the alveolar margin bears a thin groove for the dental lamina. The groove of the dental lamina begins posteriorly to the canine and extends up to the alveolus of the last postcanine tooth (Fig. 5b).

The mandibular symphysis is unfused, as in other prozostrodonts (e.g., Bonaparte and Barberena 2001; Bonaparte et al. 2001, 2005; Martinelli et al. 2005, 2017a; Martinelli and Rougier 2007; Soares et al. 2014; Stefanello et al. 2020). The symphysial region is elongated and projected anterodorsally (Fig. 5b). In medial view, the Meckelian groove is parallel and near the ventral border of the horizontal ramus of the dentary (Fig. 5b). The location of the groove is similar to that of other specimens of *Pr. brasiliensis* (UFRGS-PV-0248-T; CAPPA/UFSM 0123). In this view, the trough for the postdentary bones is located in the dorsoventral half of the posterior portion of the dentary. This trough extends anteriorly to the Meckelian groove (Fig. 5b).

As in the holotype UFRGS-PV-0248-T and mammaliaforms (e.g., *M. oehleri*; Kermack et al. 1981), the articular process is well defined, forming the posteriormost point of the dentary (Fig. 5a–b). Although elongate, it shows no evidence of an articular condyle. The coronoid is preserved in the right lower jaw, largely fused to the ascending ramus of the dentary. The coronoid process is anteroposteriorly wide and dorsoventrally tall (Fig. 5b). It develops posteriorly to the last postcanines, similar to other specimens of *Pr. brasiliensis* (UFRGS-PV-0248-T; CAPPA/UFSM 0123).

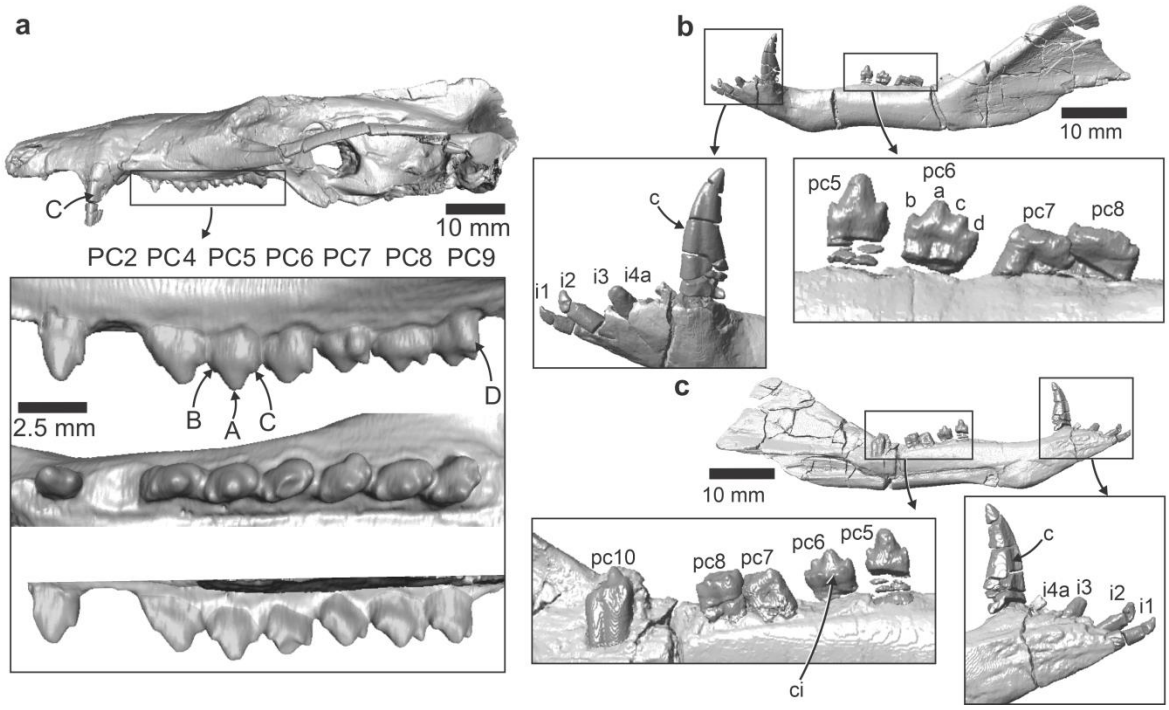

Fig. 6 Cranium and left lower jaw of *Prozostrodon brasiliensis* (CAPPA/UFSM 0210) from the Late Triassic of southern Brazil. Tridimensional model of the cranium (**a**) highlighting the left postcanine series in labial, occlusal, and lingual views (top to bottom in box). Tridimensional model of the left lower jaw highlighting in lateral (**b**) and medial (**c**) views; **b**. Details of the incisors and canine (anterior box) and postcanines (posterior box); **c**. Details of the postcanines (anterior box) and incisors and canine (posterior box). Abbreviations: *i* lower incisor; *ia* lower incisor alveolus; *c* lower canine; *C* upper canine*; ci* lingual cingulum; *pc* lower postcanine; *Pc* upper postcanine.

Lower Dentition Based on the alveoli and preserved right and left lower dentitions, the dental count for CAPPA/UFSM 0210 is four incisors (i), one canine (c), and ten postcanines (pc) (i4/c1/pc10) (Figs. 5a–b, 6b–c), as in the holotype UFRGS-PV-0248-T. The right lower jaw preserves only the crown base of the fourth incisor. The

micro-CT revealed three incisor alveoli, probably i1, i2, and i3 (Fig. 5b). In addition, near to canine, there is a complete crown of an isolated incisor tooth in the rock matrix. The crown of this incisor is long, and its tip is slightly curved.

There are three left lower incisors preserved. The i1 and i2 are complete, similar in size and shape. The crown of these first incisors is tall, and its tips are curved posteriorly. The i3 preserves only half of the crown. The micro-CT data indicate an incisor alveolus near the canine, interpreted as the i4 (Figs. 5a, 6b–c).

Both the right and left canines are well-preserved. The canine does not present serrations on its mesial and distal edges, differing from the holotype, which has tiny serrations on the distal portion (UFRGS-PV-0248-T). The crown is distally curved, with the mesial edge convex, whereas the distal one is slightly concave. There is a diastema between the canine and the alveolus to the first postcanine (Figs. 5a–b, 6b–c).

The lower postcanine series of CAPPA/UFSM 0210 includes ten functional teeth. They present with non-serrated cusps (Figs. 5a–b, 6b–c). The overall pattern of cusp disposition observed in postcanines with preserved crowns consists of three to four cusps arranged in line along the labial margin of the crown, with a continuous, cuspidate lingual cingulum. The cusps are vertically directed (Fig. 6b–c). There is a large main cusp (a) on the mesial half of the crown, followed by two or three smaller mesial and distal functional cusps (b, c, and d, respectively). Cusp a is larger than cusp c. The cusp b is positioned in the mesial portion of the crown, whereas cusp d is positioned more distally and is comparatively smaller than the other cusps (Fig. 6b–c). The height pattern among all cusps is a>c>b>d.

Only two postcanine teeth are preserved in the right postcanine series, plus eight alveoli, making for ten teeth (Fig. 5b). The preserved teeth are interpreted as pc4 and

pc5 due to the probable presence of three alveoli between the canine and the two preserved postcanine crowns (pc4 and pc5). Distally to these teeth, there are five alveoli, with the last tooth, at the end of the tooth row, unerupted inside the bone. Three-dimensional reconstructions show the presence of this replacement postcanine, which can be interpreted as pc10. The crowns of pc4-5 are damaged to some degree. They have three aligned cusps, a main cusp (a) and mesial (b) and distal (c) cusps, respectively. The pc4 is displaced from the alveolus, partially exposing the root. In addition, the crown of this tooth appears to be slightly inclined distally (Fig. 5b).

The left postcanine series preserves five postcanine teeth plus five alveoli (Figs. 5a, 6b–c). The preserved teeth are considered the pc5-8 due to the presence of four alveoli between the canine and the first preserved postcanine tooth (pc5). They show a continuous, multi-cuspidate lingual cingulum (Fig. 6c). The pc5 has three aligned cusps (a-c), whereas the pc6 has an additional cusp (d) labially displaced in comparison to a-c. The crowns of pc7-8 are damaged to some degree, preserving only half of the crown. The crown of the pc9 is missing, having only the alveolus. Distally to this alveolus, there is functional tooth pc10, with four aligned cusps (a-d) (Figs. 5a, 6b–c).

Measure	mm
basal skull length	93.93
parietals length at midline	26.7
snout length	42.1
length of secondary palate	41.0
length of secondary palatal shelf of maxilla	19.6
length of secondary palatal shelf of palatine	13.7
orbit height	6.7
zygomatic arch height	3.6
zygomatic arch lateromedial thickness	2.1
skull greatest width at occipital plate	36.4
skull greatest height at occipital plate	19.5
greatest length of right lower jaw	65.2
greatest length of left lower jaw	70.3
greatest height of right lower jaw	14.3
greatest height of left lower jaw	15.2
length of complete right upper tooth row	40.1
length of complete left upper tooth row	40.3
length of postcanine right upper tooth row	19.1
length of postcanine left upper tooth row	18.2
left upper canine height	8.7
length of complete right lower tooth row	37.7
length of complete left lower tooth row	41.1
length of postcanine right lower tooth row	24.8
length of postcanine left lower tooth row	24.4
right lower canine height	9.4
left lower canine height	8.8

Table 1. Craniomandibular and dental measurements of *Prozostrodon brasiliensis* (CAPPA/UFSM 0210) (taken according to Oliveira et al. 2010).

Phylogenetic analysis

The phylogenetic analysis recovered four most parsimonious trees of 488 steps each (consistency index, 0.453; retention index, 0.774) (Figs. 7–8). *Lumkuia fuzzi* nests as the basalmost member of Probainognathia (Figs. 7–8), corroborating some previous hypotheses (Hopson and Kitching 2001; Ruta et al. 2013; Martínez et al. 2013; Stefanello et al. 2018; Kerber et al. 2022; Benoit et al. 2022). *Protheriodon estudianti* emerges as the sister taxon to Prozostrodontia as recovered by Martinelli et al. (2016). The clade Prozostrodontia (Figs. 7–8) is supported by four character state transformations in the strict consensus tree: osseous palate extends more than 45% of skull length (36: 0→1); unfused dentary symphysis (82: 1→0); upper postcanine roots are constricted, with longitudinal groove (106: 0→1); and lower postcanine roots are constricted, with longitudinal groove (107: 0→1).

Prozostrodon brasiliensis and *Pseudotherium argentinus* are recovered in a sister taxon relationship, which is supported by the vomer with a vertical septum extending posteriorly to the level of the secondary palate (29: 1→0); prootic and opisthotic fused to form the petrosal (49: 0→1); route of the venous drainage exiting from the back of the cavum epiptericum via a lateral flange vascular canal (56: 1→2); maxillary and mandibular branches (V_{2+3}) of the trigeminal nerve exit via two foramina present between the petrosal and alisphenoid (57: 0→1); presence of a vertical component of a lateral flange of prootic (59: 0→1); differentiated paroccipital process (62: 0→1); and anteriormost one-cusped tooth not present in adults (103: 0→1). The clade containing both species is here established as Prozostrodontidae nov. (Figs. 7–8), which is the sister group to all the other prozostrodonts. *Therioherpeton cargnini* is recovered as the

earliest member of the group of non-prozostrodontid prozostrodonts, the same position as some previous studies (Liu and Olsen 2010; Soares et al. 2014; Martinelli et al. 2017a, 2017b).

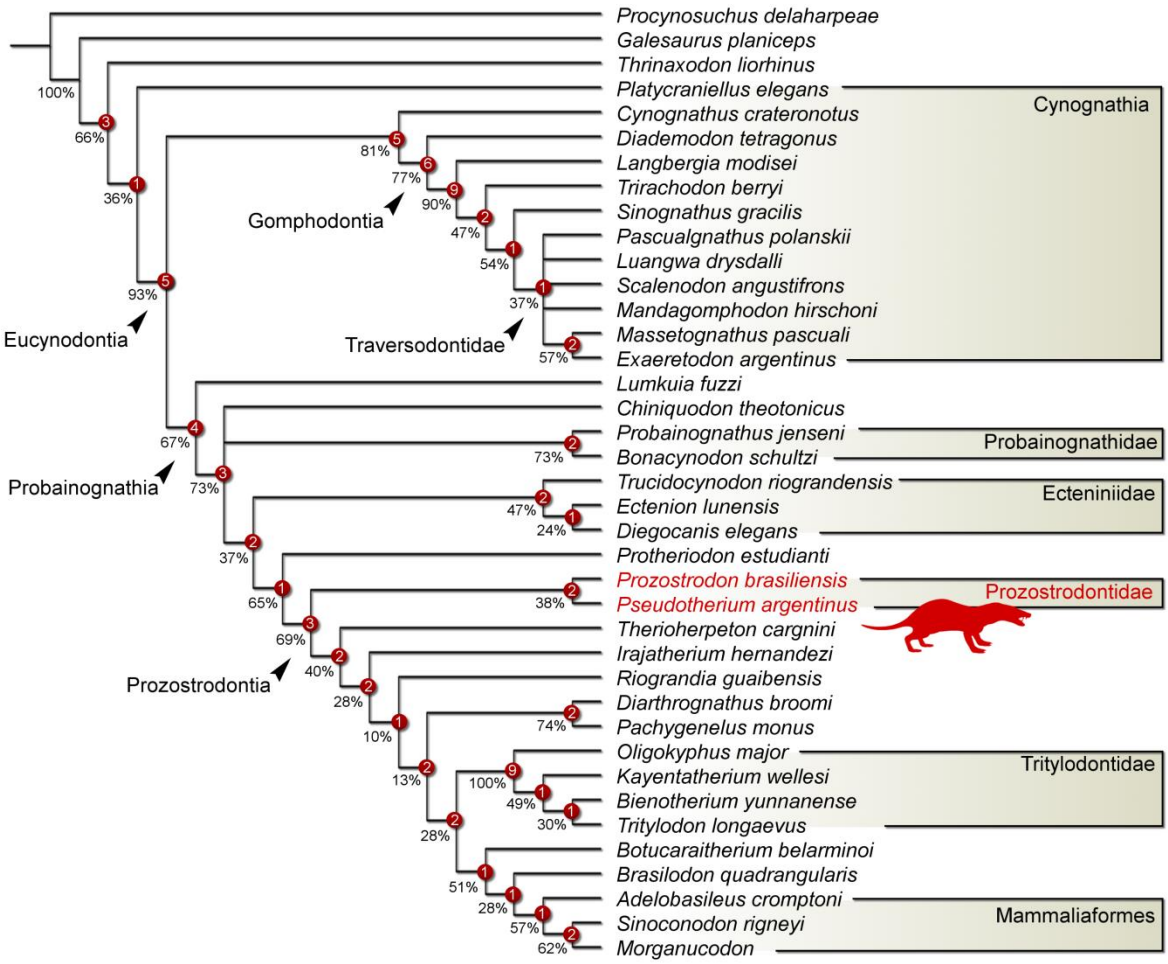

Fig. 7 Strict consensus of the phylogenetic analysis of Eucynodontia, showing the Bootstrap value and Bremer support (red circles). Silhouette highlighted in red represented the Prozostrodontidae clade nov.

Discussion and conclusions

Western Gondwana experienced sub-humid conditions in some intervals of the Carnian, possibly associated with the Carnian Pluvial Event (CPE) (Bernardi et al. 2018; Dal Corso et al. 2020; Holz and Scherer 2000; Mancuso et al. 2021). The higher humidity may have given rise to new environments (and ecological niches), possibly more diverse floristically, and, consequently faunistically, due to the greater availability of resources. An important step in the evolution of probainognathians occurred during this moment – the origin and early diversification of prozostrodonts (Liu and Olsen 2010; Martinelli et al. 2016, 2017a, 2017b). According to the support measurements of our analysis, this group is one of the best-supported probainognathian clades (Fig. 7).

The specimen reported here is the best-preserved skull of a Carnian prozostrodont. It is referred to *Prozostrodon brasiliensis* based on shared characteristics with the holotype (see emended diagnosis). However, the new specimen displays some differences with the holotype (UFRGS-PV-0248-T) and referred specimen (UFRGS-PV-0543-T), as follows:

i. CAPPA/UFSM 0210 has slightly smaller size than UFRGS-PV-0248-T and UFRGS-PV-0543-T, a trait explained by differences between the ontogenetic stages of the specimens.

ii. CAPPA/UFSM 0210 presents an inverted V-shaped fronto-nasal suture, while in UFRGS-PV-0248-T and UFRGS-PV-0543-T this suture is transverse. Jasinoski and Abdala (2017) demonstrated that although there are some variations, there is a general pattern in the ontogeny of *Thrinaxodon liorhinus* in which younger individuals tend to show an inverted V-shaped suture while adults tend to have a transverse suture.

iii. CAPPA/UFSM 0210 displays a longer rostrum (muzzle) than UFRGS-PV-0248-T. Comprehensive studies of the cynodont skull ontogeny have been shown different patterns of the allometric growth of the rostrum compared with the skull length: isometry (Abdala and Giannini 2000; Jasinoski and Abdala 2017; Wynd et al. 2021); negative allometry (Abdala and Giannini 2002), and positive allometry (Jasinoski et al. 2015). Upon the proposal of synonymy of *Brasilodon quadrangularis* and *Brasilitherium riograndensis* (e.g., Liu and Olsen 2010), it can be observed that smaller specimens of this prozostrodont (e.g., UFRGS-PV-594-T, UFRGS-PV-929-T; Bonaparte et al. 2003, 2005) have relatively longer rostrum than ontogenetically older specimens (e.g., UFRGS-PV-628-T, UFRGS-PV-1043-T; Bonaparte et al. 2005, 2012; Botha-Brink et al. 2018). Further, it was a feature used to differentiate both species (Bonaparte et al. 2003, 2005). Hence, the variation in specimens of *Pr*. *brasiliensis* can be related to ontogeny, but other explanations, such as individual variation, cannot be excluded. Considering that growth strategies are highly variable amongst the different cynodont groups, only further specimens will permit to elucidate this feature properly.

iv. CAPPA/UFSM 0210 has ten functional upper postcanines, whereas the holotype has eight. However, the number and the complexity of sectorial postcanines can be variable in cynodonts during the ontogeny (see Crompton 1963; Martinelli et al. 2005; Martinelli and Bonaparte 2011; Abdala et al. 2013; Norton et al. 2020). The holotype UFRGS-PV-0248-T also presents variation between the left and right series. It has seven plus one in eruption in the upper right and six plus one in the left upper side (Bonaparte and Barberena 2001);

v. CAPPA/UFSM 0210 does not have serrations on the mesial nor distal edge of the upper/lower canines. The holotype of *Pr. brasiliensis* had no evidence of serrated

margins (e.g., Bonaparte and Barberena 2001) until its recent re-preparation at the UFRGS by one of us. It permitted the identification of an irregular serrated distal margin only in the left lower canine, near the apex of the crown. We cannot properly assert the condition of this feature in the remaining canines of the holotype (e.g., the mesial edge of the lower/upper canines or in the mesial/distal margins of the upper canines). Consequently, the difference between the specimens from the Marchezan site (CAPPA/UFSM 0210; Pacheco et al. 2017) and the holotype may reflex a feature that varies across ontogeny or individual variations. Although serrations on canines and/or postcanines have been used as diagnostic traits for some probainognathian taxa (e.g., Martínez and Forster 1996; Oliveira et al. 2010; Martinelli et al. 2016) other relevant features accompany the proposal for a different taxon.

vi. Some differences in the complexity of the lingual cingulum of the lower postcanines of CAPPA/UFSM 0123 and the holotype of *Pr. brasiliensis* were highlighted and explained by the variability of tooth morphologies during postcanine replacement by Pacheco et al. (2017). Changes in tooth morphology in the same tooth locus are common among cynodonts (e.g., Hopson 1973; Martinelli and Bonaparte 2011; Abdala et al. 2013; Northon et al. 2020) and the same examples can be used to explain the subtle differences in the crown configuration of CAPPA/UFSM 0210.

Although little is known about the ontogeny of non-mammaliaform probainognathians, some of these differences can be explained by ontogenetic (or interspecific) variation based on comparisons with other cynodont ontogenetic stages/series (e.g., Rigney 1938; Crompton 1963; Abdala et al. 2013; Jasinoski et al. 2015; Jasinoski and Abdala 2017). Our suggestion is that CAPPA/UFSM 0210 is not a juvenile, but is younger than the other skulls assigned to this taxon (i.e., Bonaparte and

Barberena 2001; Kerber et al. 2020). The same considerations are valid for CAPPA/UFSM 0123, the other specimen from Marchezan site described by Pacheco et al. (2017). An alternative hypothesis, which appears to be less parsimonious, is that CAPPA/UFSM 0210 would be a distinct species of *Pr. brasiliensis.*

The new data support the hypothesis of Liu and Olsen (2010), where *Pr. brasiliensis* nests as an early-diverging prozostrodont; also supported by subsequent studies (e.g., Soares et al. 2014; Martinelli et al. 2017a; Wallace et al. 2019; Kerber et al. 2022) even when less complete taxa were included (Martinelli et al. 2017b; Lukic-Walther et al. 2018). Other analyses did not include *Pr. brasiliensis* (e.g., Ruta et al. 2013), or the prozostrodontian clade was not recovered (Gaetano et al. 2022).

The completeness of the new specimen of *Pr. brasiliensis* improved the phylogenetic score sampling of this taxon considerably, revealing a sister relationship between *Pr. brasiliensis* and the coeval Argentinean species *Pseudotherium argentinus*. This latter taxon was first recovered as closely related to the bizarre herbivorous Tritylodontidae (Wallace et al. 2019), but later positioned closer to *Botucaraitherium belarminoi* and more derived cynodonts with sectorial postcanine dentitions (Kerber et al. 2022). The morphological resemblance between *Pr. brasiliensis* and *Ps. argentinus*, coupled with our phylogenetic hypothesis, supports the proposition of the Prozostrodontidae clade. It represents the earliest radiation of Carnian prozostrodonts in Gondwana. This is the sister-group lineage to *Therioherpeton cargnini* and other more derived probainognathians, including tritheledontids, tritylodontids, brasilodontids, and mammaliaforms.

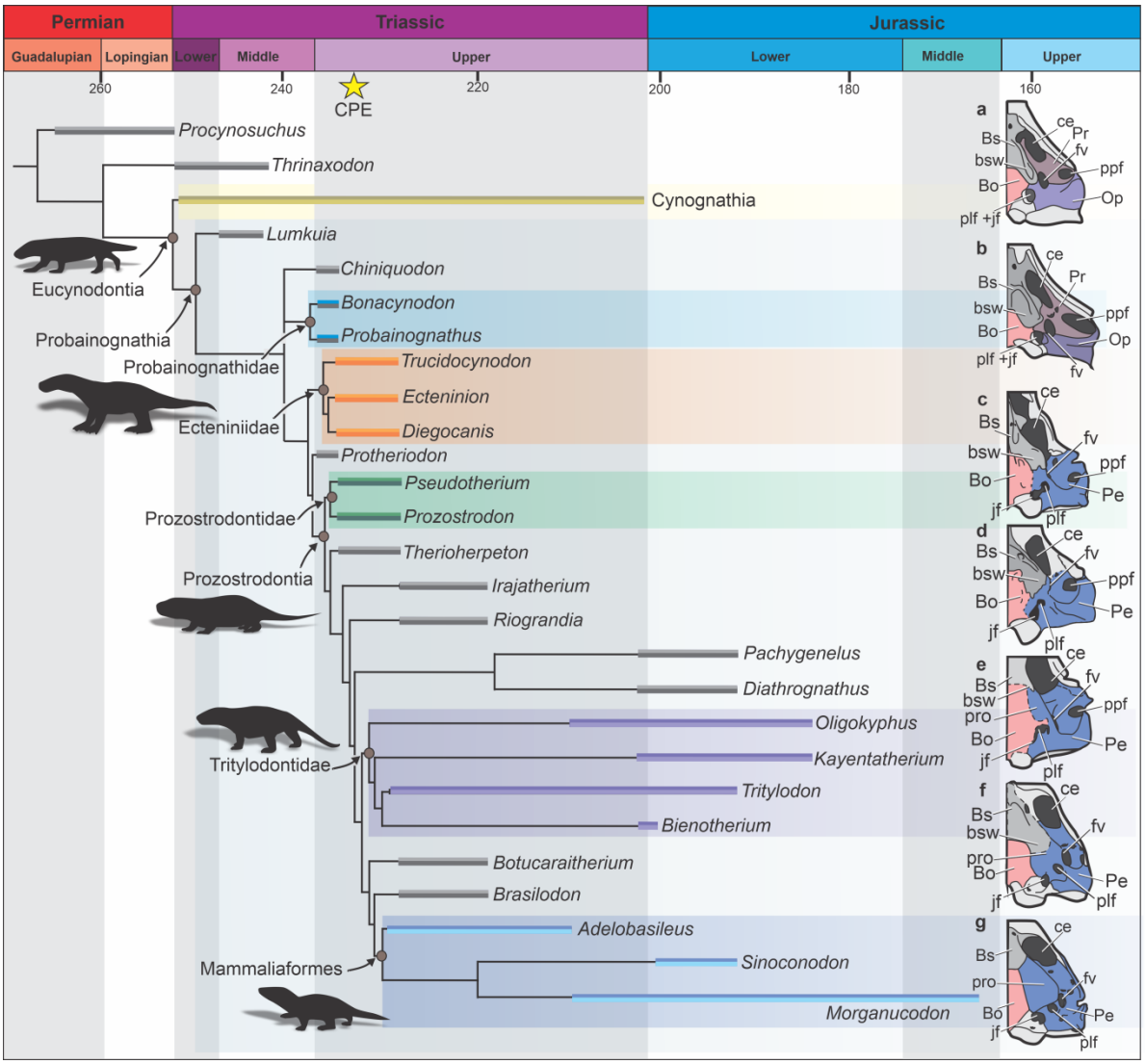

Fig. 8 Strict consensus of the phylogenetic analysis of Probainognathia and evolutionary modifications of the cynodont basicranium (**a–g**): **a**. *Thrinaxodon liorhinus*; **b**. *Probainognathus jenseni*; **c**. *Pseudotherium argentinus*; **d**. *Prozostrodon brasiliensis*; **e**. *Brasilodon quadrangularis*; **f**. *Adelobasileus cromptoni*; **g**. *Morganucodon oehleri*. Clades highlighted in: yellow, Cynognathia; orange, Ecteniniidae; green, Prozostrodontidae; purple, Tritylodontidae; blue, Mammaliaformes. Abbreviations: *Bo* basioccipital; *Bs* basisphenoid; *bsw* basisphenoid wing; *ce* cavum epiptericum; *CPE* Carnian Pluvial Event; *fv* fenestra vestibuli; *jf* jugular foramen; *Op* opisthotic; *Pe*

petrosal; *plf* perilymphatic foramen; *ppf* pterygoparoccipital foramen; *Pr* prootic; *pro* promontorium. Sources: a–b, f, redrawn from Luo (1994); c, from Wallace et al. (2019); e, from Rodrigues et al. (2013); g, from Luo et al. (1995). Clade names as defined by Hopson and Kitching (2001), Liu and Olsen (2010), Martinelli et al. (2016), and Abdala (2019) (note that the definition of Mammaliaformes by Abdala 2019 differs from the original conception by Rowe 1988).

The specimen provides information on the posterior region (including the basicranium) of the cranium of *Pr. brasiliensis*, which was hitherto unknown. The basicranial evolution of non-mammaliaform cynodonts is accompanied by changes in the configuration of the bones that form the cochlear housing (e.g., Luo 1994, 2001; Luo et al. 1995, 2001) (Fig. 8). In this context, prozostrodontids are particularly interesting, filling a gap in the evolutionary pathway of the basicranium. In the plesiomorphic condition, exemplified in non-eucynodont cynodonts (e.g., *Thrinaxodon liorhinus*; Luo 1994), the basisphenoid wing (=parasphenoid ala) is well-developed and reaches the dorsal edge of a well-rimmed fenestra vestibuli (Fig. 8a). In the early probainognathians (e.g., *Probainognathus jenseni*, early Carnian), the basisphenoid wing becomes shorter, not reaching the fenestra vestibuli (Luo 1994). However, the prootic and opisthotic are still not fused (Fig. 8b). During the late Carnian, *Ps. argentinus* and *Pr. brasiliensis* still present a similarly developed basisphenoid wing, but they show the emergence of the petrosal bone, formed by the fusion of prootic and opisthotic (Fig. 8c–d). Before discovering *Ps. argentinus* (Wallace et al. 2019), this feature was known only in tritylodontids, some tritheledontids, *Brasilodon quadrangularis,* and mammaliaforms (Wible 1991; Rodrigues et al. 2013; Wallace et al. 2019). During the early Norian,

Adelobasileus cromptoni and *B. quadrangularis* (Luo 1994; Luo et al. 1995; Bonaparte et al. 2005; Rodrigues et al. 2013) display a more shortened basisphenoid wing and the basioccipital is medially reduced (Fig. 8e–f). In both taxa, the pars cochlearis is more exposed ventrally, and there is a ventrolateral eminence on the petrosal surface – the promontorium. In *Morganucodon oehleri* and other mammaliaforms (Luo 1994), the basisphenoid and basioccipital do not overlap the pars cochlearis, and the promontorium is fully developed (Fig. 8g).

The modifications during the formation of the promontorium can be traced in the taxa mentioned above, increasing the number of features that once were thought to be exclusive to mammaliaforms, such as the presence of the petrosal bone (Fig. 8). The presence of this single bone possibly makes the inner ear more rigid and, therefore, better isolated and less susceptible to interference (Luo 2001), a crucial modification regarding the ear evolution in mammals. Coupled with these modifications, members of the prozostrodontian clade achieved other important derived traits such as the reduction/absence of the prefrontal and postorbital, lack of postorbital bar and slender zygomatic arch, unfused dentary symphysis, less rate of tooth replacement, constricted roots with two separated innervation canals, basoendothermy, a well-developed preacetabular portion of the iliac blade, reduced postacetabular portion, the medial position of the lesser trochanter and distinct greater trochanter in the femur, among other features (e.g., Bonaparte and Barberena 2001; Liu and Olsen 2010; Martinelli and Soares 2016; Guignard et al. 2018; Araújo et al. 2022).

The phylogenetic relationships of *Pr. brasiliensis* and *Ps. argentinus*, two coeval cynodonts from late Carnian beds, reinforce the faunistic similarity shared between Brazil and Argentina (Schultz et al. 2020; Novas et al. 2021) during the Late Triassic.

This is particularly interesting because Prozostrodontidae is not the only endemic clade from South America related to the early radiation of Probainognathia. Ecteniniids (medium-sized carnivorous cynodonts) are solely recovered from the Carnian beds of South America (Martínez et al. 2013; Stefanello et al. 2018). We suggest that the origin and the early radiation of these two endemic groups may have been concomitant with the CPE.

Acknowledgments Marcelo Ricardo Sánchez-Villagra and Alexandra Wegmann for helping us scan the skull. Márcio L. Castro, who made the specimen drawings. Cesar Leandro Schultz (UFRGS) and Museu Vicente Palloti for access to the specimens under their care. Christian Kammerer and an anonymous reviewer for their helpful discussions and comments that improved the first version of this manuscript.

Funding Conselho Nacional de Desenvolvimento Científico e Tecnológico [LK (422568/2018-0; 309414/2019-9); RTM (404095/2021-6); SDS (308223/2019-5)]; Fundação de Amparo à Pesquisa do RS [LK (21/2551-0002030-0); RTM (21/2551-0000680-3)]; Coordenação de Aperfeiçoamento de Pessoal de Nível Superior [LK (PrInt 8881.310240/2018-01); MS (88882.428054/2019-01)]; Paleontological Society International Research Program (PalSIRP) [LK (2018); AGM (2016/2017-2018)]; CONICET, Ginko Foundation [AGM].

Authors' contributions MS, AGM, RTM, and LK, led the writing of the main manuscript text and the supplemental text and performed the phylogenetic analysis with inputs from SDS. MS carried out specimen preparation. LK performed the µCT scanning of the specimen and segmented the reconstructed images. MS, RTM, and LK designed and prepared the figures. All authors contributed to the study's design and the manuscript's drafting, provided final approval for publication, and agree to be held accountable for the work performed herein.

Declarations

Competing interests The authors declare no competing financial interests.

References

Abdala F (2019) Permo-Jurassic cynodonts: the early road to mammalness. Encyclopedia of Geology 2:1–21. https://doi.org/10.1016/B978-0-12-409548-9.12020-2

Abdala F, Giannini NP (2000) Gomphodont cynodonts of the Chañares Formation: the analysis of an ontogenetic sequence. J Vertebr Paleontol 20(3):501–506.

Abdala F, Giannini NP (2002) Chiniquodontid cynodonts: systematic and morphometric considerations. Palaeontology 45:1151–1170.

Abdala F, Jasinoski SC, Fernandez V (2013) Ontogeny of the Early Triassic cynodont *Thrinaxodon liorhinus* (Therapsida): dental morphology and replacement. J Vertebr Paleontol 33(6):1408–1431. https://doi.org/10.1080/02724634.2013.775140

Araújo R, David R, Benoit J, Jacqueline L, Spoor F, Stoessel A, Barrett P, Maisano J, Ekdale E, Orliac M, Luo Z-X, Martinelli A, Hoffman E, Sidor C, Martins R, Angielczyk K (2022) Inner ear biomechanics reveals a Late Triassic origin for mammalian endothermy. Nature 607:726–7311. https://doi.org/10.1038/s41586-022-04963-z

Barberena MC, Bonaparte JF, Teixeira AMS (1987) *Thrinaxodon brasiliensis* sp. nov., a primeira ocorrência de cinodontes galessauros para o Triássico do Rio Grande do Sul. In: X Congresso Brasileiro de Paleontologia (Rio de Janeiro) 10:67−74.

Benoit J, Nxumalo M, Norton LA, Fernandez V, Gaetano LC, Rubidge B, Abdala F (2022) Synchrotron scanning sheds new light on *Lumkuia fuzzi* (Therapsida, Cynodontia) from the Middle Triassic of South Africa and its phylogenetic placement. J African Earth Sci 196:104689. https://doi.org/10.1016/j.jafrearsci.2022.104689

Benoit J, Ruf I, Miyamae JA, Fernandez V, Rodrigues PG, Rubidge BS (2019) The evolution of the maxillary canal in Probainognathia (Cynodontia, Synapsida): Reassessment of the homology of the infraorbital foramen in mammalian ancestors. J. Mamm Evol 27:329–348. https://doi.org/10.1007/s10914-019-09467-8

Benton MJ, Wu F (2022) Triassic Revolution. Front Earth Sci 10:899541. https://doi.org/10.3389/feart.2022.899541

Bernardi M, Gianolla P, Petti FM, Mietto P, Benton MJ (2018) Dinosaur diversification linked with the Carnian Pluvial Episode. Nat Commun 9(1499):1–10. https://doi.org/10.1038/s41467-018-03996-1

Bonaparte JF, Barberena MC (1975) A possible mammalian ancestor from the Middle Triassic of Brazil (Therapsida-Cynodontia). J Paleontol 49:931–936.

Bonaparte JF, Barberena MC (2001) On two advanced carnivorous cynodonts from the Late Triassic of Southern Brazil. In: Jenkins JrFA, Shapiro MD, Owerkowicz T (eds) Studies in Organismic and Evolutionary Biology in honor of Crompton AW. Bull Mus Comp Zool Harv Univ 156, pp. 59–80.

Bonaparte JF, Ferigolo J, Ribeiro AM (2001) A primitive Late Triassic 'ictidosaur' from Rio Grande do sul, Brazil. Palaeontology 44:623–635. https://doi.org/10.1111/1475-4983.00194

Bonaparte JF, Martinelli AG, Schultz CL (2005) New information on *Brasilodon* and *Brasilitherium* (Cynodontia, Probainognathia) from the Late Triassic of Southern Brazil. Rev Bras de Paleontol 8:25–46. https://doi.org/10.4072/rbp.2005.1.03

Bonaparte JF, Martinelli AG, Schultz CL, Rubert R (2003) The sister group of mammals: small cynodonts from the Late Triassic of Southern Brazil. Rev Bras de Paleontol 5:5–27.

Bonaparte JF, Soares MB, Martinelli AG (2012) Discoveries in the Late Triassic of Brazil improve knowledge on the origin of mammals. Historia Natural, Tercera Serie 2:5–30.

Botha-Brink J, Soares MB, Martinelli AG (2018) Osteohistology of Late Triassic prozostrodontian cynodonts from Brazil. PeerJ 6:e5029. https://doi.org/10.7717/peerj.5029

Cohen KM, Finney SC, Gibbard PL, Fan J-X (2013) The ICS International Chronostratigraphic Chart. Episodes J Int Geosci 36:199–204. https://doi.org/10.18814/epiiugs/2013/v36i3/002

Crompton AW (1963) The evolution of the mammalian jaw. Evolution 17(4):431–439.

Crompton AW, Luo Z-X (1993) Relationships of the Liassic mammals *Sinoconodon*, *Morganucodon oehleri*, and *Dinnetherium*. In: Szalay FS, Novacek MJ, Mckenna MC (eds) Mammal Phylogeny: Mesozoic Differentiation, Multituberculates, Monotremes, Early Therians and Marsupials. Springer-Verlag, New York, New York, pp. 30–44.

Dal Corso J, Bernardi M, Sun Y, Song H, Seyfullah LJ, Preto N, Gianolla P, Ruffell A, Kustatscher E, Roghi G, Merico A. Hohn S, Schmidt AR, Marzoli A, Newton RJ, Wignall PB, Benton MJ (2020) Extinction and dawn of the modern world in the Carnian (Late Triassic). Sci Adv 6(38):eaba0099. https://doi.org/10.1126/sciadv.aba0099

Furin S, Preto N, Rigo M, Roghi G, Gianolla P, Crowley JL, Bowring SA (2006) High-precision U-Pb zircon age from the Triassic of Italy: Implications for the Triassic time scale and the Carnian origin of calcareous nanoplankton and dinosaurs. Geology 34:1009–1012. https://doi.org/10.1130/0091-7613(2007)35[146:HUZAFT]2.0.CO;2

Gaetano LC, Abdala F, Seoane FD, Tartaglione A, Schulz M, Otero A, Leardi JM, Apaldetti C, Krapovickas V, Steimbach E (2022) A new cynodont from the Upper Triassic Los Colorados Formation (Argentina, South America) reveals a novel paleobiogeographic context for mammalian ancestors. Sci Rep 12(6451):1–13. https://doi.org/10.1038/s41598-022-10486-4

Goloboff PA, Catalano SA (2016) TNT version 1.5, including a full implementation of phylogenetic morphometrics. Cladistics 32:221–238. https://doi.org/10.1111/cla.12160

Guignard ML, Martinelli AG, Soares MB (2018) Reassessment of the postcranial anatomy of *Prozostrodon brasiliensis* and implications for postural evolution of nonmammaliaform cynodonts. J Vertebr Paleontol 38:e1511570. https://doi.org/10.1080/02724634.2018.1511570

Jasinoski SC, Abdala F (2016) Cranial ontogeny of the Early Triassic basal cynodont *Galesaurus planiceps*. Anat Rec 300(2):353–381. https://doi.org/10.1002/ar.23473

Jasinoski SC, Abdala F, Fernandez V (2015) Ontogeny of the Early Triassic cynodont *Thrinaxodon liorhinus* (Therapsida): Cranial morphology. Anat Rec 298(8):1440–1464. https://doi.org/10.1002/ar.23116

Holz M, Scherer CMS (2000) Sedimentological and paleontological evidence of paleoclimatic change during the South Brazilian Triassic: the register of a global trend towards a humid paleoclimate. Zentbl Geol Paläontologie 11–12:1589–1609.

Hopson JA (1973) Endothermy, small size, and the origin of mammalian reproduction. The American Naturalist, 107(955):446-452.

Hopson JA (1990) Cladistic analysis of therapsid relationships. J Vertebr Paleontol 10:28A.

Hopson JA, Kitching JW (2001) A probainognathian cynodont from South Africa and the phylogeny of nonmammalian cynodonts. Bull Mus Comp Zool Harv Univ 156:5–35.

Hopson JA, Rougier GW (1993) Braincase structure in the oldest known skull of a therian mammal: implications for mammalian systematics and cranial evolution. Am J Sci 293:268–299.

Kerber L, Martinelli AG, Müller RT, Pretto FA (2022) A new specimen provides insights into the anatomy of *Irajatherium hernandezi*, a poorly known probainognathian

cynodont from the Late Triassic of southern Brazil. Anat Rec 305:3113–3132. https://doi.org/10.1002/ar.24830

Kerber L, Martinelli AG, Rodrigues PG, Ribeiro AM, Schultz CL, Soares MB (2020) New record of *Prozostrodon brasiliensis* (Eucynodontia: Prozostrodontia) from its type-locality (Upper Triassic, southern Brazil): comments on the endocranial morphology. Rev Bras de Paleontol 23:259–269. https://doi.org/10.4072/rbp.2020.4.04

Kermack KA, Mussett F, Rigney HW (1981) The skull of *Morganucodon*. Zool J Linn Soc 71:1–158.

Langer MC, Ramezani J, Da Rosa ÁAS (2018) U-Pb age constraints on dinosaur rise from south Brazil. Gondwana Res 57:133–40. https://doi.org/10.1016/j.gr.2018.01.005

Liu J, Olsen P (2010) The phylogenetic relationships of Eucynodontia (Amniota, Synapsida). J Mamm Evol 17:151–176. https://doi.org/10.1007/s10914-010-9136-8

Lucas SG, Hunt AP (1990) The oldest mammal. N M J Sci 30:41–49.

Lucas SG, Luo Z-X (1993) *Adelobasileus* from the Upper Triassic of West Texas: the oldest mammal. J Vertebr Paleontol 13:309–334. https://doi.org/10.1080/02724634.1993.10011512

Lukic-Walther M, Brocklehurst N, Kammerer CF, Fröbisch J (2018) Diversity patterns of nonmammalian cynodonts (Synapsida, Therapsida) and the impact of taxonomic practice and research history on diversity estimates. Paleobiology 45:56–69. https://doi.org/10.1017/pab.2018.38

Luo Z-X (1994) Sister-group relationships of mammals and transformations of diagnostic mammalian characters. In: Fraser NC, Sues H-D (eds) In the Shadow of the

Dinosaurs: Early Mesozoic Tetrapods. Cambridge University Press, Cambridge, New York, pp. 98–128.

Luo Z-X (2001) Inner ear and its bony housing in tritylodontids and implications for evolution of mammalian ear. Bull Mus Comp Zool 156:81–97.

Luo Z-X, Crompton AW, Lucas SG (1995) Evolutionary origins of the mammalian promontorium and cochlea. J Vertebr Paleontol 15:113–121.

Luo Z-X, Crompton AW, Sun A-L (2001) A new mammaliaform from the Early Jurassic and evolution of mammalian characteristics. Science 292:1535–1540.

Mancuso AC, Horn BLD, Benavente CA, Schultz CL, Irmis RB (2021) The paleoclimatic context for South American Triassic vertebrate evolution. J South Am Earth Sci 110:103321. https://doi.org/10.1016/j.jsames.2021.103321

Martinelli AG, Bonaparte JF (2011) Postcanine replacement in *Brasilodon* and *Brasilitherium* (Cynodontia, Probainognathia) and its bearing in cynodont evolution. In: Calvo J, Porfiri J, González Riga B, dos Santos D (eds) Dinosaurios y Paleontología desde América Latina. Anales del III Congreso Latinoamericano de Paleontología. Mendoza: Editorial de la Universidad Nacional de Cuyo, pp. 179–186.

Martinelli AG, Bonaparte JF, Schultz CL, Rubert R (2005) A new tritheledontid (Therapsida, Eucynodontia) from the Late Triassic of Rio Grande do Sul (Brazil) and its phylogenetic relationships among carnivorous non-mammalian eucynodonts. Ameghiniana 42:191–208.

Martinelli AG, Eltink E, Da-Rosa ÁAS, Langer MC (2017a) A new cynodont (Therapsida) from the *Hyperodapedon* Assemblage Zone (upper Carnian-Norian) of southern

Brazil improves the Late Triassic probainognathian diversity. Pap Palaeontol 3:401–423. https://doi.org/10.1002/spp2.1081

Martinelli AG, Kammerer CF, Melo TP, Paes Neto VD, Ribeiro AM, Da-Rosa ÁAS, Schultz CL, Soares MB (2017c) The African cynodont *Aleodon* (Cynodontia, Probainognathia) in the Triassic of southern Brazil and its biostratigraphic significance. PloS One 12(6):e0177948. https://doi.org/10.1371/journal.pone.0177948

Martinelli AG, Rougier GW (2007) On *Chaliminia musteloides* Bonaparte (Cynodontia, Tritheledontidae) and the phylogeny of the Ictidosauria. J Vertebr Paleontol 27:442–460. https://doi.org/10.1671/0272-4634(2007)27[442:OCMETF]2.0.CO;2

Martinelli AG, Soares MB (2016) Evolution of South American cynodonts. Contribuciones del Museo Argentino de Ciencias Naturales “Bernardino Rivadavia” 6:183–197.

Martinelli AG, Soares MB, de Oliveira TV, Rodrigues PG, Schultz CL (2017b) The Triassic eucynodont *Candelariodon barberenai* revisited and the early diversity of stem prozostrodontians. Acta Palaeontol Pol 62:527–542. https://doi.org/10.4202/app.00344.2017

Martinelli AG, Soares MB, Schwanke C (2016) Two new cynodonts (Therapsida) from the Middle-early Late Triassic of Brazil and comments on South American probainognathians. PLoS One 11:e0162945. https://doi.org/10.1371/journal.pone.0162945

Martínez RN, Fernández E, Alcober, OA (2013) A new non-mammaliaform eucynodont from the Carnian-Norian Ischigualasto Formation, northwestern Argentina. Rev Bras de Paleontol 16:61–76. https://doi.org/10.4072/rbp.2013.1.05

Martínez RN, Forster CA (1996) The skull of *Probelesodon sanjuanensis*, sp. nov., from the Late Triassic Ischigualasto Formation of Argentina. J Vertebr Paleontol 16:285–291

Martínez RN, May CL, Forster CA (1996) A new carnivorous cynodonts from the Ischigualasto Formation (Late Triassic, Argentina), with comments on eucynodont phylogeny. J Vertebr Paleontol 16:271–284.

Norton LA, Abdala F, Rubidge BS, Botha J (2020) Tooth replacement patterns in the Early Triassic epicynodont *Galesaurus planiceps* (Therapsida, Cynodontia). PloS One 15(12):e0243985. https://doi.org/10.1371/journal.pone.0243985

Novas FE, Agnolin FL, Ezcurra MD, Müller RT, Martinelli AG, Langer MC (2021) Review of the fossil record of early dinosaurs from South America, and its phylogenetic implications. J South Am Earth Sci 110:103341. https://doi.org/10.1016/j.jsames.2021.103341

Oliveira TV, Soares MB, Schultz CL (2010) *Trucidocynodon riograndensis* gen. nov. et sp. nov. (Eucynodontia), a new cynodont from the Brazilian Upper Triassic (Santa Maria Formation). Zootaxa 2382:1–71. https://doi.org/10.11646/zootaxa.2382.1.1

Oliveira TV, Soares MB, Schultz CL, Rodrigues CN (2011) A new carnivorous cynodont (Synapsida, Therapsida) from the Brazilian Middle Triassic (Santa Maria Formation): *Candelariodon barberenai* gen. et sp. nov. Zootaxa 3027:19–28. https://doi.org/10.11646/zootaxa.3027.1.3

Owen R (1861) Palaeontology, or a Systematic Summary of Extinct Animals and their Geological Relationships. Adam and Black, Edinburgh.

Pacheco CP, Martinelli AG, Pavanatto AEB, Soares MB, Dias-da-Silva S (2017) *Prozostrodon brasiliensis*, a probainognathian cynodont from the Late Triassic of

Brazil: second record and improvements on its dental anatomy. Hist Biol 30:475–485. https://doi.org/10.1080/08912963.2017.1292423

Pacheco C, Müller RT, Langer M, Pretto FA, Kerber L, Silva SD (2019) *Gnathovorax cabreirai*: a new early dinosaur and the origin and initial radiation of predatory dinosaurs. PeerJ 7:e7963. https://doi.org/10.7717/peerj.7963

Rigney HW (1963) A specimen of *Morganucodon* from Yunnan. Nature 197:1122–1123.

Rigney HW (1938) The morphology of the skull of a young *Galesaurus planiceps* and related forms. J Morphol 63(3):491–529.

Rodrigues PG, Ruf I, Schultz CL (2013) Digital reconstruction of the otic region and inner ear of the non-mammalian cynodont *Brasilitherium riograndensis* (Late Triassic, Brazil) and its relevance to the evolution of the mammalian ear. J Mamm Evol 20:291–307. https://doi.org/10.1007/s10914-012-9221-2

Romer AS (1970) The Chañares (Argentina) Triassic reptile fauna. VI. A chiniquodontid cynodont with an incipient squamosal-dentary jaw articulation. Breviora 344:1–18.

Rougier GW, Wible JR, Hopson JA (1992) Reconstruction of the cranial vessels in the Early Cretaceous mammal *Vincelestes neuquenianus*: implications for the evolution of the mammalian cranial vascular system. J Vertebr Paleontol 12:188–216.

Ruffell A, Simms MJ, Wignall PB (2015) The Carnian Humid Episode of the Late Triassic: a review. Geol Mag 153:271–284. https://doi.org/10.1017/S0016756815000424

Ruta M, Botha-Brink J, Mitchell SA, Benton MJ (2013) The radiation of cynodonts and the ground plan of mammalian morphological diversity. Proc R Soc Lond B Biol Sci 280(1769):20131865. https://doi.org/10.1098/rspb.2013.1865

Sidor CA, Hancox PJ (2006) *Elliotherium kersteni*, a new tritheledontid from the Lower Elliot Formation (Upper Triassic) of South Africa. J Paleontol 80:333–342. https://doi.org/10.1666/0022-3360(2006)080[0333:EKANTF]2.0.CO;2

Schultz CL, Martinelli AG, Soares MB, Pinheiro FL, Kerber L, Horn LDB, Pretto FA, Müller RT, Melo T (2020) Triassic faunal successions of the Paraná Basin, southern Brazil. J South Am Earth Sci 104:102846. https://doi.org/10.1016/j.jsames.2020.102846

Soares MB, Martinelli AG, Oliveira TV (2014) A new prozostrodontian cynodont (Therapsida) from the Late Triassic *Riograndia* Assemblage Zone (Santa Maria Supersequence) of Southern Brazil. An Acad Bras Cienc 86:1673–1691. https://doi.org/10.1590/0001-3765201420140455

Soares MB, Schultz CL, Horn BLD (2011) New information on *Riograndia guaibensis* Bonaparte, Ferigolo & Ribeiro, 2001 (Eucynodontia, Tritheledontidae) from the Late Triassic of southern Brazil: Anatomical and biostratigraphic implications. An Acad Bras Cienc 83:329–354. https://doi.org/10.1590/S0001-37652011000100021

Stefanello M, Kerber L, Martinelli AG, Dias-da-Silva S (2020) A new prozostrodontian cynodont (Eucynodontia, Probainognathia) from the Upper Triassic of Southern Brazil. J Vertebr Paleontol 40:e1782415. https://doi.org/10.1080/02724634.2020.1782415

Stefanello M, Müller RT, Kerber L, Martínez RN, Dias-Da-Silva S (2018) Skull anatomy and phylogenetic assessment of a large specimen of Ecteniniidae (Eucynodontia: Probainognathia) from the Upper Triassic of southern Brazil. Zootaxa 4457:351–378. https://doi.org/10.11646/zootaxa.4457.3.1

Wallace RV, Martínez R, Rowe T (2019) First record of a basal mammaliamorph from the early Late Triassic Ischigualasto Formation of Argentina. PLoS One 14:e0218791. https://doi.org/10.1371/journal.pone.0218791

Wible JR (1991) Origin of Mammalia: the craniodental evidence reexamined. J Vertebr Paleontol 11:1–28.

Wynd B, Abdala F, Nesbitt, SJ (2022) Ontogenetic growth in the crania of *Exaeretodon argentinus* (Synapsida: Cynodontia) captures a dietary shift. PeerJ 10:e14196. https://doi.org/10.7717/peerj.14196

Supplementary Material for: A complete skull of a stem mammal from the Late Triassic of Brazil illuminates the early evolution of prozostrodonts

Micheli Stefanello[1,2]. Agustín G. Martinelli[3]. Rodrigo T. Müller[1,2]. Sérgio Dias-da-Silva[1]. Leonardo Kerber[1,2]

[1]Programa de Pós-Graduação em Biodiversidade Animal, Universidade Federal de Santa Maria, Av. Roraima, 1000, 97105-900, Santa Maria, RS, Brazil

[2]Centro de Apoio à Pesquisa Paleontológica da Quarta Colônia, Universidade Federal de Santa Maria (CAPPA/UFSM), Rua Maximiliano Vizzotto, 598, 97230-000, São João do Polêsine, RS, Brazil

[3]Sección Paleontologia de Vertebrados, Museo Argentino de Ciencias Naturales "Bernardino Rivadavia", Av. Ángel Gallardo, 470, C1405 DJR, Buenos Aires, Argentina

1. Modifications to the character scoring

Character 1. *Prozostrodon brasiliensis* changes from 2 to 1. Comments: The premaxillary extranasal process is large but does not contact the nasal, based on UFRGS-PV-0248-T and CAPPA/UFSM 0210.

Character 2. *Prozostrodon brasiliensis* changes from 1 to 0. Comments: The septomaxilla facial process is long, far beyond the posterior border of the external nares, based on UFRGS-PV-0248-T and CAPPA/UFSM 0210.

Character 15. *Prozostrodon brasiliensis* changes from 2 to 1. Comments: The palatine meets the frontal but two elements without significant contribution to the medial orbit wall, based on UFRGS-PV-0248-T and CAPPA/UFSM 0210.

Character 18. *Prozostrodon brasiliensis* changes from 1 to 0. Comments: The anteroventral corner of the zygomatic arch lies at the same level as the postcanine line, based on UFRGS-PV-0248-T and CAPPA/UFSM 0210.

Character 29. *Prozostrodon brasiliensis* and *Pseudotherium argentinus* change from 1 to 0. Comments: Vomer with vertical septum, based on UFRGS-PV-0248-T and CAPPA/UFSM 0210 for *Pr. brasiliensis* and PVSJ 882 for *Ps. argentinus* (see Wallace et al. 2019, Figs. 3–4 and 10–11).

Character 46. *Prozostrodon brasiliensis* and *Pseudotherium argentinus* change from 2 to 1. Comments: We codified both taxa as 1, because although the basisphenoid is slightly shorter than *Probainognathus jenseni*, it is not as short as in *Adelobasileus cromptoni* and *Brasilodon quadrangularis*.

Character 47. *Prozostrodon brasiliensis* and *Pseudotherium argentinus* change from 1 to 0. Comments: We codified both taxa as 0, because the state 1 was created by Luo et al. (2001) to represent the condition found in *Adelobasileus cromptoni* and *Sinoconodon rigneyi*, which clearly differ from the condition found in *Pr. brasiliensis* and *Ps. argentinus*. *A. cromptoni* and *S. rigneyi* display the pars cochlearis exposed ventrally with a marked promontorium, a condition necessary to evidence this state.

Character 50. *Pseudotherium argentinus* changes from 1 to 0. Comments: We opted to codify this character as 0 for *Ps. argentinus* and *Prozostrodon brasiliensis*, since both cynodonts have a similar condition. Promontorium, is defined as a ventrolateral eminence of the pars cochlearis of the petrosal, enclosing the bony cochlear canal (Luo

et al. 1995). In both taxa, the pars cochlearis is still covered anteriorly by the basisphenoid wing, and probably medially by the basioccipital (although the limits between both regions are not totally clear because of the fusion of both bones). In both taxa, there is no eminence as that present in *Brasilodon quadrangularis* (UFRGS-PV-1043-T). In the latter taxon, the basisphenoid wing is more reduced compared to *Ps. argentinus* and *Pr. brasiliensis*; consequently, the pars cochlearis is more exposed ventrally.

Character 52. *Prozostrodon brasiliensis* changes from 1 to 0. *Adelobasileus cromptoni* changes from 2 to 1. Comments: We opted to codify this character as 0 for *Pr. brasiliensis*, since the prootic floor is open ventrally for trigeminal ganglion, based on CAPPA/UFSM 0210. Whereas in *A. cromptoni*, it is partially open in the area of the cavum epiptericum (see Lucas and Luo 1993, Fig. 8).

Character 66. *Pseudotherium argentinus* changes from 1 to 0. Comments: The tabular is present, based on PVSJ 882 (see Wallace et al. 2019, Figs. 3–4).

Character 81. *Probainognathus jenseni*, *Pachygenelus monus*, *Sinoconodon rigneyi*, and *Morganucodon oehleri* change from 2 to 1. Comments: This character describes the shape of the squamosal articulation surface for the mandible. Originally, Character 81 was a three-state character statement and state 0 read “absent.” However, Wallace et al. (2019) changed the definition of the states for this character.

Character 94. *Prozostrodon brasiliensis* changes from 0 to 1. Comments: Four upper incisors, based on UFRGS-PV-0248-T and CAPPA/UFSM 0210.

Character 103. *Prozostrodon brasiliensis* changes from 1 to 1 and 2. *Pseudotherium argentinus* changes from 0 to ?. Comments: We opted to codify this character as 1 and 2 for *Pr. brasiliensis*, since that the anteriormost one-cusped tooth is presents only in

juvenile or absent, based on UFRGS-PV-0248-T and CAPPA/UFSM 0210. The condition of *Ps. argentinus* is uncertain.

Character 106. *Prozostrodon brasiliensis* and *Therioherpeton cargnini* change from 0 to 1. Comments: The upper postcanines have constricted roots, with longitudinal grooves, based on UFRGS-PV-0248-T and CAPPA/UFSM 0210 for *Pr. brasiliensis*, and MVP 05.22.04 for *T. cargnini* (see Martinelli et al. 2017a, Fig. 10).

Character 107. *Prozostrodon brasiliensis* changes from 0 to 1. Comments: The lower postcanines have constricted roots, with longitudinal grooves, based on UFRGS-PV-0248-T, CAPPA/UFSM 0210, and CAPPA/UFSM 0123 (see Pacheco et al. 2017, Figs. 2–4).

Character 147. *Pseudotherium argentinus* changes from 0 to 1. Comments: The cusps of the upper middle and posterior postcanines are mesiodistally asymmetrical and vertically oriented, with the main cusp (A) and accessory mesial (B) and distal (C).

2. Character List

The following morphological character list was used in the present phylogenetic analysis. It uses the data matrix proposed by Liu and Olsen (2010) with subsequent additions (Soares et al. 2014; Martinelli et al. 2016, 2017b; Wallace et al. 2019; Kerber et al. 2022; Benoit et al. 2022), and with the character definition modifications ([37; 63] Kerber et al. 2022) and the new characters ([146-148] and [149-154]), as suggested by Kerber et al. (2022) and Benoit et al. (2022), respectively. Italicized acronyms indicate differences in how the character is written between present study and previous author(s). Acronyms refer to authors and their published character numbers: R, Rowe (1988); W, Wible (1991); WH, Wible and Hopson (1993); LL, Lucas and Luo (1993); L,

Luo (1994); LC, Luo and Crompton (1994); M, Martínez et al. (1996); HK, Hopson and Kitching (2001); LCS, Luo et al. (2001); B, Bonaparte et al. (2003); SS, Sidor and Smith (2004); MA, Martinelli et al. (2005); BO, Bonaparte et al. (2005); SH, Sidor and Hancox (2006); A, Abdala (2007); MR, Martinelli and Rougier (2007); LO, Liu and Olsen (2010); SMO, Soares et al. (2014); WMR, Wallace et al. (2019); BE, Benoit et al. (2022).

1. Premaxillary extranasal process: absent or with very little exposure (0); large but not contacting nasal (1); contacting nasal (2). [*R2*, *W36*, L82, MMF14, A0]
2. Septomaxilla facial process: long, far beyond the posterior border of the external nares (0); short, almost limited in the external nares (1). [*SS1, A1*, LO2]
3. Snout in relation to the temporal region (to the posterior border, not the parietal crest): longer (0); subequal (1); shorter (2). [*A10*, LO3]
4. Paracanine fossa in relation to the upper canine: anteromedial (0), medial or posteromedial (1), anterior (2), paracanine fossa absent (3). [A13]
5. Premaxilla forms posterior border of the incisive foramen: absent (0), present (1). [M19, HK1, B21, BO27, MA24, *A12,* LO5]
6. Maxillary platform lateral to the teeth series: absent (0); present (1). [M15, HK77, BO15, *A22*, LO6]
7. Maxilla: excluded from (0), or participates in (1) border of subtemporal fenestra. [R15, W14, *L62*, M16, A20]
8. Profile of skull roof: nearly flat (0); remarkably concave (the parietal crest is higher than the extension of anterior surface) (1); convex (the parietal crest is lower than the extension of anterior surface) (2). [*SS7, A64*, LO8]

9. Parietal foramen: present (0); absent (1). [R8, W12, LL34, L64, M31, HK7, B24, BO34, MA28, A6]
10. Interparietal (postparietal) in adult: separate bone in adult (0); fused with other bones (1). [R21, W15, *LL36*, M34]
11. Lateral expansion of braincase in parietal region: absent (0); well-developed (1). [*L67, M33*, *LO11*]
12. Parietal crest posteriorly extending close to or reach the posteriomost position of the occipital crest: absent (0); present (1). [LO12]
13. Prefrontal: present (0); absent (1). [R4, W1, M28, HK3, B22, BO30, MA25, A3]
14. Postorbital bar and postorbital: present (0); postorbital present but not forming postorbital bar (1); both absent (2). [*R7, W2, LL33, L55, M29, HK5, B23, B40, BO31, BO32, MA 50, A5*, LO14]
15. Palatine: do not meet the frontal (0); meets frontal but two elements without significant contribution to medial orbit wall (1); meets frontal and two elements with significant contribution to medial orbit wall (2). [*R6, R31, W17, W37, L56, L60, M24, M30, HK23, B29, BO46, MA38, A62*, LO15]
16. Sphenopalatine foramen: absent (0); present (1). [*L57, M26*, LO16]
17. Zygomatic arch dorsoventral height relative to skull length: moderately deep (10~18%) (0); very deep (>18%) (1); slender (2) (<10%). [*R16, W40, L54, M39, HK18, SS5, BO40, MA33, A68*, LO17]
18. The anteroventral corner of the zygomatic arch: lie at the same level as (0); or remarkably higher than (1) the postcanine line. [LO18]

19. Infraorbital process: absent (0); suborbital angulation between maxilla and jugal (1); descending process of the jugal (2). [*M18*, *HK21*, *HK41*, *A25*, *B38*, *BO29*, *BO44*, *MA36*, *MA46*, A69, LO19]
20. Zygomatic arch dorsal extent: below middle of orbit (0); above middle of orbit but still level within orbit (1); beyond the upper border of the orbit (2). [*HK19*, LO20]
21. Posterior extension of jugal along zygomatic arch: extending back near quadratojugal notch of squamosal (0), extending back near squamosal glenoid (1), reduced and receding from glenoid (2). [*L28*, LO21]
22. The posteroventral process of jugal: low (0); high, forming more than half height of zygomatic arch (1). [*HK20*, *BO43, A70*, LO22]
23. The width of temporal fossa: reach greatest near middle (0); same throughout or little change (1); strongly increase backward, the posterior width much bigger than the anterior width (2). [*HK39*, *BO42, MA44*, A73, LO23]
24. Squamosal groove for external auditory meatus: without or with an incipient depression (0); deep (1). [*M55*, *HK22*, *B28*, *SS18*, *BO45*, *MA37*, *A72*, LO24]
25. Posterior extension of the squamosal dorsal to the squamosal sulcus in zygomatic arch: incipient (0); well developed (1) [*A71*, LO25]
26. The notch separating lambdoidal crest from zygomatic arch: shallow (0); deep, “V”-shape (1). [*HK43, SS17, BO55, A74*, LO26]
27. Palatine: excluded from subtemporal border of orbit (0); participates in subtemporal border by displacing pterygoid posteriorly (1). [L58]
28. Vomer exposure in incisive foramen (at anterior ends of maxillae on palate): present (0); absent (1). [*M21*, LO28]

29. Vomer: with (0) or without (1) vertical septum extending posterior to level of secondary palate. [SH63]

30. Ectopterygoid: does not contact maxilla (0); contacts maxilla (1); absent (2). [*R32*, *HK9, SS15, A19*, LO30]

31. Interpterygoid vacuity in adults between pterygoid flanges: present (0); absent (1). [M27, HK10, B25, BO35, MA29, A24]

32. Secondary palatal plate on maxilla reaches midline: absent (0); present (1). [HK12, SS11, *A15*, LO32]

33. Secondary palatal plate on palatine reaches midline: absent (0); present (1). [HK13, SS12, *A15*, LO33]

34. Posterior extent of osseous secondary palate: far from (0), close to or beyond (1) rear upper postcanine row. [R30, W16, *L68*, M23, LCS40, *HK14, B26*, *BO36*, *MA30, A17*, LO34]

35. The posterior end of secondary osseous palate relative to anterior border of orbit: anterior (0); about equal level (1); posterior (2). [HK15, B27, BO38]

36. Osseous palate extension: 45% of skull length or less (0); more than 45% of skull length (1). [A16]

37. Length of palatine relative to maxilla in secondary palate: (0) shorter; (1) about equal; (2) longer. [M22, *HK40*, *B37*, *BO53*, *MA45, A18*, LO37]

38. Middle of pterygoid: smooth (0); a boss (1); a distinct median crest (2). [*LL12, L71*, *A25*, LO38]

39. The nasopharyngeal roof posterior to the transverse process of pterygoid: narrow, deep, ventrally forms a keel (0); wide, flat, the narrowest place greater than half the width of the transverse process (1). [LO39]

40. Quadrate ramus of pterygoid: present (0); absent (1). [R38, W47, *LC10*, M40, HK30, B34, BO52, SS20, MA43, A29]

41. Quadrate articulation with quadrate ramus of epipterygoid: absent (0); present (1). [*LC11*, M53, *A30*, LO41]

42. Frontal-epipterygoid contact: present (0), absent (1). [*R39*, *W48*, *L61*, HK35, SS24, A63]

43. Epipterygoid ascending process at level of trigeminal foramen: greatly expanded (0); moderately expanded (1). [HK32, B35, A66]

44. The anterior part of the basisphenoid: narrow (0); wide, and the width greater than half the width of the transverse process (1). [*L69, LCS44*, LO44]

45. Parasphenoid ala: at the same level as the basicranium (0); ventrally expanded below the basicranium (1). [*HK17*, *BO39*, *MA32,* A28, LO45]

46. Basisphenoid wing (parasphenoid ala): long, border the fenestra vestibuli (0); slightly reduced and excluded from oval window, overlap the entire prootic cochlear housing (1); greater reduced and overlapping a part of the pars cochlearis (cochlear housing) (2); basisphenoid does not overlap the petrosal pars cochlearis (3). [*R40, W49*, L74*, M41, M49, LCS37, A27*, LO46]

47. Overlap of the basioccipital to the pars cochlearis: entire cochlear housing (0); the medial side of the promontorium (1); no overlapping (2). [LCS 38]

48. Internal carotid foramina in basisphenoid: present (0); absent (1). [*R42*, *W50*, *WH23*, LL14, L72, M45, HK26, B31, BO48, MA40, A26]

49. Prootic and opisthotic: separated (0); fused at early ontogenetic stage to form petrosal (=periotic) (1). [R51, W5, WH29, L34, BO56, A36]

50. Promontorium (Pars cochlearis of petrosal): absent (0); present (1). [R52, W6, *LL1*, *L35,* LCS9, *BO57*, A34]

51. Internal auditory meatus: open (0); walled (1). [*R53, W7, WH12, L39, M47, HK36, B36,* A37]

52. The trigeminal ganglion (semilular ganglion): open ventrally (0); partial prootic floor (1); complete prootic floor (2). [W54, A33]

53. Lateral trough floor anterior to the tympanic aperture of the prootic canal and/or the primary facial foramen: absent (0); present (1). [*R49, LL6, L43, M44,* LCS 15]

54. Vascular foramen in the posterior part of the lateral flange (Foramen “X” of (Rougier et al., 1992) (p205)): absent (0); present (1). [*LL30*, *L53, M43*, LCS29]

55. Foramen and passage of prootic sinus on lateral trough: absent (0); present (1). [*R50, W28, LL3, L45, MA49, BO58, A35*, LO55]

56. Route of the venous drainage exiting from the back of the cavum epiptericum: only lateral flange vascular groove (0); absent (1); lateral flange vascular canal present (foramina on lateral surface) (2). [W53, WH22, *HK27*, LO56]

57. Maxillary and mandibular branch (V2+3) of the trigeminal nerve exit: via single foramen between prootic and epipterygoid (0); via two foramina between prootic and epipterygoid (1); via separate foramina, some enclosed by anterior lamina of prootic (petrosal) (2). [*L50, M48, HK28, B33 BO51, SS27, MA42, A65*, LO57]

58. Pterygoparoccipital foramen: squamosal does not contribute to enclosure of foramen (0); squamosal contributes to enclosure of foramen (1); open (2). [*LL23*, *L51*]

59. Vertical component of lateral flange of prootic (“L-shaped” and forming a vertical wall to pterygoparoccipital foramen): absent (0); present (1). [*L52*, LCS25]

60. Anterior part of paroccipital process: the lateral aspect covered by the squamosal (0); exposed due to dorsally withdrawn of the squamosal (1). [*L47*, LCS22]

61. Hyoid (stapedial) muscle fossa on the paroccipital process: absent (0); present (1). [R55, W56, WH35, LL7, L40, M59, LCS32, MA48, BO61, *A38*, LO61]

62. Paroccipital process: undifferentiated (0); differentiated (1). [*R56, W18, L46, L47, M50, LCS21, LCS30, BO66*, *A43*, *LO62*]

63. Fenestra rotunda separation from jugular foramen: (0) confluent; (1) partially separated by finger-like projection from postero-lateral wall of jugular foramen; (2) completely separated. [R60, W29, *LL10*, *L42*, M46, *HK42*, LCS33, *B39*, *BO60*, A40]

64. Articulation of the paroccipital process with the quadrate: absent (0); present (1). [*R19, W41, M52, HK29, A32*, LO64]

65. Paroccipital process in the base of the posttemporal fossa: absent (0); present (1). [*HK24, A44*, LO65]

66. Tabular: present (0), absent (1). [R22, LL19, L80, *LCS 47*, LO66]

67. The relationship of hypoglossal foramen (condylar foramen) with the jugular foramen: confluent or sharing a depression (0); at least one foramen completely separated from the jugular foramen (1). [*LL11, L75, M51, LCS39, BO65*]

68. Shape of the occipital condyles (in lateral view): bulbous (0); ovoid to cylindrical (1). [*LL15, L77,* LCS51]

69. Rotation of dorsal plate relative to trochlear axis on quadrate: less than 10 degree (0); about 45 degrees (1); around 90 degrees (2); parallel to trochlear axis (3). [L30, LC1]

70. Curvature of the contact facet on the posterior side of the dorsal plate of quadrate: flat or convex (0); concave (1). [*L29, LC2, M56*, LO70]

71. Size of the lateral trochlear condyle relative to the medial trochlear condyle on quadrate: the lateral condyle larger than the medial condyle (0); the medial condyle equal or larger than the lateral condyle (1). [*LC3*, LO71]
72. Shape of the trochlear of quadrate: cylindrical (0); trough-shaped (1). [LC4]
73. Lateral margin of the dorsal plate of quadrate: straight (0); flaring posteriorly (1); flaring and rotated posteromedially (2). [LC5]
74. Medial margin of the dorsal plate of quadrte: straight (0); flaring anteriorly (1); flaring and rotated anterolaterally (2). [LC6]
75. Dorsal margin of dorsal plate of quadrate: retains pointed angle (0); has rounded margin (1) [L31, LC7]
76. Lateral notch and neck of quadrate (separation of the lateral margin of the contact facet from the trochlear): the lateral notch is absent or poorly developed (0); lateral notch developed, separating the lateral margin of the contact facet from the lateral end of the trochlear (1); lateral notch is broader and separation of the lateral margin of contact facet for the trochlear is wider, the lateral margin is shifted medially (2); development of the neck with raise the contact facet away from the trochlear (3). [*L32*, LC8]
77. Articulation of the quadrate with the squamosal: via concave recess in the squamosal (0); covered dorsally by the squamosal (1); little or no contact with the squamosal (2). [*WH7*, *LC12,* M54, *HK31, A60*, LO77]
78. Articulation of the quadrate with the stapes: via a broad recess on the medial margin and the median end of the trochlear (0); the stapedial contact restricted to the medial end of the trochlear (1); via a projection from the medial margin of the dorsal plate (2);

via a medial vertical ridge in the neck (3); via a projection from the neck of the quadrate (4). [*R20, W42*, *L33*, LC14]

79. Craniomandibular articulation; quadrate/articular (0); main quadrate/articular, secondary surangular/squamosal (1); incipient dentary/squamosal (2); main dentary/squamosal (3). [*R66*, *R67*, *W9*, *W60, L23*, *L24*, *M60*, *HK25*, *LCS 70*, *B30*, *SS19*, *BO26*, *MA39*, *A58*, LO79]
80. Craniomandibular articulation: lies around the same height (0), much lower (1) or remarkably higher (2) than the postcanine line. [*L25, A59*, LO80]
81. Shape of squamosal articulation surface for mandible: small and medially or anteromedially facing facet (0); wide, ventrally directed glenoid cavity (1). [*L26*, *B19*, *BO37*, *MA22*, *A57*, LO81]
82. Dentary symphysis: unfused (0); fused (1). [R68, W10, L19, LCS56, HK44, B17, SS34, BO21, MA21, A61]
83. Lateral ridge of the dentary: absent (0); incipient (1); moderatly developed (2); strongly projected (3). [A47]
84. Angle of the dentary: close to the position of postorbital bar (0); close to the jaw joint (1). [*A54*, LO84]
85. Position of dentary-surangular dorsal contact relative to postorbital bar and jaw joint: around midway (0); closer to jaw joint (1). [*H48, A55*, LO85]
86. Mediolateral thickening of the anterior margin of the coronoid process: absent (0); present (1). [M66, H50, A51]
87. Splenial: large and deep, reaches ventral border of the dentary (0); reduced to thin splint covering dentary groove (1). [M64]

88. Postdentary bones: large, with tall surangular (0); angular, surangular, and prearticular reduced in height and lying in dentary groove (1); further reduced to single gracile rod in postdentary trough (2). [R74, W59, M65, H49]
89. Reflected lamina of angular posterior extent relative to distance from angle of dentary to jaw joint: greater than 1/2 the distance (0); less than l/2 the distance (1). [H51]
90. Reflected lamina of angular shape: spoon-shaped plate with slight depressions (0); hook-like lamina (1); reduced to thin process (2) [*M62*, *H52*, *SS44*, A56]
91. Mandibular movement during occlusion: orthal movement during power stroke (0); posteriorly directed power stroke (1); moderate rotation along the longitudinal axis in power stroke (2). [*R79*, *W62, L2,* LCS74, *B2, BO2*, LO91]
92. Postcanine occlusion: lack consistent contact relationship (0); bilateral, interdigitating occlusion between multiple cusps (1); precise unilateral occlusion (2) [*R84*, *R86*, *W33*, *L1*, *L14, M8, LCS 73, LCS 81*, *B1*, *BO1*, *MA1, A87*, LO92]
93. Relationships of wear facet to main cusp: wear facet absent (0); simple longitudinal facet on crown (1); main cusp bears two distinct facets (2); multiple cusps with each cusp bearing one or two transverse and crescentic facets (3). [*L17, B16, MA19, BO20*, LO93]
94. Upper incisors number: five or more (0); four (1); three or less (2). [*R81, W63, L5, M1, HK53, B3*, SS45, BO3, MA3, A76]
95. Lower incisor number: four or more (0); three (1); two or less (2). [L5, M2, HK54, B4, SS46, BO4, MA4, A77]
96. Incisor size: all of similar size (0); some incisors large (1). [HK56, *B5, B6*, *BO5*, *MA5*, *MA6, MA7,* A78, LO96, SMO96]

97. Incisor cutting margins: smoothly ridged (0); serrated (1); denticulated (2). [*HK55, A79*, LO97]

98. Distinct upper incisor/canine diastema: present (0); absent (1). [*A81*, LO98]

99. Upper canine: large (0); reduced in size (<10% of skull length) (1); absent (2). [*L6*, HK57, A83]

100. Lower canine: large (0); reduced in size (1); absent (2). [L6, HK58, A84]

101. Canine serrations: absent (0); present (1). [HK59, A8]

102. Upper postcanine morphology: sectorial without or with incipient cingulum broadening the crown (0); sectorial with a well-developed lingual cingulum (1); bucco-lingually expanded (2). [*L13*, *M5*, *M9*, *HK60*, *HK62*, *A7*, *SS51*, *SS55, B10, BO8, A89*, LO102]

103. Anteriormost one-cusped tooth: present till adult (0); present only in juvenile (1); absent (2). [LO103]

104. Posteriormost gomphodont postcanine(s) in adults: absent (0); absent in juvenile but present in adult (1); present from juvenile (2). [HK80]

105. Posterior postcanines with strongly curved main cusp: absent (0); present (1). [*S52*, A90]

106. Upper postcanine roots: single (0); constricted root, with longitudinal groove (1); divided into two longitudinal aligned roots (2); multiple roots (more than two) (3). [*R88, W65, W66, L9, M6, LCS77, B8, BO6, MA9*, *A95*, *LO106, SMO106*]

107. Lower postcanine roots: single (0); constricted root, with longitudinal groove (1); divided (2). [*R88*, W65, *L9*, M7, *B8, BO6*, *MA9, A94*, *LO107, SMO107*]

108. Buccal (external) cingulum on sectorial upper postcanines: absent (0); present (1). [*R85, HK61, B9, BO7, MA10, A91*, LO108]

109. Number of upper cusps in transverse row: one (0); two (1); three or more (2). [HK63, A92]

110. Position of upper transverse cusp row on crown: midcrown (almost to posterior margin) (0); on anterior half of crown (1); at posterior margin (no posterior cingulum) (2). [HK64]

111. Central cusp of upper transverse row: absent (0), midway between buccal and lingual cusps (1); closer to lingual cusp (2). [HK65]

112. Arrangement of main cups of upper postcanines: in single longitudinal row (0); multiple cusps in multiple rows (1). [L13, LCS78]

113. Interlocking of lower postcanines: absent (0); distal cuspule ‘d’ of anterior molar fits into embayment between cusp ‘b’ and cusp ‘e’ of the succeeding molar (1). [L11, B14, BO18]

114. Number of lower cusps in transverse row: two (0), three or more (1). [*HK73*, LO114]

115. Lingual cingulum on lower postcanine: present (0); vestigial or absent (1) [*L12*, *LCS80, B11*, *B12*, *BO9*, *BO10*, S*S56, A93*, LO115]

116. Lower posterior basin: absent (0); present (1). [HK75]

117. Axis of posterior part of maxillary tooth row: directed lateral to subtemporal fossa (0); directed toward center of fossa (1); directed toward medial rim of the fossa and diverged (2); directed toward medial rim of the fossa and parallel (3). [*R80*, *M12, HK78*, *B13*, *MA17*, *MA20*, *BO14*, *BO16*, *BO17, A86*, LO117]

118. Upper tooth series posterior extension: below the orbit and anterior to the subtemporal fenestra (0); anterior to the orbit (1); behind the anterior border of the subtemporal fenestra (2). [*HK79, A75*, LO118]

119. Postcanine replacement pattern: alternating (0); delayed (1); at most single replacement for one position (2); sequential addition of postcanines, no replacement (3). [*L7, HK81, LCS89, B7*, LO119]

120. Vertebral centra: amphicoelous (0); platycoelous (1). [R108, HK101, B51, BO78, MO61]

121. Axis centrum: cylindrical (0) or depressed (1). [R98]

122. Dens: absent or vestigial (0) or strongly developed (1) [R99]

123. Posterior thoracic vertebrate (or middle of the dorsal vertebrate): neural spines slightly inclined or nearly vertical (0) or strongly inclined (1). [*R102*, LO123]

124. Anapophysis: absent (0); present (1). [LO124]

125. Expanded costal plates on dorsal ribs: absent (0); present (1). [HK82]

126. Lumbar costal plates with ridge overlapping preceding rib: absent (0); present (1). [HK83]

127. Acromion process: absent (0); weak to moderate (1); strongly developed and close to level of glenoid (2). [R115, HK85]

128. Scapular constriction below the acromion process: absent (0); present (1). [HK86]

129. Scapular elongation between the acromion and glenoid: absent (0); present (1). [HK87, *B41, BO68*, *MO51*, LO129]

130. Procoracoid in glenoid: present (0); barely present or absent (1). [R116, HK88, B42, BO 71, MO52]

131. Procoracoid contact with scapula: greater than coracoid contact (0); equal to or less than coracoid contact (1). [HK89, B43, BO72, MO53]

132. Humeral ectepicondylar foramen: present (0); absent (1). [R124, HK90, B44, BO73, MO54]

133. Ulnar olecranon process: unossified or poorly ossified (0); well ossified (1). [*R128, HK91, B45, MO55*, LO133]

134. Manual digit III phalanx number: four (0); three (1). [HK92]

135. Manual digit IV phalanx number: four (0); three (1). [HK93]

136. Dorsal profile of ilium: strongly convex (0); flat to concave (1). [R130, HK96, B48, BO75]

137. Length of anterior process of ilium anterior to acetabulum (relative to diameter of acetabulum): less than 1.5 (0); greater than 1.5 (1). [HK94, B46, BO74, MO56]

138. Lateral surface of iliac blade: concave or nearly flat (0); convex (1); a longitudinal ridge divides it into dorsal and ventral moieties (1). [*R131*, LO138]

139. Posterior iliac spine: robust and extends beyond acetabulum (0); reduced to small nub that lies entirely anterior to acetabulum (1). [R132, *R133*, LO139]

140. Cotyloid (acetabular) notch: lies between the ischial and iliac part of the acetabulum, mainly on ilium (0); between acetabular facet and pubic process of the ischium, on ischium (1). [*R134*, LO140]

141. The diameter of the obturator foramen greater than that of the acetabulum: absent (0); present (1). [*R139*, LO141]

142. Femoral head: rounded and predominately in plane of shaft (0); subspherical and inflected dorsally (1). [R141]

143. Greater trochanter separated from femoral head by distinct notch: absent (0); present (1). [R143, HK98, B49, BO76, MO59]

144. Lesser trochanter position: on ventromedial surface of femoral shaft (0); on medial surface of femoral shaft (1). [R144, HK100, B50, BO77, MO60]

145. Lesser trochanter location near the level of the femoral head: absent (0); present (1). [BO80, MO63]

146. Posterior portion of secondary palate almost at the level of the tip of the postcanine upper teeth, forming a deep groove between the hard palate and the tooth row: (0) absent; (1) present. [MR]

147. Morphology of upper middle and posterior postcanines for taxa with sectorial teeth (see Ch. 102): (0) symmetrical postcanines with main cusp A and small mesial and distal accessory cusps; (1) mesiodistally asymmetrical postcanines with main cusp A and accessory mesial (usually one) and distal ones vertically oriented; (2) mesiodistally asymmetrical postcanines with main cusp A and accessory mesial (if present) and distal ones strongly curved posteriorly; (3) mesiodistally symmetrical postcanines with bulbous main cusp A and accessory ones; (4) leaf-shaped postcanines. This character was employed to improve the variability of sectorial teeth of character 102 used by several authors. [WMR]

148. Number of upper postcanine teeth in adults: (0) no greater than 10; (1) greater than 11. [SH]

149. Cochlear canal: absent or shallow (forms a short triangular extension of the vestibule at best) (0), excavates a deep recess that can be easily separated from the rest of the vestibule (1). [BE]

150. Maxillary canal external nasal ramus: present (0), reduced or absent (1). [BE]

151. Maxillary canal internal nasal and superior labial rami: present (0), reduced or absent (1). [BE]

152. Lacrimal duct and zygomaticofacial canal: fused (0), separated (1). [BE]

153. Maxillary antrum and maxillary canal: fused (0), separated (1). [BE]

154. Anteroposteriorly elongated maxillary antrum: absent (0), present (1). [BE]

References

Abdala F (2007) Redescription of *Platycraniellus elegans* (Therapsida, Cynodontia) from the Lower Triassic of South Africa, and the cladistic relationships of eutheriodonts. Palaeontology 50:591–618. https://doi.org/10.1111/j.1475-4983.2007.00646.x

Benoit J, Nxumalo M, Norton LA, Fernandez V, Gaetano LC, Rubidge B, Abdala F (2022) Synchrotron scanning sheds new light on *Lumkuia fuzzi* (Therapsida, Cynodontia) from the Middle Triassic of South Africa and its phylogenetic placement. J African Earth Sci 196:104689. https://doi.org/10.1016/j.jafrearsci.2022.104689

Bonaparte JF, Martinelli AG, Schultz CL (2005) New information on *Brasilodon* and *Brasilitherium* (Cynodontia, Probainognathia) from the Late Triassic of Southern Brazil. Rev Bras de Paleontol 8:25–46. https://doi.org/10.4072/rbp.2005.1.03

Bonaparte JF, Martinelli AG, Schultz CL, Rubert R (2003) The sister group of mammals: small cynodonts from the Late Triassic of Southern Brazil. Rev Bras de Paleontol 5:5–27.

Hopson JA, Kitching JW (2001) A probainognathian cynodont from South Africa and the phylogeny of nonmammalian cynodonts. Bull Mus Comp Zool Harv Univ 156:5–35.

Kerber L, Martinelli AG, Müller RT, Pretto FA (2022) A new specimen provides insights into the anatomy of *Irajatherium hernandezi*, a poorly known probainognathian cynodont from the Late Triassic of southern Brazil. Anat Rec 1–21. https://doi.org/10.1002/ar.24830

Liu J, Olsen P (2010) The phylogenetic relationships of Eucynodontia (Amniota, Synapsida). J Mamm Evol 17:151–176. https://doi.org/10.1007/s10914-010-9136-8

Lucas SG, Luo Z-X (1993) *Adelobasileus* from the Upper Triassic of West Texas: the oldest mammal. J Vertebr Paleontol 13:309–334. https://doi.org/10.1080/02724634.1993.10011512

Luo Z-X (1994) Sister-group relationships of mammals and transformations of diagnostic mammalian characters. In: Fraser NC, Sues H-D (editors). The Shadow of the Dinosaurs: Early Mesozoic Tetrapods. Cambridge University Press, Cambridge, New York. 98–128.

Luo Z-X, Crompton AW (1994) Transformation of the quadrate (incus) through the transition from non-mammalian cynodonts to mammals. J Vertebr Paleontol 14:341–74.

Luo Z-X, Crompton AW, Lucas SG (1995) Evolutionary origins of the mammalian promontorium and cochlea. J Vertebr Paleontol 15:113–121.

Luo Z-X, Crompton AW, Sun A-L (2001) A new mammaliaform from the Early Jurassic and evolution of mammalian characteristics. Science 292:1535–1540.

Martinelli AG, Rougier GW (2007) On *Chaliminia musteloides* Bonaparte (Cynodontia, Tritheledontidae) and the phylogeny of the Ictidosauria. J Vertebr Paleontol 27: 442–460. https://doi.org/10.1671/0272-4634(2007)27[442:OCMETF]2.0.CO;2

Martinelli AG, Bonaparte JF, Schultz CL, Rubert R (2005) A new tritheledontid (Therapsida, Eucynodontia) from the Late Triassic of Rio Grande do Sul (Brazil) and its phylogenetic relationships among carnivorous non-mammalian eucynodonts. Ameghiniana 42:191–208.

Martinelli AG, Eltink E, Da-Rosa ÁAS, Langer MC (2017a) A new cynodont (Therapsida) from the *Hyperodapedon* Assemblage Zone (upper Carnian-Norian) of southern Brazil improves the Late Triassic probainognathian diversity. Pap Palaeontol 3:401–423. https://doi.org/10.1002/spp2.1081

Martinelli AG, Soares MB, de Oliveira TV, Rodrigues PG, Schultz CL (2017b) The Triassic eucynodont *Candelariodon barberenai* revisited and the early diversity of stem prozostrodontians. Acta Palaeontol Pol 62:527–542. https://doi.org/10.4202/app.00344.2017

Martinelli AG, Soares MB, Schwanke C (2016) Two new cynodonts (Therapsida) from the Middle-early Late Triassic of Brazil and comments on South American probainognathians. PLoS One 11:e0162945. https://doi.org/10.1371/journal.pone.0162945

Martínez RN, May CL, Forster CA (1996) A new carnivorous cynodonts from the Ischigualasto Formation (Late Triassic, Argentina), with comments on eucynodont phylogeny. J Vertebr Paleontol 16:271–284.

Pacheco CP, Martinelli AG, Pavanatto AEB, Soares MB, Dias-da-Silva S (2017) *Prozostrodon brasiliensis*, a probainognathian cynodont from the Late Triassic of Brazil: second record and improvements on its dental anatomy. Hist Biol 30:475–485. https://doi.org/10.1080/08912963.2017.1292423

Rowe T (1988) Definition, diagnosis, and origin of Mammalia. J Vertebr Paleontol 8:241–64.

Sidor CA, Smith RMH (2004) A new galesaurid (Therapsida: Cynodontia) from the Lower Triassic of South Africa. Palaeontology 47:535–56. https://doi.org/10.1111/j.0031-0239.2004.00378.x

Sidor CA, Hancox PJ (2006) *Elliotherium kersteni*, a new tritheledontid from the Lower Elliot Formation (Upper Triassic) of South Africa. *J Paleontol* 80:333–342. https://doi.org/10.1666/0022-3360(2006)080[0333:EKANTF]2.0.CO;2

Soares MB, Martinelli AG, Oliveira TV (2014) A new prozostrodontian cynodont (Therapsida) from the Late Triassic *Riograndia* Assemblage Zone (Santa Maria Supersequence) of Southern Brazil. An Acad Bras Cienc 86:1673–1691. https://doi.org/10.1590/0001-3765201420140455

Wallace RV, Martínez R, Rowe T (2019) First record of a basal mammaliamorph from the early Late Triassic Ischigualasto Formation of Argentina. PLoS One 14:e0218791. https://doi.org/10.1371/journal.pone.0218791

Wible JR (1991) Origin of Mammalia: the craniodental evidence reexamined. J Vertebr Paleontol 11:1–28.

Wible JR, Hopson JA (1993) Basicranial evidence for early mammal phylogeny. In: Szalay FS, Novacek MJ, McKenna MC (editors). Mammal Phylogeny: Mesozoic Differenctiation, Multituberculates, Monotremes, Early Therians, and Marsupials. New York, Springer-Verlag. pp. 42–62.

CONSIDERAÇÕES FINAIS

3 CONCLUSÕES

Nesta presente tese de doutorado, a morfologia, taxonomia e filogenia de três novos espécimes de cinodontes não-mamaliaformes do Triássico Superior do Rio Grande do Sul é analisada. Os dois primeiros espécimes estudados, CAPPA/UFSM 0262 e CAPPA/UFSM 0208, correspondem a um novo gênero e espécie de cinodonte prozostrodonte não-mamaliaforme, *Agudotherium gassenae* Stefanello et al., 2020a. O novo táxon consiste em um dentário esquerdo com canino e dentes pós-caninos bem preservados (holótipo, CAPPA/UFSM 0262) e um dentário direito com incisivos, canino e dentes pós-caninos pouco informativos (parátipo, CAPPA/UFSM 0208). *Agudotherium gassenae* difere claramente de outros cinodontes não-mamaliaformes carnianos e norianos conhecidos por possuir uma combinação única de características, tais como: um dentário robusto, com o corpo do dentário dorsoventralmente profundo e com margem ventral retilínea; um sulco Meckeliano longo e dorsoventralmente alto, disposto retilineamente na metade dorsoventral do dentário; ausência de serrilhas nas bordas mesial e distal do canino; e dentes pós-caninos setoriais não serrilhados, com cúspides inclinadas posteriormente, apresentando cíngulo lingual restrito aos cantos mesiolingual e distolingual das coroas. A nova espécie fornece evidências adicionais para a diversidade de cinodontes probainognátios não-mamaliaformes, bem como para o conhecimento da irradiação adaptativa de Prozostrodontia, ocorrida durante o Triássico Superior que levou ao surgimento de vários grupos, incluindo os Mammaliaformes.

O terceiro material analisado, CAPPA/UFSM 0210, compreende um novo e mais completo espécime de *Prozostrodon brasiliensis* (BARBERENA; BONAPARTE; TEIXEIRA, 1987), representado por um crânio completo excepcionalmente bem preservado, com dentários desarticulados. Dada à completude do espécime, o novo material de *P. brasiliensis*, fornece informações anatômicas adicionais para a região posterior do crânio, ajudando a compreender as principais transformações evolutivas sofridas nessa região. Os novos dados anatômicos, por meio de análises filogenéticas, revelam um novo clado endêmico de cinodontes sul-americano. Prozostrodontidae, formado pela relação de táxon-irmão entre *P. brasiliensis* e *Pseudotherium argentinus* Wallace; Martínez; Rowe, 2019, ilustra a primeira radiação de prozostrodontes carnianos para o Gondwana ocidental e reforça a similaridade faunística compartilhada entre os dois países vizinhos, Brasil e Argentina.

REFERÊNCIAS BIBLIOGRÁFICAS DO TEXTO INTEGRADOR

ABDALA, F. Redescription of *Platycraniellus elegans* (Therapsida, Cynodontia) from the Lower Triassic of South Africa, and the cladistic relationships of eutheriodonts. **Palaeontology**, v. 50, p. 591–618, 2007.

ABDALA, F. et al. South American Middle Triassic continental faunas with Amniotes: Biostratigraphy and Correlation. **Palaeontologia Africana**, v. 44, p. 83–87, 2009.

ABDALA, F. et al. Non-mammaliaform cynodonts from western Gondwana and the significance of Argentinean forms in enhancing understanding of the group. **Journal of South American Earth Sciences**, v. 104, p. 102884, 2020.

ABDALA, F.; BARBERENA, M. C.; DORNELLES, J. E. A new species of the traversodontid cynodont *Exaeretodon* from the Santa Maria Formation (Middle/Late Triassic) of southern Brazil. **Journal of Vertebrate Paleontology**, v. 22, n. 2, p. 313–325, 2002.

ABDALA, F.; JASINOSKI, S. C.; FERNANDEZ, V. Ontogeny of the Early Triassic cynodont *Thrinaxodon liorhinus* (Therapsida): dental morphology and replacement. **Journal of Vertebrate Paleontology**, v. 33, p. 1408–1431, 2013.

ABDALA, F.; GAETANO, L. C. The Late Triassic record of cynodonts: time of innovations in the mammalian lineage. **The late Triassic world**, Springer, p. 407–445, 2018.

ABDALA, F.; NEVELING, J.; WELMAN, J. A new trirachodontid cynodont from the lower levels of the Burgersdorp Formation (Lower Triassic) of the Beaufort Group, South Africa and the cladistic relationships of Gondwanan gomphodonts. **Zoological Journal of the Linnean Society**, v. 147, p. 383–413, 2006.

ABDALA, F.; RIBEIRO, A. M. A new therioherpetid cynodont from the Santa Maria Formation (middle Late Triassic), southern Brazil. **Geodiversitas**, v. 22, p. 589–596, 2000.

ABDALA, F.; RIBEIRO, A. M. Distribution and diversity patterns of Triassic cynodonts (Therapsida, Cynodontia) in Gondwana. **Palaeogeography, Palaeoclimatology, Palaeoecology**, v. 286, p. 202–217, 2010.

ABDALA, F.; RIBEIRO, A. M.; SCHULTZ, C. L. A rich cynodont fauna of Santa Cruz do Sul, Santa Maria Formation (Middle–Late Triassic), southern Brazil. **Neues Jahrbuch für Geologie und Paläontologie**, Monatshefte, p. 669–687, 2001.

ALLIN, E. F. Evolution of the mammalian middle ear. **Journal of Morphology**, v. 147, p. 403–438, 1975.

ALLIN, E. F. The auditory apparatus of advanced mammal-like reptiles and early mammals. In: HOTTON, III. N.; MACLEAN, P. D.; ROTH, J. J.; ROTH, E. C. (Editors) **The Ecology and**

Biology of Mammal-like Reptiles. Washington DC: Smithsonian Institution Press. p. 283–294, 1986.

ALLIN, E. F.; HOPSON, J. A. Evolution of the auditory system in Synapsida ("Mammal-like Reptiles" and primitive mammals) as seen in the fossil record. In: WEBSTER, D. B.; FAY, R. R.; POPPER, A. N. (Editors). **The evolutionary biology of hearing.** New York: Springer-Verlag. p. 587–614, 1992.

ARAÚJO, R. et al. Inner ear biomechanics reveals a Late Triassic origin for mammalian endothermy. **Nature**, p. 1–6, 2022.

ARAÚJO, D. C.; GONZAGA, T. D. Uma nova especie de *Jachaleria* (Therapsida, Dicynodontia) do Triassico do Brasil. In: **Actas del II Congreso Argentino de Paleontología y Biostratigrafía/I Congresso Latinoamericano de Paleontología**. Buenos Aires, p. 159–174, 1980.

BARBERENA, M. C.; BONAPARTE, J. F.; TEIXEIRA, A. M. S. *Thrinaxodon brasiliensis* sp. nov., a primeira ocorrência de cinodontes galessauros para o Triássico do Rio Grande do Sul. In: **Anais do X Congresso Brasileiro de Geologia, Rio de Janeiro**, v. 1, p. 67–74, 1987.

BONAPARTE, J. F. Sobre nuevos terápsidos Triásicos hallados en el centro de la Provincia de Mendoza, (Therapsida, Dicynodontia y Cynodontia). **Acta Geológica Lilloana**, v. 8, p. 95–100, 1966.

BONAPARTE, J. F. *Cynognathus minor* n. sp. (Therapsida-Cynodontia). Nueva evidencia de vinculación faunística Afro-Sudamericana a principios del Triásico. **Gondwana Stratigraphy**, I.U.G.S., Coloquio Mar del Plata, v. 1967, p. 273–281, 1969.

BONAPARTE, J. F. Los tetrápodos del sector superior de la Formación Los Colorados, La Rioja, Argentina (Triásico Superior). **Opera Lilloana**, v. 22, p. 1–183, 1971.

BONAPARTE, J. F. et al. The sister group of Mammals: small cynodonts from the Late Triassic of southern Brazil. **Revista Brasileira de Paleontologia**, v. 5, p. 5–27, 2003.

BONAPARTE, J. F. et al. La fauna local de Faxinal do Soturno, Triásico Tardío de Rio Grande do Sul, Brasil. **Revista Brasileira de Paleontologia**, v. 13, p. 233–246, 2010.

BONAPARTE, J. F.; BARBERENA, M. C. A possible mammalian ancestor from the Middle Triassic of Brazil (Therapsida-Cynodontia). **Journal of Paleontology**, p. 931–936, 1975.

BONAPARTE, J. F.; BARBERENA, M. C. On two advanced carnivorous cynodonts from the Late Triassic of Southern Brazil. In: JENKINS, JR. F. A.; SHAPIRO, M. D.; OWERKOWICZ, T. (Editors) Studies in Organismic and Evolutionary Biology in honor of Crompton AW. **Bulletin of the Museum of Comparative Zoology at Harvard College**, v. 156, p. 59–80, 2001.

BONAPARTE, J. F.; FERIGOLO, J.; RIBEIRO, A. M. A primitive Late Triassic 'ictidosaur' from Rio Grande do Sul, Brazil. **Palaeontology**, v. 44, n. 4, p. 623-635, 2001.

BONAPARTE, J. F.; MARTINELLI, A. G.; SCHULTZ, C. L. New information on *Brasilodon* and *Brasilitherium* (Cynodontia, Probainognathia) from the Late Triassic of southern Brazil. **Revista Brasileira de Paleontologia**, v. 8, p. 25–46, 2005.

BONAPARTE, J. F.; MIGALE, L. A. Protomamíferos y Mamíferos Mesozoicos de América del Sur. Museo de Ciencias Naturales Carlos Ameghino. **Mercedes**, v. 442, p. 1–441, 2010.

BONAPARTE, J. F.; SOARES, M. B.; MARTINELLI, A. G. Discoveries in the Late Triassic of Brazil improve knowledge on the origin of mammals. Historia Natural, Fundación Felix de Azara, **Tercera Serie**, v. 2, p. 5–30, 2012.

BONAPARTE, J. F.; SOARES, M. B.; SCHULTZ, C. L. A new non-mammalian cynodont from the Middle Triassic of southern Brazil and its implications for the ancestry of Mammals. **Bulletin of the New Mexico Museum of Natural History & Science**, v. 37, p. 599–607, 2006.

BONAPARTE, J. F.; SUES, H. D. A new species of *Clevosaurus* (Lepidosauria: Rhynchocephalia) from the upper Triassic of Rio Grande do Sul, Brazil. **Palaeontology**, v. 49, n. 4, p. 917–923, 2006.

BOTHA, J.; ABDALA, F.; SMITH, R. The oldest cynodont: new clues on the origin and early diversification of the Cynodontia. **Zoological Journal of the Linnean Society**, v. 149, p. 477–492, 2007.

BOTHA-BRINK, J.; SOARES, M. B.; MARTINELLI, A. G. Osteohistology of Late Triassic prozostrodontian cynodonts from Brazil. **PeerJ**, v. 6, p. e5029, 2018.

CABRERA, A. El primer hallazgo de terápsidos en la Argentina. **Notas del Museo de La Plata**, v. 8, n. 55, p. 317–331, 1943.

CROMPTON, A. W. Postcanine occlusion in Cynodonts and Tritylodonts. Bulletin of the British Museum (Natural History), **Geology**, v. 21, p. 29–71, 1972.

CROMPTON, A. W. The dentitions and relationships of the southern African Triassic mammals, *Erythrotherium parringtoni* and *Megazostrodon rudnerae*. Bulletin of the British Museum (Natural History). **Geology**, v. 24, p. 397–437, 1974.

CROMPTON, A. W. et al. Structure of the nasal region of non-mammalian cynodonts and mammaliaforms: speculations on the evolution of mammalian endothermy. **Journal of Vertebrate Paleontology**, v. 37, p. e1269116, 2017.

CROMPTON, A. W.; HYLANDER, W. L. Changes in mandibular function following the acquisition of a dentary-squamosal jaw articulation. In: HOTTON, III. N.; MACLEAN, P. D.; ROTH, J. J.; ROTH, E. C. (Editors). **The Ecology and Biology of Mammal-like Reptiles.** Washington DC: Smithsonian Institution Press. p. 263–281, 1986.

CROMPTON, A. W.; LUO, Z.-X. Relationships of the Triassic mammals *Sinoconodon*, *Morganucodon oehleri*, and *Dinnetherium*. In: SZALAY, F. S.; NOVACEK, M. J.; MCKENNA, M. C. (Editors) **Mammal Phylogeny: Mesozoic Differentiation, Multituberculates, Monotremes, Early Therians and Marsupials.** New York: Springer-Verlag, p. 30–44, 1993.

FERIGOLO, J.; LANGER, M. C. A Late Triassic dinosauriform from south Brazil and the origin of the ornithischian predentary bone. **Historical Biology**, v. 19, n. 1, p. 23–33, 2007.

GUIGNARD, M. L.; MARTINELLI, A. G.; SOARES, M. B. Reassessment of the postcranial anatomy of *Prozostrodon brasiliensis* and implications for postural evolution of nonmammaliaform cynodonts. **Journal of Vertebrate Paleontology**, v. 38, p. e1511570, 2018.

HILLENIUS, W. J. The evolution of nasal turbinates and mammalian endothermy. **Paleobiology**, v. 18, p. 17–29, 1992.

HILLENIUS, W. J. Turbinates in therapsids: evidence for Late Permian origins of mammalian endothermy. **Evolution**, v. 48, p. 207–229, 1994.

HOPSON, J. A. Postcanine replacement in the gomphodont cynodont *Diademodon*. In: KERMACK, D. M.; KERMACK, K. A. (Editors). **Early mammals. Zoological Journal of the Linnean Society**, v. 50, p. 1–21, 1971.

HOPSON, J. A. Cladistic analysis of therapsid relationships. **Journal of Vertebrate Paleontology**, v. 10, n. 3, p. 28A, 1990.

HOPSON, J. A.; BARGHUSEN, H. An analysis of Therapsid relationships. **The ecology and biology of mammal-like reptiles**. Washington DC, p. 83–106, 1986.

HOPSON, J. A.; KITCHING, J. W**.** A probainognathian cynodont from South Africa and the Phylogeny of nonmammalian Cynodonts. **Bulletin of the Museum of Comparative Zoology**, v. 156, p. 5–35, 2001.

HORN, B. L. D. et al. A new third-order sequence stratigraphic framework applied to the Triassic of the Paraná Basin, Rio Grande do Sul, Brazil, based on structural, stratigraphic and paleontological data. **Journal of South American Earth Sciences**, v. 55, p. 123–132, 2014.

HUENE, F. F. Von. **Die Fossilien Reptilien des Südamerikanischen Gondwanalands.** C.H. Beck'sche Verlag, Münich, p. 332, 1936.

KAMMERER, C. F. A new taxon of cynodont from the *Tropidostoma* Assemblage Zone (upper Permian) of South Africa, and the early evolution of Cynodontia. **Palaeontology**, v. 2, p. 387–397, 2016.

KERBER, L. et al. A new specimen provides insights into the anatomy of *Irajatherium hernandezi*, a poorly known probainognathian cynodont from the Late Triassic of southern Brazil. **The Anatomical Record**, p. 1–21, 2022.

KERMACK, K. A.; MUSSETT, F.; RIGNEY, H. W. The lower jaw of *Morganucodon*. **Zoological Journal of the Linnean Society**, v. 53, p. 87–175, 1973.

KEMP, T. S. **Mammal-like Reptiles and the Origin of Mammals.** Academic Press, London, p. 363, 1982.

KEMP, T. S. **The Origin and Evolution of Mammals.** Oxford: University Press, p. 342, 2005.

KEMP, T. S. Acoustic transformer function of the postdentary bones and quadrate of a nonmammalian cynodont. **Journal of Vertebrate Paleontology**, v. 27, n. 2, p. 431–44, 2007.

KEMP, T. S. The origin and radiation of therapsids. In: CHINSAMY-TURAN, A. (Editor.). **The Forerunners of Mammals: Radiation. Histology. Biology.** Bloomington: Indiana University Press, p. 3–28, 2012.

KIELAN-JAWOROWSKA, Z.; CIFELLI, R. L.; LUO, Z.-X. **Mammals from the Age of Dinosaurs.** Origins, Evolution, and Structure. New York: Columbia University Press, p. 630, 2004.

LANGER, M. C.; RAMEZANI, J.; DA ROSA, Á. A. U-Pb age constraints on dinosaur rise from south Brazil. **Gondwana Research**, v. 57, p. 133–140, 2018.

LANGER, M. C. et al. The continental Tetrapod bearing Triassic of south Brazil. **Bulletin of the New Mexico Museum of Natural History and Science**, v. 41, p. 201–218, 2007.

LAUTENSCHLAGER, S. et al. Morphological evolution of the mammalian jaw adductor complex. **Biological Reviews**, v. 92, p. 1910–1940, 2016.

LINNAEUS, C. **Systema naturae per regna tria naturae, secundum classes, ordines, genera, species, cum characteribus, differentiis, synonymis, locis.** Regnum animale. Editio decima, reformata. Laurentii Salvii, Stockholm, 1758.

LIU, J.; ABDALA, F. Phylogeny and taxonomy of the Traversodontidae. In: **Early evolutionary history of the Synapsida.** Springer Netherlands, p. 255–279, 2014.

LIU, J.; OLSEN, P. E. The phylogenetic relationships of Eucynodontia (Amniota, Synapsida). **Journal of Mammalian Evolution**, v. 17, p. 151–176, 2010.

LIU, J.; SUES, H.-D. Dentition and tooth replacement of *Boreogomphodon* (Cynodontia, Traversodontidae) from the Upper Triassic of North Carolina, USA. **Vertebrata Pal Asiatica**, v. 48, p. 169–184, 2010.

LUCKETT, W. P. An ontogenetic assessment of dental homologies in therian mammals. In: SZALAY, F. S.; NOVACEK, M. J.; MCKENNA, M. C. (Editors) **Mammal Phylogeny: Mesozoic Differentiation, Multituberculates, Monotremes, Early Therians, and Marsupials.** New York: Springer-Verlag. p. 182–204, 1993.

LUO, Z.-X. Sister-group relationships of mammals and transformations of diagnostic mammalian characters. In: **The Shadow of the Dinosaurs.** Cambridge University Press, Cambridge, p. 98–128, 1994.

LUO, Z.-X. Inner ear and its bony housing in tritylodontids and implications for evolution of mammalian ear. **Bulletin of the Museum of Comparative**, v. 156, p. 81–97, 2001.

LUO, Z.-X. Transformation and diversification in early mammal evolution. **Nature**, v. 450, n. 7172, p. 1011–1019, 2007.

LUO, Z.-X. Developmental patterns in Mesozoic evolution of mammal ears. **Annual Review of Ecology, Evolution and Systematics**, v. 42, p. 355–380, 2011.

LUO, Z.-X. et al. Mandibular and dental characteristics of Late Triassic mammaliaform *Haramiyavia* and their ramifications for basal mammal evolution. **Proceedings of National Academy of Sciences of the USA**, v. 112, p. E7101–E7109, 2015.

LUO, Z.-X.; CROMPTON, A. W.; LUCAS, S. G. Evolutionary origins of the mammalian promontorium and cochlea. **Journal of Vertebrate Paleontology**, v. 15, p. 113–121, 1995.

LUO, Z.-X.; MANLEY, G. A**. Origins and early evolution of mammalian ears and hearing function.** p. 207–252, 2020.

LUO, Z.-X.; SCHULTZ, J. A.; EKDALE, E. G. Evolution of the middle and inner ears of mammaliaforms: the approach to mammals. In: **Evolution of the vertebrate ear.** Springer, Cham, p. 139–174, 2016.

LUO, Z.-X.; WIBLE, J. R. A new Late Jurassic digging mammal and early mammalian diversification. **Science**, v. 308, p. 103–107, 2005.

MAIER, W.; HEEVER, J. V. D.; DURAND, F. New therapsid specimens and the origin of the secondary hard and soft palate. **Journal of Zoological Systematic and Evolutionary Research**, v. 34, p. 9–19, 1996.

MANLEY, G. A. Evolutionary paths to mammalian cochleae. **Journal of Association of Research on Otolaryngology**, v. 13, p. 733–743, 2012.

MARSOLA, J. C. et al. New sauropodomorph and cynodont remains from the Late Triassic *Sacisaurus* site in southern Brazil and its stratigraphic position in the Norian Caturrita Formation. **Acta Palaeontologica Polonica**, v. 63, p. 653–669, 2018.

MARTINELLI, A. G. et al. A new tritheledontid (Therapsida, Eucynodontia) from the Late Triassic of Rio Grande do Sul (Brazil) and its phylogenetic relationships among carnivorous non-mammalian eucynodonts. **Ameghiniana**, v. 42, n. 1, p. 191–208, 2005.

MARTINELLI, A. G. et al. The African cynodont *Aleodon* (Cynodontia, Probainognathia) in the Triassic of southern Brazil and its biostratigraphic significance. **Plos One**, v. 12, n. 6, p. e0177948, 2017a.

MARTINELLI, A. G. et al. A new cynodont from the Santa Maria Formation, South Brazil, improves Late Triassic probainognathian diversity. **Palaeontology**, v. 3, p. 401–423, 2017b.

MARTINELLI, A. G. et al. *Brasilodon quadrangularis*, *Brasilitherium riograndensis* and *Minicynodon maieri* (Cynodontia): taxonomy, ontogeny and tooth replacement. In: **Paleontologia em Destaque, Boletim de Resumos XXV Congresso Brasileiro de Paleontologia**, Ribeirão Preto, SP, Brazil, p. 189, 2017c.

MARTINELLI, A. G.; BONAPARTE, J. F. Postcanine replacement in *Brasilodon* and *Brasilitherium* (Cynodontia, Probainognathia) and its bearing in cynodont evolution. In: CALVO, J.; PORFIRI, J.; GONZÁLEZ RIGA, B.; DOS SANTOS, D. (Editors) **Dinosaurios y Paleontología desde América Latina.** Anales del III Congreso Latinoamericano de Paleontología. Mendoza: Editorial de la Universidad Nacional de Cuyo. p. 179–186, 2011.

MARTINELLI, A. G.; ROUGIER, G. W. On *Chaliminia musteloides* Bonaparte (Cynodontia, Tritheledontidae) and the phylogeny of the Ictidosauria. **Journal of Vertebrate Paleontology**, v. 27, p. 442–460, 2007.

MARTINELLI, A. G.; SOARES, M. B. **Evolution of South American cynodonts.** Contribuciones Científicas del Museo Argentino de Ciencias Naturales “Bernardino Rivadavia”, v. 6, p. 183–197, 2016.

MARTINELLI, A. G.; SOARES, M. B.; SCHWANKE, C. Two New Cynodonts (Therapsida) from the Middle-Early Late Triassic of Brazil and Comments on South American Probainognathians. **Plos One**, v. 11, n. 10, p. e0162945, 2016.

MARTÍNEZ, R. N.; FERNANDEZ, E.; ALCOBER, O. A. A new Nonmammaliaform Eucynodont from the Carnian-Norian Ischigualasto Formation, northwestern Argentina. **Revista Brasilera de Paleontología**, v. 16, p. 61–76, 2013.

MARTÍNEZ, R. N.; FORSTER, C. A. The skull of *Probelesodon sanjuanensis*, sp. nov., from the Late Triassic Ischigualasto Formation of Argentina. **Journal of Vertebrate Paleontology**, v. 16, p. 285–291, 1996.

MARTÍNEZ, R. N.; MAY, C. L.; FORSTER, C. A. A new carnivorous cynodonts from the Ischigualasto Formation (Late Triassic, Argentina), with comment on eucynodont phylogeny. **Journal of Vertebrate Paleontology**, v. 16, p. 271–284, 1996.

MELO, T. P. et al. New occurrences of massetognathine traversodontids and chiniquodontids (Synapsida, Cynodontia) from the early Late Triassic *Santacruzodon* Assemblage Zone (Santa Maria Supersequence, southern Brazil): Geographic and biostratigraphic implications. **Journal of South American Earth Sciences**, v. 115, p. 103757, 2022.

MIRON, L. R. et al. *Siriusgnathus niemeyerorum* (Eucynodontia: Gomphodontia): The youngest South American traversodontid? **Journal of South American Earth** Sciences, v. 97, p. 102394, 2020.

MÜLLER, R. T. A new theropod dinosaur from a peculiar Late Triassic assemblage of southern Brazil. **Journal of South American Earth Sciences**, v. 107, p. 103026, 2021.

MUSSER, A. M. et al. First australian non-mammalian cynodont: new evidence for the unusual nature of Austrália Cretaceous Vertebrates. In: **Conference on Australasian Vertebrate Evolution, Paleontology and Systematics**, v. 93, p. 47, 2009.

O'MEARA, R. N.; DIRKS, W.; MARTINELLI, A. G. Enamel formation and growth in non-mammalian cynodonts. **Royal Society open science**, v. 5, p. 172293, 2018.

OLIVEIRA, T. V.; SOARES, M. B.; SCHULTZ, C. L. *Trucidocynodon riograndensis* gen. nov. et sp. nov. (Eucynodontia), a new cynodont from the Brazilian Upper Triassic (Santa Maria Formation). **Zootaxa**, v. 2382, p. 1–71, 2010.

OLIVEIRA, T. V. et al. A new carnivorous cynodont (Synapsida, Therapsida) from the Brazilian Middle Triassic (Santa Maria Formation): *Candelariodon barberenai* gen. et sp. nov. **Zootaxa,** v. 3027, p. 19–28, 2011.

OWEN, R. **Palaeontology, or a Systematic Summary of Extinct Animals and Their Geological Relationships.** Adam and Black, Edinburgh, p. 463, 1861.

PAVANATO, A. E. B. et al. A new cynodont-bearing fossiliferous site from the Upper Triassic of southern Brazil, with taphonomic remarks and description of a new traversodontid taxon. **Journal of South American Earth Sciences**, v. 88, p. 179– 196, 2018.

RODRIGUES, P. G.; RUF, I.; SCHULTZ, C.; L. Digital reconstruction of the otic region and inner ear of the non-mammalian cynodont *Brasilitherium riograndensis* (Late Triassic, Brazil) and its relevance to the evolution of the mammalian ear. **Journal of Mammalian Evolution**, v. 20, p. 291, 2013.

ROUGIER, G. W.; WIBLE, J. Major changes in the ear region and basicranium of early mammals. In: CARRANO, M.; GAUDIN, T. J.; BLOB, R.; WIBLE. J. R. (Editors) **Amniote Paleobiology: Phylogenetic and Functional Perspectives on the evolution of mammals, birds, and reptiles.** Chicago: University of Chicago Press, p. 269–311, 2006.

ROUGIER, G. W.; WIBLE, J.; HOPSON, J. A. Reconstruction of the cranial vessels in the Early Cretaceous mammal *Vincelestes neuquenianus*: implications for the evolution of the mammalian cranial vascular system. **Journal of Vertebrate Paleontology**, v. 12, p. 188–216, 1992.

ROMER, A. S. The Chañares (Argentina) Triassic reptile fauna. VI. A chiniquodontid cynodont with incipient squamosal dentary jaw articulation. **Breviora**, v. 344, p. 1–18, 1970.

ROWE, T. Definition, Diagnosis and Origin of Mammalia. **Journal of Vertebrate Paleontology**, v. 8, p. 241–264, 1988.

ROWE, T.; MACRINI, T. E.; LUO, Z.-X. Fossil evidence on origin of the mammalian brain. **Science**, v. 332, p. 955–957, 2011.

ROWE, T.; SHEPHERD, G. M. Role of ortho-retronasal olfaction in mammalian cortical evolution. **Journal of Comparative Neurology**, v. 524, n. 3, 471–495, 2016.

RUBEN, J. A. et al. The evolution of mammalian endothermy. In: CHINSAMY-TURAN, A. (Editor.). **The Forerunners of Mammals: Radiation. Histology. Biology.** Bloomington: Indiana University Press. p. 273–286, 2012.

RUF, I. et al. Nasal anatomy of the nonmammaliaform cynodont *Brasilitherium riograndensis* (Eucynodontia, Therapsida) reveals new insight into mammalian evolution. **Anatomical Record**, v. 297, n. 11, p. 2018–2030, 2014.

RUTA, M. et al. The radiation of cynodonts and the ground plan of mammalian morphological diversity. **Proceedings of the Royal Society of London B: Biological Sciences**, v. 280, p. 1865, 2013.

SEELEY, H. G. Researches on the structure, organization, and classification of the Fossil Reptilia. Part IX, Section 3**. On *Diademodon*. Philosophical Transactions of the Royal Society of London**, v. 185, p. 1029–1041, 1894.

SIDOR, C. A. Evolutionary trends and the origin of the mammalian lower jaw. **Paleobiology**, v. 29, p. 605–640, 2003.

SIDOR, C. A.; HANCOX, P. J. *Elliotherium kersteni*, a new tritheledontid from the Lower Elliot Formation (Upper Triassic) of South America. **Journal of Paleontology**, v. 80, p. 333–342, 2006.

SIDOR, C. A.; HOPSON, J. A. Ghost lineages and "mammalness": assessing the temporal pattern of character acquisition in the Synapsida. **Paleobiology**, v. 24, p. 254–273, 1998.

SOARES, M. B. Cinodontes fósseis brasileiros revelam os primeiros passos da evolução dos mamíferos. **Ciência e Cultura**, v. 67, p. 39–45, 2015.

SOARES, M. B.; DORNELLES, J. E. F. Cinodontes, a chave para a origem dos mamíferos. **Vertebrados fósseis de Santa Maria e região**, p. 15–208, 2009.

SOARES, M. B.; MARTINELLI, A. G.; OLIVEIRA, T. V. A new prozostrodontian cynodont (Therapsida) from the Late Triassic *Riograndia* Assemblage Zone (Santa Maria Supersequence) of Southern Brazil. **Anais da Academia Brasileira de Ciências**, v. 86, p. 1673–1691, 2014.

SOARES, M. B.; SCHULTZ, C. L.; HORN, B. L. D. New information on *Riograndia guaibensis* Bonaparte, Ferigolo & Ribeiro, 2001 (Eucynodontia, Tritheledontidae) from the Late Triassic of

southern Brazil: anatomical and biostratigraphic implications. **Anais da Academia Brasileira de Ciências**, v. 83, p. 329–354, 2011.

STEFANELLO, M. et al. A new prozostrodontian cynodont (Eucynodontia, Probainognathia) from the Upper Triassic of Southern Brazil. **Journal of Vertebrate Paleontology**, v. 40, p. e1782415, 2020a.

STEFANELLO, M. et al. 3D models related to the publication: A new prozostrodontian cynodont (Eucynodontia, Probainognathia) from the Upper Triassic of southern Brazil. **MorphoMuseuM**, ISSN: 2274-0422, 2020b.

STEFANELLO, M. et al. A complete skull of a stem mammal from the Late Triassic of Brazil illuminates the early evolution of prozostrodontians. **Journal of Mammalian Evolution**. **Em revisião.**

SULEJ, T. et al. A new early Late Triassic non-mammaliaform eucynodont from Poland. **Historical Biology**, v. 32, p. 80–92, 2018.

SULEJ, T. et al. The earliest-known mammaliaform fossil from Greenland sheds light on origin of mammals. **Proceedings of the National Academy of Sciences**, v. 117, p. 26861–26867, 2020.

WALLACE, R. V.; MARTÍNEZ, R.; ROWE, T. First record of a basal mammaliamorph from the early Late Triassic Ischigualasto Formation of Argentina. **PLoS One**, v. 14, p. e0218791, 2019.

WATABE, M.; TSUBAMOTO, T.; TSOGTBAATAR, K. A new Tritylodontid Synapsid from Mongolia. **Acta Palaeontologica Polonica**, v. 52, p. 263–274, 2007.

WIBLE, J. R.; HOPSON, J. A. Basicranial evidence for early mammal phylogeny. In: SZALAY, F. S.; NOVACEK, M. J.; MCKENNA, M. C. (Editors) **Mammal Phylogeny: Mesozoic Differentiation, Multituberculates, Monotremes, Early Therians and Marsupials.** New York: Springer Verlag, p. 45–62, 1993.

ZERFASS, H. et al. Sequence stratigraphy of continental Triassic strata of Southernmost Brazil: a contribution to Southwestern Gondwana palaeogeography and palaeoclimate. **Sedimentary Geology**, v. 161, p. 85–105, 2003.